International PhD program in Cardiovascular Pathophysiology and Therapeutics

CardioPaTh
Cardiovascular
Pathophysiology
& Therapeutics

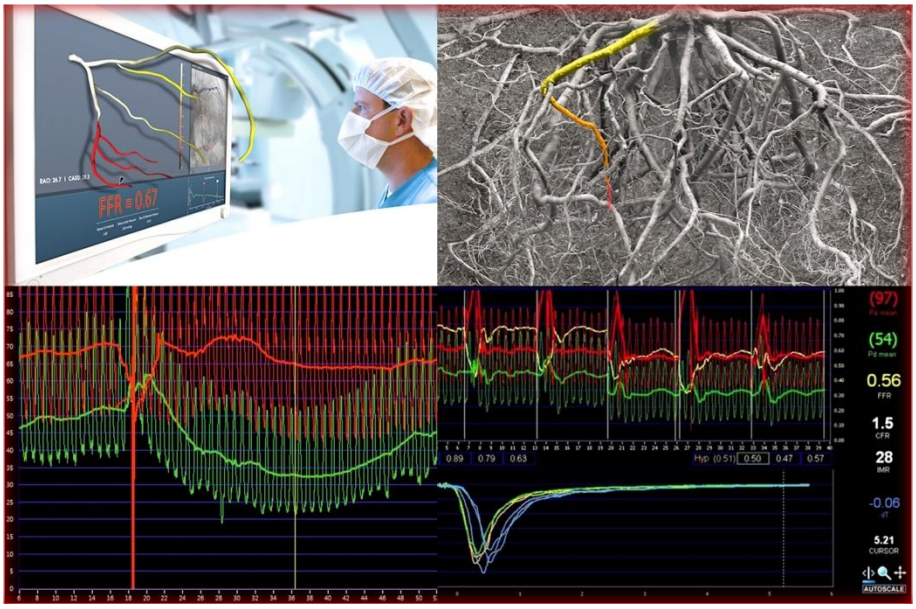

New perspectives in percutaneous coronary intervention based on an integrated approach of imaging and physiology

PhD thesis

Mariano Pellicano MD, MSc

Università degli Studi di Napoli Federico II
Cardiovascular Center OLV Aalst
INSELSPITAL
UNIVERSITÄTSSPITAL BERN
HÔPITAL UNIVERSITAIRE DE BERNE
Alta specialità del cuore
Montevergine
Professionalità, dedizione e ricerca

New perspectives in percutaneous coronary intervention based on an integrated approach of imaging and physiology

PhD thesis

Mariano Pellicano MD, MSc

28/09/1981 Cosenza (Italy)

Promotor: Prof. Bernard De Bruyne

Cardiovascular Center Aalst, OLV Clinic, Aalst, Belgium

Co-promotor: Prof. Tullio Tesorio

Montevergine Clinic, Mercogliano (AV), Italy

Naples, 21/01/2019

University Federico II of Naples, Faculty of Medicine,

Via Pansini n. 5, 80131 Naples, Italy

"The real voyage of discovery consists not in seeking new lands but seeing with new eyes"

Marcel Proust

Contents

Part II. Fractional flow reserve and natural history of stable coronary artery disease

Part III. Fractional flow reserve in special clinical settings

Part IV. Angiography-derived FFR technologies

Part V. Platelet and microvascular function

interventions in coronary bifurcations.
In Press on International Journal of Cardiology-
Published online: December 3, 2018

Part VII. Discussion and conclusions

CHAPTER 1

General introduction and outline of the thesis

Since its first description, invasive coronary angiography has been uniformly accepted to define the presence and extent of obstructive coronary artery disease (CAD), and to guide revascularization[1]. However coronary angiography produces 2-dimensional silhouette images of the 3-dimensional vascular lumen. Because angiographic stenosis severity is reported as a ratio of the stenosis' minimal lumen diameter to the adjacent "normal" reference segment, accuracy is limited by the inability to identify both "diseased" and "normal" vessel segments, particularly in the setting of diffuse CAD. Additional artifacts including contrast streaming, branch overlap, vessel foreshortening, calcifications, and ostial origins further contribute to the uncertainty of the angiographic interpretation of coronary stenosis severity. Despite numerous attempts to evaluate complex anatomy, the angiographer is still confronted with a visual dilemma in which no single view, or even multiple views, provides an answer. Considering these limitations, coronary anatomy alone, even with the highest resolution and a perfect repeatability, will never be sufficient to predict physiological behaviour of a single stenosis[2,3], particularly for those between 30% and 80% diameter stenosis[4-6]. The main unknowns are the myocardial mass depending from the stenotic segment and the microvascular function. Both will determine maximal myocardial blood.

In contrast fractional flow reserve (FFR) is a flow index, defined as the ratio of maximal hyperemic myocardial blood flow in the presence of a stenosis

to the physiologic maximal hyperemic myocardial blood flow in the same territory but in the absence of any stenosis[7-9]. As such, its value is influenced and integrates hyperaemic flow, which itself depends on stenosis severity, myocardial mass, and its microvascular function. Since mass and microvascular function are not likely to change in a given patients before and after revascularization, FFR indicates to what extent hyperaemic myocardial flow will increase after percutaneous coronary intervention (PCI) (i.e. normalization of the epicardial resistance)[10,11]. FFR overcomes the visual-functional mismatch and stands alone in measuring ischemia in the catheterization laboratory with validated and durable clinical data supporting its use for predicting outcomes. Fifteen-year outcome data from the DEFER (Deferral vs. performance of percutaneous coronary intervention of functionally nonsignificant coronary stenosis) study demonstrate that postponing PCI in vessels with an FFR >0.75 is safe and associated with a low rate of clinical endpoints[12], whereas the FAME-2 (Fractional Flow Reserve versus Angiography for Multivessel Evaluation-2) study, among others, showed that patients with an abnormal FFR (i.e., lesion-specific ischemia) benefit more from revascularization than continued optimal medical therapy[13-15].

Faced with this scenario, the almost systematic use of FFR in catheterization laboratory in different anatomical settings would seem almost intuitive and obvious, especially if we consider the clear indications of the European and American guidelines on myocardial revascularization[16,17]. Nevertheless, the penetration of physiology-based guidance varies significantly across continents, countries, centers, and operators, ranging from 3% to 30% of the total volume of coronary revascularizations. Several factors have been proposed to explain the variability in FFR assessment adoption, such as

differences in equipment, reimbursement policies, and operator choice. Other investigators have suggested concerns regarding adenosine side effects, costs, and time[18,19]. Therefore, the ability to derive FFR values from routinely performed coronary angiograms, without the need for a pressure guidewire or hyperemic stimulus, could have an important impact on daily clinical practice by streamlining the workflow within the catheterization laboratory and avoiding the need for invasive coronary measurements. Several image-based FFR methodologies have recently been introduced. In this thesis we report the first multicenter validation studies of the two angiography derived-FFR technologies that are gaining ground in interventional cardiology practice: FFR_{angio} and QFR.

It is unclear whether FFR can predict which patients will actually have an increase in myocardial perfusion after PCI[20]. Although the goal of PCI is to increase coronary blood flow by relieving epicardial coronary stenosis, early explorations showed that successful stenting increased coronary flow reserve (CFR) in only 80% of patients[21]. This surprising failure to normalize CFR in all PCI patients was attributed to a combination of diffuse downstream atherosclerosis, or acutely induced or preexisting microvascular dysfunction. Microvascular dysfunction alone can cause ischemic symptoms in the absence of epicardial obstruction[22-24] and probably contributes to persistent ischemia despite successful revascularization[25]. However, use of CFR to assess the microcirculation independently is limited in that CFR interrogates the flow status of both the epicardial artery and the microcirculation. Also the dependence on resting haemodynamics is an important theoretical limitation for the use of CFR as a primary diagnostic tool in ischemic heart disease[26,27].

In this sense, Fearon WF et colleagues setted up a novel index of microcirculatory resistance (IMR), defined as distal coronary pressure divided by the inverse of the hyperemic mean transit time (a correlate to absolute flow), measured simultaneously with the coronary pressure wire[28-32]. The advantages of IMR include that is relatively easy to measure and can be performed simultaneously while measuring FFR without any extra equipment, is specific for the microvasculature and is independent from the hemodynamic variability[33-35]. Still, it is not known whether therapeutic reduction of IMR (e.g. with an intracoronary vasodilator) confers clinical benefits. Nor is it known whether, in patient with stable CAD, treatment decisions based on an IMR threshold might have prognostic benefits (as has been shown to be the case with FFR). Also during IMR assessment an intrinsic variability of resting mean transit time (Tmn_{rest}) of 7-10%, and Tmn_{hyp} of 4-8% have been reported.

With this in mind, aiming to a quantitative assessment of the microcirculation independent of operators and the presence of epicardial stenoses, a recent development of a dedicated monorail infusion catheter (Rayflow™, Hexacath, Paris, France) has simplified the measurement of absolute coronary flow (Q) and microvascular resistance (R) in the cathlab, opening a new window to the coronary microcirculation. The present method relies on a simple basic principle. Three parameters should be known: the infusion rate of saline (in mL/min), the temperature of the saline when it enters the coronary tree (in degrees), and the temperature of the blood when saline and blood have been mixed in the distal part of the artery (in degrees). This rule of three allows the calculation of absolute Q[36]. The calculated flow is hyperemic flow because it has been shown that the infusion of saline at room temperature through the RayFlow catheter

reliably uniformly induces maximal hyperemia[37]. A major advantage of this method is that—in contrast to Doppler or index of microcirculatory resistance—it is completely operator independent. The saline infusion can be continued until a true steady state is achieved (typically within 10–15 seconds), and during the entire measurement sequence, the operator does not touch the patient nor any catheter. In this thesis we report the fist study aimed at investigate feasibility, safety, and reproducibility of catheter-based measurements of absolute coronary blood flow and microvascular resistance.

Outline of the thesis

The thesis is divided in seven part:

Part I. From pressure derived-FFR to Absolute Flow and Microvascular Resistance. In the first part of the thesis we report our research projects published in the field of coronary physiology, describing the gradual shift of attention over the years from the FFR measurements to the direct assessment of absolute coronary blood flow and microvascular resistance. The *"leitmotiv"* of this paradigm shift is represented by the research projects, presented in this section, regarding the agents inducing maximal hyperemia, starting from the intracoronary administration of adenosine to the intracoronary infusion of saline at room temperature through the Rayflow™ catheter.

Part II. Fractional flow reserve and natural history of stable coronary artery disease. In the second part of the thesis we report the cluster of

research projects that focuses on the importance of FFR assessment of epicardial stenosis in patients with stable CAD, with both single vessels disease (chapter 7) and multivessel disease (chapter 9), underlining its prognostic value.

Part III. Fractional flow reserve in special clinical settings. This section of the thesis is a collection of our research projects aimed at investigate the role of invasive functional assessment in patients in whom coronary artery bypass graft (CABG) is indicated, which already underwent CABG and in patients with left ventricular dysfunction (LVD) and/or heart failure (HF). We also provide a description of the impact on clinical decision making of guiding catheter disengagement during FFR assessment of intermediate coronary stenoses (chapter 11) and the FFR measurements in symptomatic patients with Myocardial Bridge (chapter 12).

Part IV. Angiography-derived FFR technologies. We report in these sections the first-in man validations studies of the two main technologies in the field of angiography-derived FFR: FFR_{angio} and QFR.

Part V. Platelet and microvascular function. This part of the thesis is a collection of research projects aimed to evaluate the microvascular dysfunction with IMR in patients with stable CAD undergoing elective PCI. We investigated a) the protective rule of prasugrel vs. clopidogrel on microcirculation (chapter 24) b) the effect of G894T polymorphism on

residual platelet reactivity and on the risk of periprocedural myocardial infarction (PMI) (chapter 25); c) the impact of serum uric acid levels on high residual platelet reactivity after PCI (chapter 26); d) the procedure related microvascular activation in long lesions treated with bioresorbable vascular scaffold versus everolimus-eluting stent implantation (chapter 27).

Part VI: Percutaneous coronary interventions in bifurcation lesions: from bench tests to clinical outcome. This section of the thesis focuses on the topic of PCI in bifurcation lesions. Regarding the bench tests, we describe the procedural steps in vitro of the reversed single string technique (chapter 29) and we report the validation of resorbable magnesium scaffold (RMS) in various non-bifurcation and bifurcation anatomies using standard interventional techniques (chapter 30). Concerning the clinical evaluation, we describe the clinical applicability of the single-string bifurcation stenting technique (chapter 28) and we report the results of the P2BiTO registry, regarding the major clinical, anatomic and procedural determinants of mid-term clinical outcomes in all comer patient population undergoing PCI in bifurcations (chapter 31).

Part VII: Discussion and conclusions. The last section of the thesis is a broad discussion of the addressed topics with the conclusions.

Part I

From pressure derived-FFR to Absolute Flow and Microvascular Resistance

CHAPTER 2

Standardization of Fractional Flow Reserve Measurements

To assess the contribution of a new diagnostic test, a hierarchical model of efficacy was proposed by Fryback and Thornbury. Although the model was developed for the evaluation of diagnostic imaging, its parameters also apply to "physiological imaging," with its attributes of: 1) technical quality; 2) diagnostic accuracy; 3) diagnostic thinking efficacy; 4) effect on therapy; 5) patient's outcome; and 6) economic aspects (Figure 1). A key feature of this model is that for a test to be efficacious at a higher level in this hierarchy, it must be efficacious at lower levels.

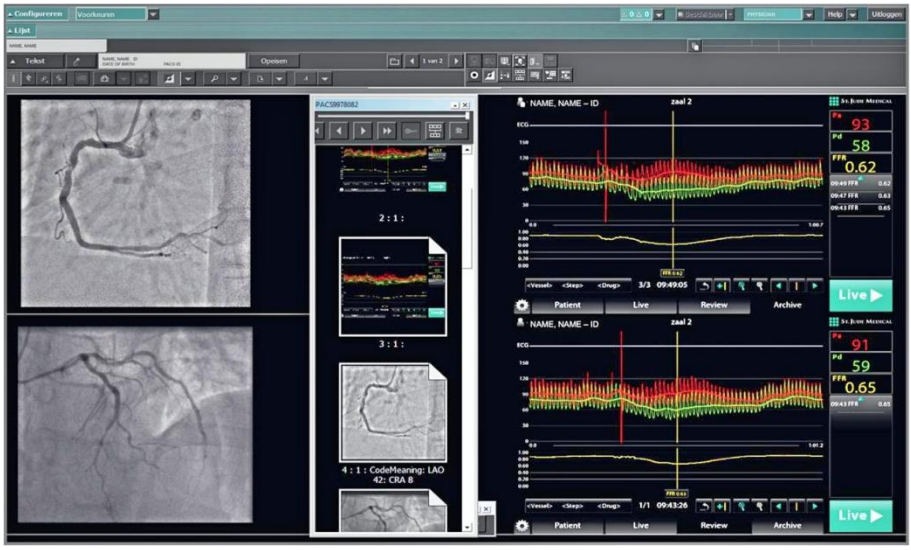

Figure 1: Fractional Flow Reserve: example of simultaneous DICOM format storage of complete physiological and angiographic information. Archiving this information (as well as intravascular ultrasound and optical coherence tomography, when available) side-by-side, in a format that is easily accessible ("same place, same time" principle) enables surgeons, interventional cardiologists, clinicians, and heart team meeting participants to be exposed to these different imaging modalities and to integrate "anatomy" and "physiology" into individual clinical decision making. CRA: cranial; DICOM: digital imaging and communications

in medicine; ECG: electrocardiogram; FFR: fractional flow reserve; LAO: left anterior oblique; P_a: aortic pressure; P_d: distal coronary pressure.

Since the first description of pressure wire-based FFR, an abundance of data pertaining to each of these criteria have been reported. Accordingly, FFR is now considered to be the reference standard for the evaluation of the ischemic potential and the expected benefit from revascularization of coronary stenosis. Moreover, FFR is increasingly being used in clinical trials as an inclusion criterion or as an endpoint and to validate new diagnostic modalities. Although all major outcomes-randomized clinical trials (RCTs) have made decisions on the basis of operator-derived FFR values, a handful of recent diagnostic accuracy studies sent tracings to physiology core laboratories for post hoc analysis. However, no matter where analysis takes place, technical or operator-related artifacts in pressure recordings should be avoided, minimized, or at least identified if they occur.

FFR is calculated from distal coronary pressure (P_d) and aortic pressure (P_a) obtained during maximal coronary hyperemia. In principle, these measurements are straightforward and almost fully automated, as illustrated in Figure 2. Yet, minor differences among practices of different laboratories have led to some heterogeneity in acquiring and interpreting the data. Because FFR-based decisions are important for patients' outcomes, and given the need for rigor and reproducibility in reading the tracings by core laboratories, the highest technical quality of FFR measurements is desirable. As FFR by itself is a highly reproducible diagnostic measure, deviations mainly derive from a lack of standardization.

Figure 2: Typical example of FFR measurement obtained after intracoronary bolus injection of adenosine. The injection of the bolus is brief so that the aortic signal (red) is interrupted during no longer than 1 to 2 s. Automated calculation of FFR corresponds to the ratio of mean distal coronary pressure (green) to mean aortic pressure during maximal hyperemia. CRA: cranial; FFR: fractional flow reserve; LAO: left anterior oblique; P_a: aortic pressure; P_d: distal coronary pressure.

Accordingly, this document proposes a standardized way of acquiring, recording, interpreting, and storing the pressure tracings for daily practice and for the purpose of clinical research through a core laboratory. Comprehensive reviews of the principle of FFR and of the FFR-based clinical outcome data have been described previously.

CHAPTER 3

Intracoronary Adenosine: Dose-Response Relationship With Hyperemia

The present study sought to establish the dosage of intracoronary (IC) adenosine associated with minimal side effects and above which no further increase in flow can be expected.

Background: Despite the widespread adoption of IC adenosine in clinical practice, no wide-ranging, dose-response study has been conducted. A recurring debate still exists regarding its optimal dose.

Methods: In 30 patients, Doppler-derived flow velocity measurements were obtained in 10 right coronary arteries (RCAs) and 20 left coronary arteries (LCAs) free of stenoses >20% in diameter. Flow velocity was measured at baseline and after 8 ml bolus administrations of arterial blood, saline, contrast medium, and 9 escalating doses of adenosine (4 to 500 µg). The hyperemic value was expressed in percent of the maximum flow velocity reached in a given artery (Q/Qmax, %).

Results: Q/Qmax did not increase significantly beyond dosages of 60 mg for the RCA and 160 mg for LCA. Heart rate did not change, whereas mean arterial blood pressure decreased by a maximum of 7% ($p < 0.05$) after bolus injections of intracoronary (IC) adenosine. The incidence of transient A-V blocks was 40% after injection of 100 µg in the RCA and was 15% after injection of 200 µg in the LCA. The duration of the plateau reached 12 13 s after injection of 100 µg in the RCA and 21 6 s after the injection of 200 µg in the LCA. A progressive prolongation of the time needed to return to

baseline was observed. Hyperemic response after injection of 8 ml of contrast medium reached 65 36% of that achieved after injection of 200 µg of adenosine (Figure 3).

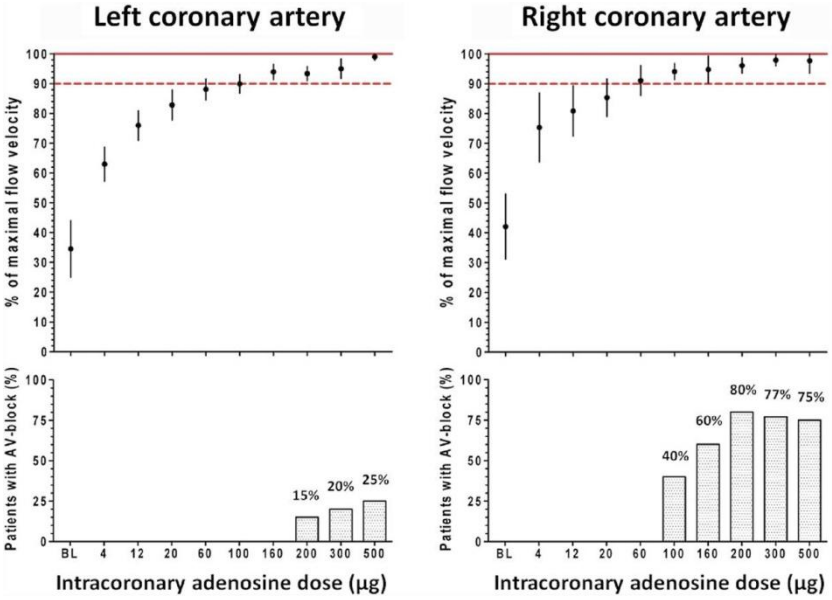

Figure 3: Intracoronary adenosine dose-flow relationship. (Top) Dose-response data for the right coronary artery (RCA) (left panel) and the left coronary artery (LCA) (right panel). The data are expressed as the percent of maximum for each patient (Q/Qmax) at each dose of intracoronary (IC) adenosine. The error bars represent the 95% confidence intervals for each value. (Bottom) The bars represent the percent of patients in whom high-grade atrioventricular (AV) block occurred with that dose of adenosine. BL: baseline.

Conclusions: This wide-ranging, dose-response study indicates that an IC adenosine bolus injection of 100 µg in the RCA and 200 µg in the LCA induces maximum hyperemia while being associated with minimal side effects.

CHAPTER 4

Saline-Induced Coronary Hyperemia: Mechanisms and Effects on Left Ventricular Function

Background: reliable method to assess volumetric maximal myocardial flow and absolute minimal microvascular resistance has been described almost 10 years ago. The method is based on the principle of coronary thermodilution by continuous infusion of saline at room temperature during steady-state hyperemia. One of the prerequisites of the thermodilution principle is the complete and instantaneous mixing of the indicator, in this case saline at room temperature. Yet, the method was hampered by technical difficulties that precluded routine application. The technique was recently simplified by the development of a dedicated rapid exchange infusion catheter and a dedicated software allowing instantaneous calculation of volumetric flow and resistance. The present work is based on an incidental observation. While performing measurements of minimal microvascular resistance in patients with mild atherosclerosis, we observed the occurrence or the increase of a pressure gradient between the coronary ostium and the distal part of the coronary artery few seconds after the start of the intracoronary infusion of saline, even before the start of adenosine infusion (Figure 4). This observation suggested that the infusion of saline at room temperature could elicit coronary hyperemia. If infusion of saline would indeed induce maximal steady-state hyperemia, this would further simplify the application of coronary thermodilution-derived quantification of myocardial flow and resistance.

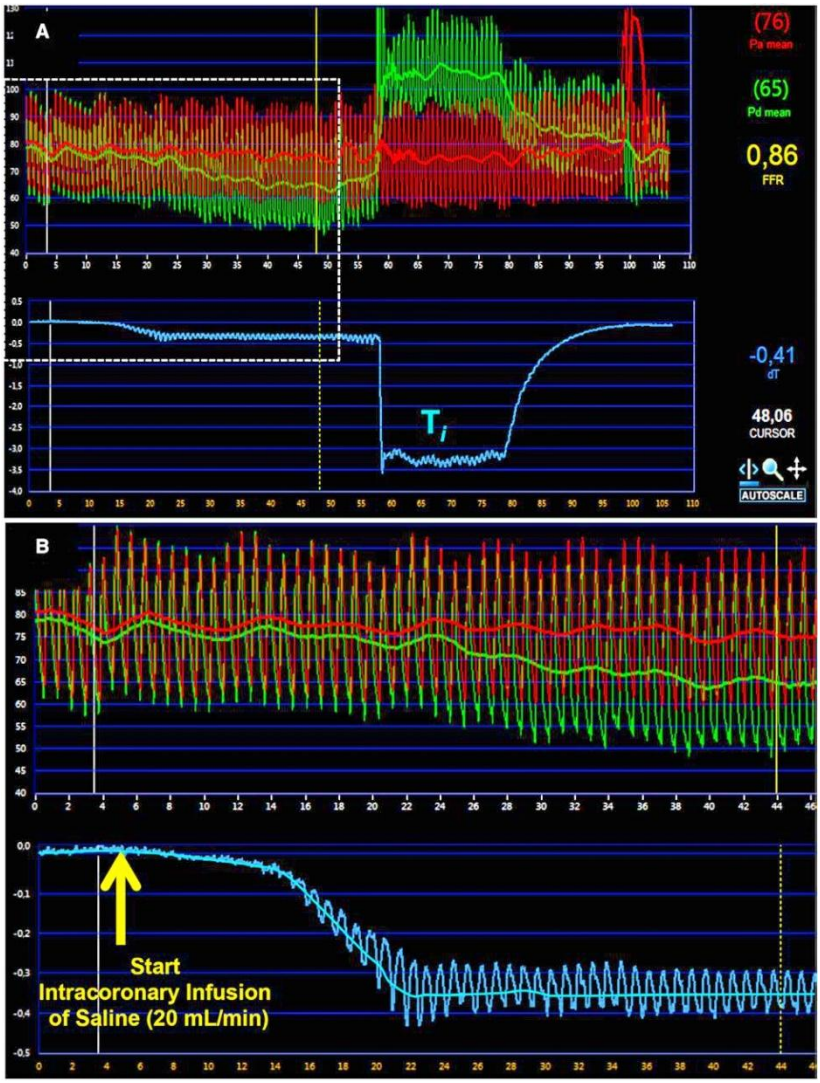

Figure 4. Example of simultaneous pressure and temperature recording in the left anterior descending coronary artery with mild diffuse atherosclerosis. A, Complete tracing of thermodilution-derived absolute flow measurements, including the moderate decline in coronary temperature (T) and the sharp decrease in temperature when the sensor is pulled back in the infusion catheter to assess the temperature of the saline when it enters the coronary artery (T*i*). B, Magnification of the rectangle delineated in A by a white broken line. Approximately 10 s after the start of the infusion of saline at room temperature at the rate of 20 mL/min (yellow arrow), the distal temperature starts to decline, reaching a plateau after ≈20 s. This decrease in temperature is paralleled by an increase in pressure gradient across the mild epicardial stenosis suggesting the occurrence of hyperemia. FFR indicates fractional flow reserve.

Aim: This study was designed to study the effects of intracoronary infusion of saline at room temperature on the coronary circulation and myocardial function in humans and to explore its mechanisms.

Methods and Results: Thirty-three patients were studied; in 24 patients, intracoronary Doppler flow velocity measurements were performed at rest, after IC adenosine, and during increasing infusion rates of saline at room temperature through a dedicated catheter with 4 lateral side holes. In 9 patients, global longitudinal strain and flow propagation velocity were assessed by transthoracic echocardiography (TTE) during a prolonged intracoronary saline infusion. Taking adenosine induced maximal hyperemia as reference, intracoronary infusion of saline at rates of 5, 10, 15, and 20 mL/min induced 6%, 46%, 111%, and 112% of maximal hyperemia, respectively (Figure 5). There was a close agreement of maximal saline- and adenosine induced CFR (intraclass correlation coefficient, 0.922; $P<0.001$). The same infusion rates given through 1 end hole (n=6) or in the contralateral artery (n=6) did not induce a significant increase in flow velocity. Intracoronary saline given on top of an intravenous (IV) infusion of adenosine did not further increase flow. Intracoronary saline infusion did not affect blood pressure, systolic, or diastolic left ventricular function. Heart rate decreased by 15% during saline infusion ($P=0.021$).

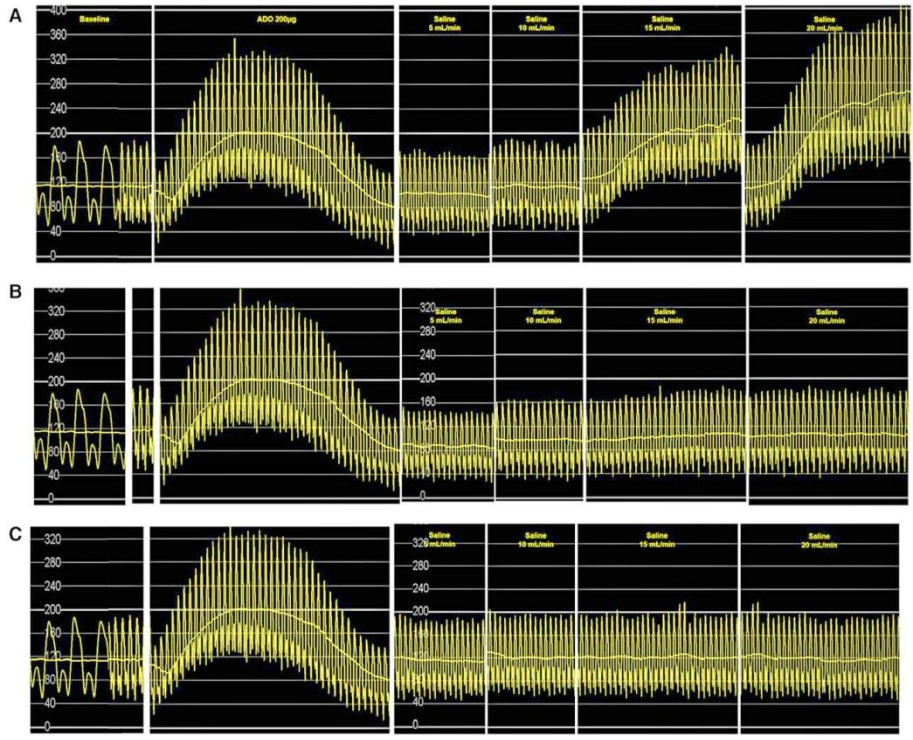

Figure 5: Representative example of coronary flow velocity tracings at baseline and after an intracoronary bolus of 200 µg of adenosine, during infusion of saline at room temperature at rates of 5, 10, 15, and 20 mL/min. A, Saline is infused through the side holes of the catheter advanced over the Doppler wire. B, Saline is infused through the distal hole of the catheter advanced over the Doppler wire. C, Saline is infused through the side holes of an infusion catheter advanced in a contralateral artery.

Conclusions: intracoronary infusion of saline at room temperature through a dedicated catheter for coronary thermodilution induces steady-state maximal hyperemia at a flow rate ≥15 mL/min. These findings open new possibilities to measure maximal absolute coronary blood flow and minimal microcirculatory resistance.

CHAPTER 5

Reduced Coronary Flow Reserve in Coronary Arteries without Stenosis: Impact of Various Hemodynamic and Clinical Parameters

Background: CFR, the ratio of hyperemic flow to baseline flow, was proposed over 40 years ago, and has been the gateway for clinical application of coronary physiology. This study aimed to evaluate the impact of various clinical and hemodynamic parameters on CFR in angiographically normal coronary arteries.

Methods: In 30 patients with stable coronary artery disease, Doppler-derived flow velocity measurements were obtained in angiographically normal coronary arteries. Flow velocity was measured during one minute under resting conditions and then after administering increasing dosages of IC adenosine boluses (4 to 500 μg).

Results: In coronary arteries without significant stenosis, CFR varied from 1.42 to 4.88 (average 2 .83±0.88). Patients were categorized into two groups using the median CFR: *low* CFR ranging from 1.42 to 2.78 and *high* CFR ranging from 2.87 to 4.88. Baseline flow velocity was significantly higher in patients with *low* CFR than in patients with *high* CFR. Hyperemic flow velocity was similar in both groups (Figure 6).

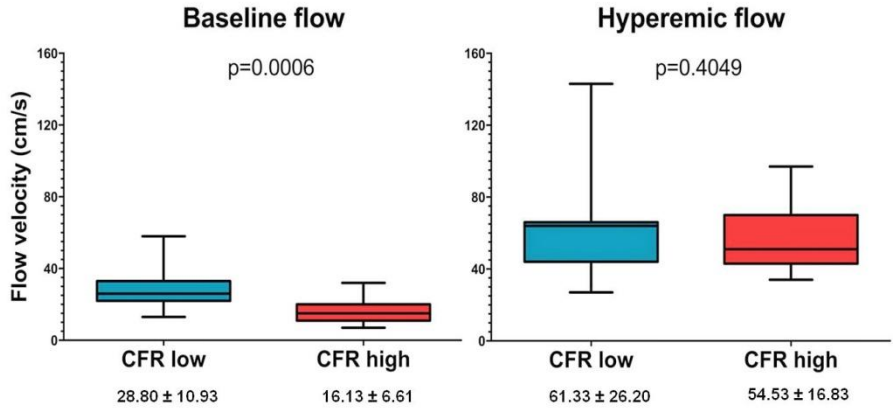

Figure 6: Baseline and hyperemic flow in the two groups.

Baseline flow velocity showed a significant correlation with the absolute value of CFR (R2=0.42, p<0.01), while hyperemic flow did not correlate with it (R2=0.04, p=0.30). A trend was observed such that, in patients with low CFR, less adenosine was needed to reach maximal hyperemia. No difference was found in any other hemodynamic or clinical or parameters between groups.

Conclusions: In coronary arteries free from significant stenosis, "resting" flow velocity appears to be a major determinant of pathologic CFR, more so than hyperemic flow.

CHAPTER 6

Catheter-Based Measurements of Absolute Coronary Blood Flow and Microvascular Resistance: Feasibility, Safety, and Reproducibility in Humans

Background: The principle of continuous thermodilution can be used to calculate absolute coronary blood flow (Q). The concomitant measurement of pressure in the distal part of the vessel allows the calculation of myocardial resistance. The recent development of a dedicated monorail infusion catheter has simplified the measurement of absolute Q and microvascular resistance (R) in the cathlab, opening a new window to the coronary microcirculation. Q (mL/min) can be calculated by continuous intracoronary infusion of saline, as previously described, according to the equation

$$Q_b = c_p \left[\frac{(T_b - T_i)}{(T_b - T)} - 1 \right] Q_i + Q_i$$

where Q_i is the saline infusion rate in mL/min, T_b is the temperature of blood in the distal coronary before infusion of saline, T_i is the temperature of the infused saline when it exits the infusion catheter, and T is the temperature of the homogenous mixture of blood and saline in the distal part of the coronary artery during infusion. The constant c_p relates to the difference between the specific temperature and density of blood and saline, and when saline is infused in blood, this is equal to 1.08. In practice, the temperature of blood (Tb, ≈37°C) is taken as a reference, and the other

temperatures are measured with respect to that value. Therefore, T_i and T stand for relative temperatures compared with T_b, and the equation is simplified as follows:

$$Q_b = 1.08\frac{T_i}{T}Q_i - 0.08Q_i$$

Since, in clinical practice, Q_i is chosen between 15 and 30 ml/min, the last part of the equation subtracts between 1.2 and 2.4 mL/min from the calculated coronary blood flow and can therefore be neglected. Consequently, the equation is further simplified to:

$$Q_b = 1.08\frac{T_i}{T}Q_i$$

Absolute microvascular resistance (R) is calculated in analogy to Ohm's law:

$$R = \frac{P_d}{Q_b}$$

where P_d is the distal coronary pressure and Q_b is the coronary blood flow.

Aim: Although data on the in vitro validation of the method and the infusion catheter have been recently published, in vivo data are lacking. The aim of the study is to explore the safety, feasibility, and reproducibility of coronary blood flow and R measurements as measured by continuous thermodilution in humans.

Methods and Results: Absolute coronary flow and R can be calculated by thermodilution by infusing saline at room temperature through a dedicated monorail catheter. The temperature of saline as it enters the vessel, the temperature of blood and saline mixed in the distal part of the vessel, and

the distal coronary pressure were measured by a pressure/temperature sensor-tipped guidewire (Figure 7).

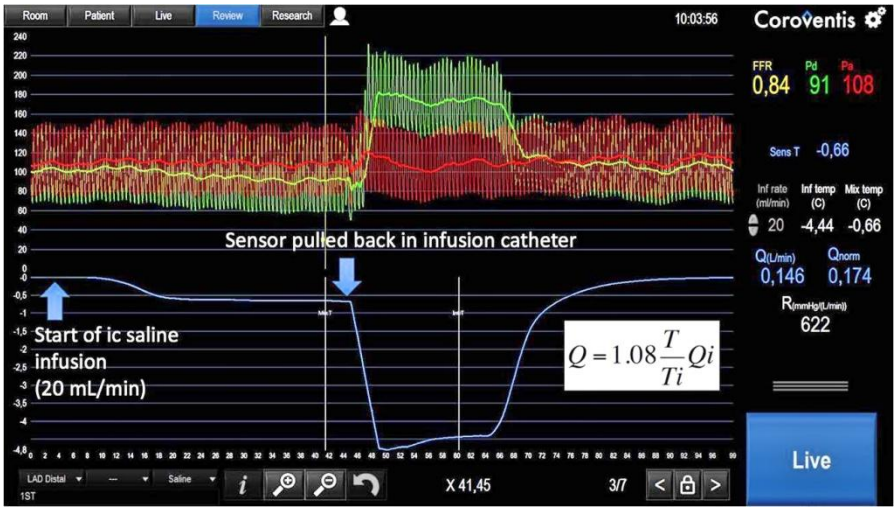

Figure 7: Thermodilution-derived absolute coronary blood flow and microvascular resistance measurement. Example of thermodilutionderived absolute microvascular resistance and coronary blood flow in a left anterior descending artery. The flow rate of the administered saline is 20 mL/min, and the calculated values of absolute coronary blood flow (Q) and microvascular resistance (R) are 0.146 L/min and 622 mm Hg/L/min, respectively. The theoretically achieved maximum blood flow in the absence of epicardial stenoses (Q_{norm}), that is, if fractional flow reserve (FFR) was equal to 1, is also displayed. Pa indicates aortic pressure; and Pd, distal coronary pressure.

The feasibility and safety of the method were tested in 135 patients who were referred for coronary angiography. No significant adverse events were observed; in 11 (8.1%) patients, bradycardia and concomitant atrioventricular block appeared transiently and were reversed immediately on interruption of the infusion. The reproducibility of measurements was tested in a subgroup of 80 patients (129 arteries). Duplicate measurements had a strong correlation both for coronary blood flow (ρ=0.841, P<0.001; intraclass correlation coefficient=0.89, P<0.001) and R (ρ=0.780, P<0.001; intraclass correlation coefficient=0.89, P<0.001). In Bland–Altman plots, there was no significant bias or asymmetry.

Conclusions: Despite some limitations, the present data confirm the feasibility, safety, and reproducibility of thermodilution-derived hyperemic coronary flow (expressed in L/min) and of coronary R measurements (expressed in mm Hg/L/min or Wood units) that can be performed simply and easily. If further confirmed and validated, this approach should allow a more quantitative and operator-independent quantification of the microvasculature and help in assessing treatment of microvascular dysfunction.

Part II

Fractional flow reserve and natural history of stable coronary artery disease

CHAPTER 7

Significance of Intermediate Values of Fractional Flow Reserve in Patients With Coronary Artery Disease

Background: FFR represents the standard of reference for invasive functional evaluation of the ischemic potential of coronary stenosis and is a valuable tool to guide percutaneous revascularization. An FFR value ≤0.75 is almost uniformly associated with signs of ischemia, whereas an FFR >0.80 is usually associated with the absence of ischemia. Based on numerous randomized trials and registries in most subsets of lesions and patients, the threshold value of 0.80 has been widely accepted to guide clinical decision making. The best treatment strategy for intermediate stenosis with FFR in the narrow gray zone of values, that is, between 0.76 and 0.80, has been questioned. Therefore, we analyzed the long-term clinical outcome of patients with an isolated stenosis within the gray zone (0.76–0.80) or immediately next to the gray zone (0.70–0.75 and 0.81–0.85).

Methods and Results: From February 1997 to June 2013, all patients with single-segment disease and an FFR value within the gray zone or within the 2 neighboring FFR strata (0.70–0.75 and 0.81–0.85) were included. Study end points consisted of major adverse cardiovascular events (death, myocardial infarction, and any revascularization) up to 5 years. Of 17 380 FFR measurements, 1459 patients were included. Of them, 449 patients were treated with revascularization and 1010 patients were treated with medical therapy (Figure 8). In the gray zone, the major adverse cardiovascular events rate was similar (37 [13.9%] versus 21 [11.2%],

respectively; P=0.3) between medical therapy and revascularization, whereas a strong trend toward a higher rate of death or myocardial infarction (MI) (25 [9.4] versus 9 [4.8], P=0.06) and overall death (20 [7.5] versus 6 [3.2], P=0.059) was observed in the medical therapy group (Figure 8). Among medical therapy patients, a significant step-up increase in major adverse cardiovascular events rate was observed across the 3 FFR strata, especially with proximal lesion location. In revascularization patients, the major adverse cardiovascular events rate was not different across the 3 FFR strata (Figure 9).

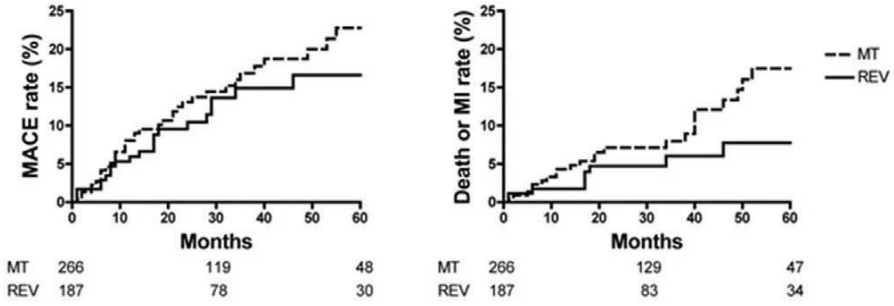

Figure 8: Cumulative rate (%) of MACE (log-rank, 0.87; P=0.3) and death or MI (log-rank, 2.96; P=0.08) in the gray-zone patients treated with medical therapy or revascularization. MACE indicates major adverse cardiovascular event; MI, myocardial infarction; MT, medical therapy; and REV, revascularization.

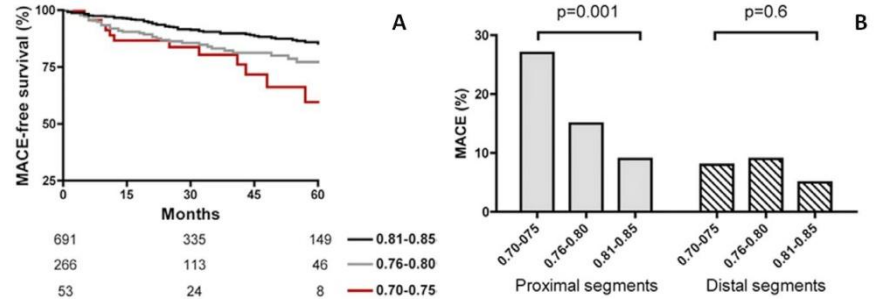

Figure 9: A) MACE-free survival (%) in patients of the medical therapy group stratified by FFR strata (log-rank, 15; P<0.001). B) MACE rate (%) in patients receiving medical therapy,

stratified according to the FFR strata, and grouped according to the location of the lesions (proximal vs distal). FFR indicates fractional flow reserve; and MACE, major adverse cardiovascular event.

Conclusions: Patients with an isolated stenosis located in a proximal coronary segment and FFR within the gray zone of 0.76 to 0.80. demonstrate a clinical outcome that is suboptimal when deferred to medical therapy alone. These data confirm the value of the 0.80 FFR threshold, and favor a revascularization strategy of coronary stenoses with FFR ≤0.80.

CHAPTER 8

Visual and Quantitative Assessment of Coronary Stenoses at Angiography Versus Fractional Flow Reserve: The Impact of Risk Factors

Background: The correlation between angiographic assessment of coronary stenoses and FFR is weak. Whether and how risk factors impact the diagnostic accuracy of angiography is unknown. We sought to evaluate the diagnostic accuracy of angiography by visual estimation (VE) and by quantitative coronary angiography (QCA) when compared with FFR and evaluate the influence of risk factors (RF) on this accuracy.

Methods and Results: In 1382 coronary stenoses (1104 patients), percent diameter stenosis by visual estimation (DS_{VE}) and by quantitative coronary angiography (DS_{QCA}) was compared with FFR. Patients were divided into 4 subgroups, according to the presence of RFs, and the relationship between DS_{VE}, DS_{QCA}, and FFR was analyzed. Overall, DS_{VE} was significantly higher than DS_{QCA} ($P<0.0001$); nonetheless, when examined by strata of DS, DS_{VE} was significantly smaller than DS_{QCA} in mild stenoses, although the reverse held true for severe stenoses. Compared with FFR, a large scatter was observed for both DS_{VE} and DS_{QCA}. When using a dichotomous FFR value of 0.80, C statistic was significantly higher for DS_{VE} than for DS_{QCA} (0.712 versus 0.640, respectively; $P<0.001$). C statistics for DS_{VE} decreased progressively as RFs accumulated (0.776 for ≤1 RF, 0.750 for 2 RFs, 0.713 for 3 RFs and 0.627 for ≥4 RFs; $P=0.0053$) (Figure 10A). Also 97 (9%) patients had diabetes mellitus, and 1007 (91%) did not have diabetes mellitus. Both groups were similar in terms of baseline and angiographic characteristics, with the

exception of higher prevalence of dyslipidemia, family history of coronary artery disease, and higher body mass index in the diabetic group. FFR was significantly higher in the diabetic group compared with the nondiabetic group (0.83 [0.76, 0.90] versus 0.81 [0.73, 0.88]; P=0.013). In ROC analyses, the DS_{VE} curve for the diabetic group had a lower C statistic compared with the nondiabetic group (0.524 versus 0.729; P<0.001;) (Figure 10B).

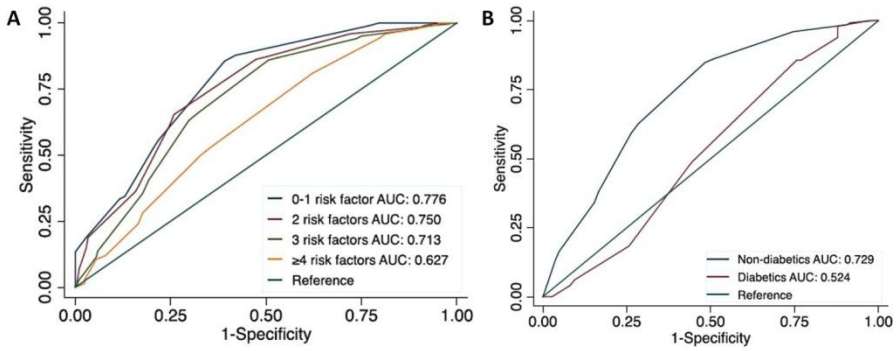

Figure 10: A) Receiver operating characteristic curves for diameter stenosis by visual estimation (DS_{VE}) according to the presence of risk factors. B) Receiver operating characteristic curves for DS_{VE} in diabetic and nondiabetic patients. AUC indicates area under the curve.

Conclusions: This study confirms the weak correlation between angiographic metrics and FFR and indicates that, despite its subjectivity, VE is more accurate in predicting physiology than QCA. The presence of risk factors markedly blur this relationship: the more risk factors, the weaker the potential of angiography to assess physiology, particularly so in diabetics. In these patients—even more than in others—a combined angiographic and functional approach is mandated for optimal clinical decision-making about revascularization.

CHAPTER 9

Angiography versus hemodynamic assessment to predict the natural history of coronary stenoses: a fractional flow reserve versus angiography in multivessel evaluation 2 (FAME 2) substudy

Background: FFR has become the standard of reference for the invasive evaluation of coronary stenosis. Nevertheless, interventional cardiologists still prefer angiography for guiding decision making about revascularization, even in the absence of any budget and logistic constraints. The angiographic thresholds of 50% or 70% diameter stenosis (DS) are still used to define obstructive coronary artery disease to risk stratify patients, justify revascularization, serve as an end point in studies on revascularization strategies, and validate other approaches. Accordingly, we investigated the spontaneous, vessel-oriented clinical outcome of patients from the FAME 2 trial (Fractional Flow Reserve Versus Angiography in Multivessel Evaluation 2) in whom no revascularization was performed but in whom both the DS and functional (FFR) severity was known. The aim of the study was to compare the accuracy of both approaches in predicting the natural history of CAD.

Methods: The present analysis included the 607 patients from the FAME 2 trial in whom no revascularization was performed. FFR varied from 0.20 to 1.00 (average 0.74±0.16), and DS (by quantitative coronary analysis) varied from 8% to 98% (average 53±15). The primary end point, defined as vessel-

oriented clinical end point (VOCE) at 2 years, was a composite of prospectively adjudicated cardiac death, vessel-related MI, vessel-related urgent, and not urgent revascularization. The stenoses were divided into 4 groups according to FFR and DS% values: positive concordance (PC) (FFR≤0.80; DS≥50%), negative concordance (NC) (FFR>0.80; DS<50%), positive mismatch (PM) (FFR≤0.80; DS<50%), and negative mismatch (NM) (FFR>0.80; DS≥50%).

Results: Clinical 2-year follow-up was available for all patients. Overall, VOCEs occurred in 26% of cases. The rate of VOCE was highest in the group of stenoses with PC (FFR ≤0.80; DS ≥50%; 125/317 lesions [39.4%]) and lowest in stenoses with an NC (FFR >0.80; DS <50%; 17/216 lesions [7.9%]). The rate of VOCEs was similar in stenoses with a PM (FFR ≤0.80; DS <50%) and with a PC (50/153 lesions [32.7%] versus 125/317 lesions [39.4%], respectively; P=0.139). In contrast, the rate of VOCEs of stenoses with a NM (FFR >0.80; DS ≥50%) was lower as compared with stenoses with a PM (16/113 lesions [14.2%] 50/153 lesions [32.7%], respectively; P=0.001) but was not significantly different compared with stenoses with an NC (17/216 [7.9%]; P=0.099). There was no significant difference in terms of lesion-related outcome between the NM (FFR >0.80; DS ≥50%) and the NC (FFR >0.80; DS <50%), although there was a trend (P=0.099) (Figure 11).

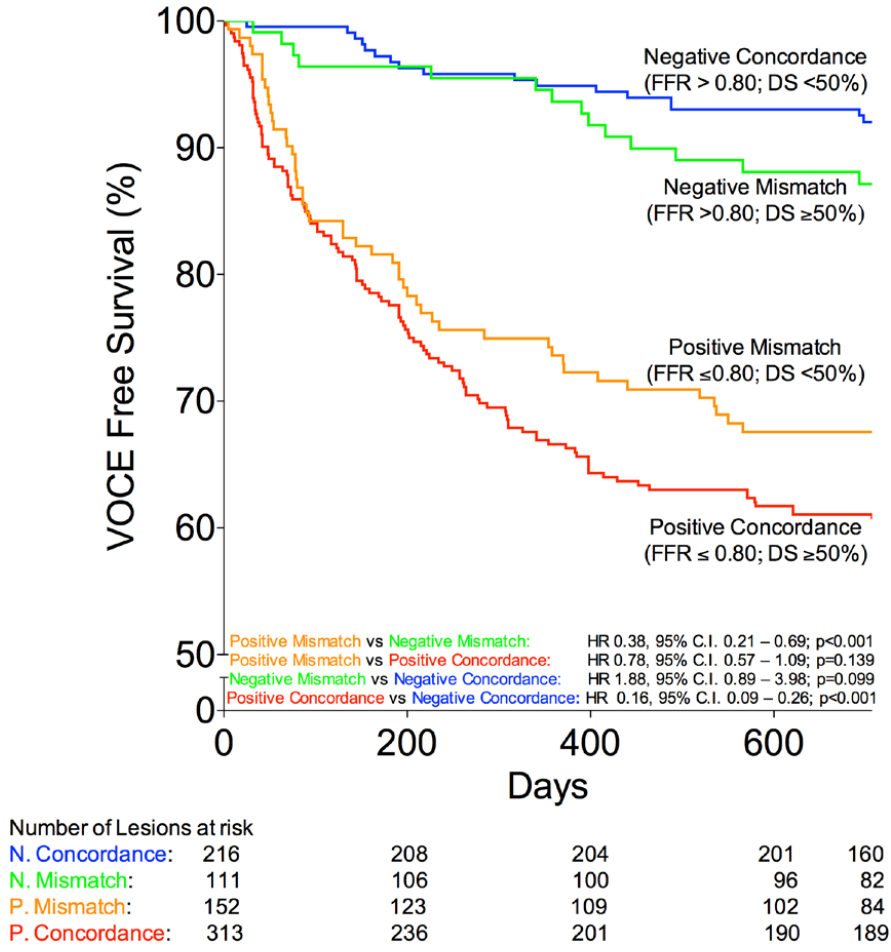

Figure 11: Kaplan–Meier survival curve of 4 groups according to the values of fractional flow reserve (FFR) and percent diameter stenosis (DS). CI indicates confidence interval; HR, hazard ratio; and VOCE, vessel-oriented clinical end point. Red, positive concordance (FFR≤0.80; DS≥50%); blue, negative concordance (FFR>0.80; DS<50%); orange, positive mismatch (FFR≤0.80; DS<50%); and green, negative mismatch (FFR>0.80; DS ≥50%).

When the angiographic cutoff was set at 70% DS, the outcome results did not change. The rate of VOCE over time was significantly larger when lesions have a DS ≥50% or when lesions have an FFR ≤0.80, but the difference between the event curves was markedly larger for FFR than for DS (Figure 12). At the univariable analysis of predictors of VOCE the global

SYNTAX score was not found to be a significant predictor for vessel-related outcome. Moreover at the multivariable analysis FFR ≤0.80 was associated with a 4.16-fold increase in the hazard of VOCE and DS ≥50% with a 1.36-fold increase. After introduction of an interaction term, FFR ≤0.80 was associated with a 7.28- fold increase in the hazard of VOCE during the first 90 days and a 3.29-fold increase in the hazard of VOCE occurring >90 days.

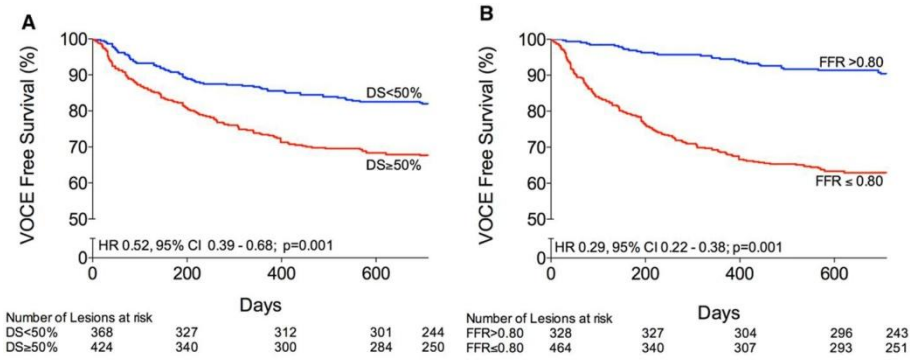

Figure 12: Kaplan–Meier survival according to the values of percent diameter stenosis (DS) and fractional flow reserve (FFR). CI indicates confidence interval; HR, hazard ratio; N, number of events; and VOCE, vessel-oriented clinical end point.

Conclusion: From this side-by-side comparison of DS and FFR to lesion-related outcome, it appears that the main determinant of the natural history of a lesion is its hemodynamic significance rather than its angiographic appearance. DS is the cornerstone of the definition of CAD. Because clinical outcome is the ultimate validation test for any new treatment or metrics, the present findings suggest that FFR should replace the 50% DS criteria for the definition of obstructive CAD.

CHAPTER 10

Coronary lesion progression as assessed by fractional flow reserve (FFR) and angiography

Background: Intermediate coronary stenoses are prevalent in patients undergoing coronary angiography and are defined as a 30-70% luminal narrowing. Nevertheless, a heterogeneity exists in the definition of clinically significant coronary stenosis depending on diagnostic tool or location. This scatter in defining the significance of stenoses is attributed to the limited ability of anatomic tools to predict the functional impact of the lesions. Accordingly, guidelines recommend deferring revascularization with FFR > 0.80, irrespective of location and angiographic appearance due to the very low event rates. This "watchful waiting" approach begs the question of how intermediate, non-revascularized lesions evolve over time, both anatomically and functionally. To date, there is an abundance of data regarding the anatomic progression of coronary lesions that has shaped our understanding of their natural history. Yet, no data exist regarding the longitudinal functional progression of the coronary stenoses assessed by FFR.

Aim: To explore the evolution of coronary lesions that had repeated physiologic evaluation by FFR as an endpoint, describe the clinical significance of longitudinal FFR change ($\Delta FFR = FFR_{follow\text{-}up} - FFR_{baseline}$), its correlation with angiographic indices and identify predictors of $FFR_{follow\text{-}up}$.

Methods and results: A retrospective, single-center analysis of 414 stenoses (331 patients) with consecutive FFR measurements at least six months apart was performed [median time interval: 24 (17, 37) months]. The change in percent diameter stenosis was 2% (-5%, 11%). FFR values at baseline and follow-up were 0.86 (0.82, 0.90) and 0.83 (0.79, 0.90) respectively (<0.0001). The median ΔFFR was -0.007 (-0.028, 0.010) per year. A significant linear correlation of $FFR_{follow\text{-}up}$ with $FFR_{baseline}$ was noted (ρ= 0.550, P<0.0001); this was also the case on a per vessel analysis (Figure 13).

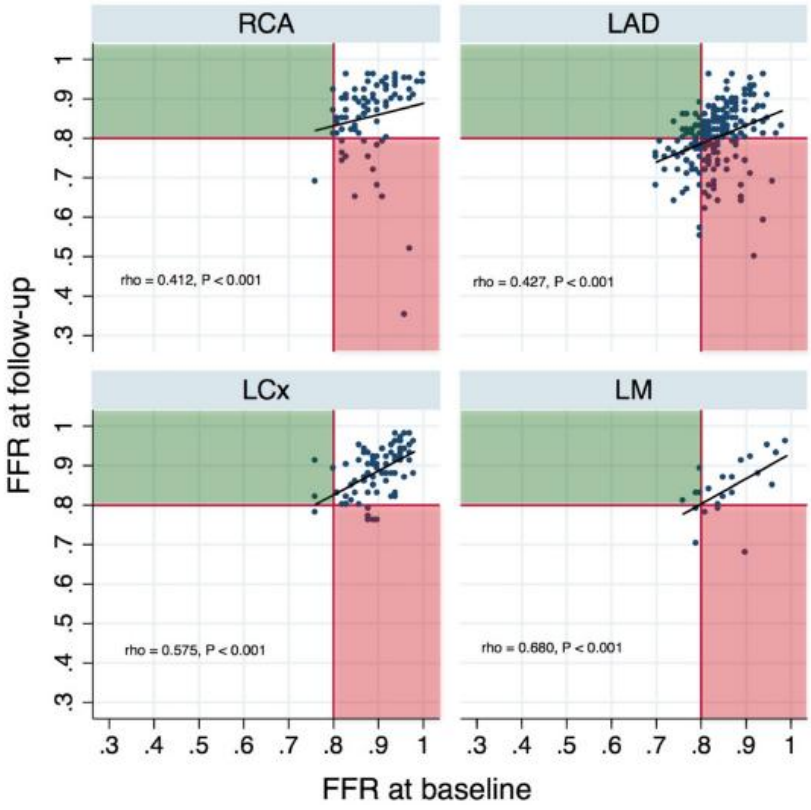

Figure 13: Scatterplot and correlations of FFR values at baseline and follow-up on a per vessel basis. The black line depict the 0.80 FFR threshold below which a lesion is clinically significant and should be revascularized. The red area includes lesions that were non-

ischemic at baseline and became ischemic at follow-up (FFR deterioration); the opposite is true for lesions in the green area (FFR improvement). Non-parametric Sperarman's ρ correlation coefficients are presented. FFR= fractional flow reserve.

Similar results were noted for DS% and MLD, while lower values at follow-up (P<0.0001 for both the Wilcoxon matched-pairs test and the mixed effects repeated measures model), while RD remained unchanged. Rates of change for %DS was 1 (-2, 5) % and for MLD –0.012 (-0.175, 0.080) mm/year. Worsening FFR (ΔFFR <-0.05) was observed in 105 (25%) stenoses, stable FFR (-0.05≤ΔFFR≤0.05) in 276 (67%) and improving FFR (ΔFFR>0.05) in 33 (8%) stenoses. The number of hemodynamically significant stenoses (FFR≤0.80) was higher at follow-up compared to baseline (33% versus 17%, P<0.0001); ΔFFR correlated weakly with delta diameter stenosis (Δ%DS, ρ=-0.111, P=0.024). FFR baseline and PCI between measurements at a non-index segment were independent predictors of FFR follow-up (R^2=0.2301). In ROC analysis, FFR baseline values predicted future clinically significant values [c-statistic: 0.736 (95% CI: 0.682 – 0.783)].

Conclusions: The findings of our study point to a slow progression rate for coronary atherosclerotic lesions, as evaluated by both angiography and FFR. Longitudinal data regarding FFR evolution are presented for the first time, with only 1 out of 4 lesions having a significant FFR worsening over a two-year period. $FFR_{baseline}$, but not angiographic indices, is an independent predictor of longitudinal functional atherosclerosis progression, predicting which lesions will require revascularization. This finding can be clinically useful in the context of forgoing repeat angiographies for patients with persistent symptoms and high baseline FFR.

Part III

Fractional flow reserve in special clinical settings

CHAPTER 11

Detect fractIonal flow reServe of Epicardial steNosis with Guiding cAtheter disenGagEment: DISENGAGE registry

Background: The application of FFR in daily practice as well as for research purposes has been standardized in order to avoid technical or operator-related artifacts in pressure recordings and interpretation. However the impact of guiding catheter (GC) at the level of the coronary ostium during FFR measurements of intermediate coronary stenoses has been poorly investigated up to date. The mere presence of a GC in the coronary ostium induces some degree of stenosis, which depends on the relative size of the GC and the coronary ostium. This results into a not fully hyperemic flow across the ostium, with an artificial decrease of the mean aortic pressure (P_a) and a final overestimation of FFR value (Figure 14).

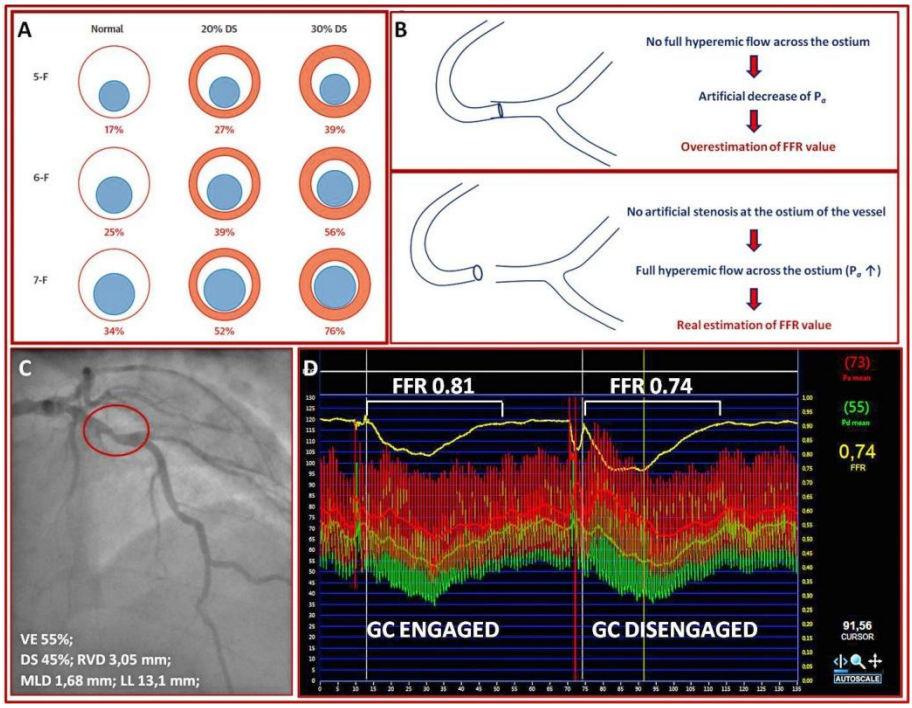

Figure 14: A) impact of different size of GCs on the relative diameter of the coronary ostium, with and without stenosis; B) mechanism of artificial decrease of the mean aortic pressure (P_a) and a final overestimation of FFR value; C) Angiographic example of intermediate stenosis and D) the corresponding FFR measurements with GC ingaged and GC disengaged. GC= guiding catheter; FFR= fractional flow reserve; VE= visual estimation; DS= diameter stenosis; RVD= reference vessel diameter; MLD= minimal lumen diameter; LL= lesion length.

Aim: In this prospective registry we aimed at investigate if the Δ $FFR_{engaged}$ – $FFR_{disengaged}$: (1) might be significantly different from the intrinsic variability of repeated FFR measurements; (2) could impact clinical decision making in intermediate coronary stenoses (e.g. changes on the FFR values from above 0.80 to below 0.75 and/or below 0.80). Also we aimed to evaluate if (3) the GC disengagement might have a different impact on stenoses related to a large amount of myocardium as compare to those related to small amount of myocardium.

Methods: Between October 2015 and December 2016, FFR was prospectively measured in 202 intermediate isolated stenosis (DS 46±10%; MLD 1.6±0.4 mm; RVD 3.0±1.6 mm; LL 15±8 mm) of 173 patients with stable angina (93%), silent ischemia (5%), and acute coronary syndrome (ACS) (2%, in non-culprit lesion). Stenoses were located on left anterior descending artery (n=124), diagonal branch (n=3), left circumflex artery (n=28), obtuse marginal branch (n=14), intermediate branch (n=5) and right coronary artery (n=28). Patients with diffuse disease, tandem lesions, left main and aorto-ostial stenosis, and culprit lesions of ST-segment elevation myocardial infarction (STEMI) and non-ST segment elevation myocardial infarction (NSTEMI) were excluded. FFR were measured with a 0.014-inch pressure guidewire (Pressure Wire Certus, St. Jude Medical, St. Paul, MN, US) with IC adenosine at the dose of 100 µg for the RCA and 200 µg for the LCA. For each stenosis, FFR was measured twice: with the GC engaged ($FFR_{engaged}$) and with the GC disengaged ($FFR_{disengaged}$). To assure the quality of the measurements, the equalization was checked with both GC engaged and disengaged, likewise the position of the wire was filmed to document the stability of the pressure sensor during the manipulation of the GC.

Results: GC disengagement was associated with a slight albeit non-significant decrease in FFR values overall ($FFR_{engaged}$ 0.84 ± 0.08 vs $FFR_{disengaged}$ 0.80 ± 0.08; Δ $FFR_{engaged}$–$FFR_{disengaged}$ 0.04 ± 0.03; p= 0,92), mainly due to an increase of the mean P_a value ($P_{a\ engaged}$ 78.7 ± 13.5 mmHg vs $P_{a\ disengaged}$ 82.9 ± 13.6; p= 0,79) rather than changes in the mean P_d value ($P_{d\ engaged}$ 66.3 ± 13 mmHg vs $P_{d\ disengaged}$ 66.6 ± 13.2 mmHg; p= 0,86) (Figure 15). However in 38 stenoses (22% patients and 19% stenoses) whose FFR values were mostly located in the 0.81-0.85 stratum, GC disengagement was associated with a shift from above to below the clinical-decision making

threshold of 0.80. Also in 50% of the stenoses (102/202) ΔFFR was ≥ 0.04, which correspond to twice the value to be expected from repeated FFR measurements (test-retest repeatability of FFR; cut-off value: 0.02). GC disengagement had a significant impact on FFR measurements of stenoses related to large amount of myocardium($\Delta FFR_{engaged}$–$FFR_{disengaged}$ proximal and mid segments 0.043 ± 0.03 vs $\Delta FFR_{engaged}$–$FFR_{disengaged}$ distal segments 0.029 ± 0.03; p= 0.028) (Figure 16).

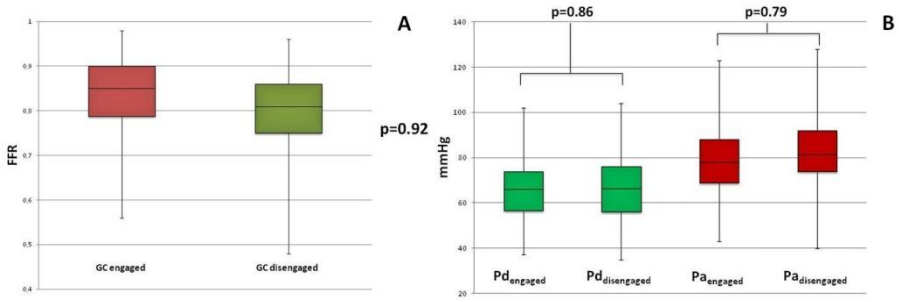

Figure 15: A) Overall FFR values changes after GC disengagement; B) P_d and P_a changes after GC disengagement. GC indicates guiding catheter.

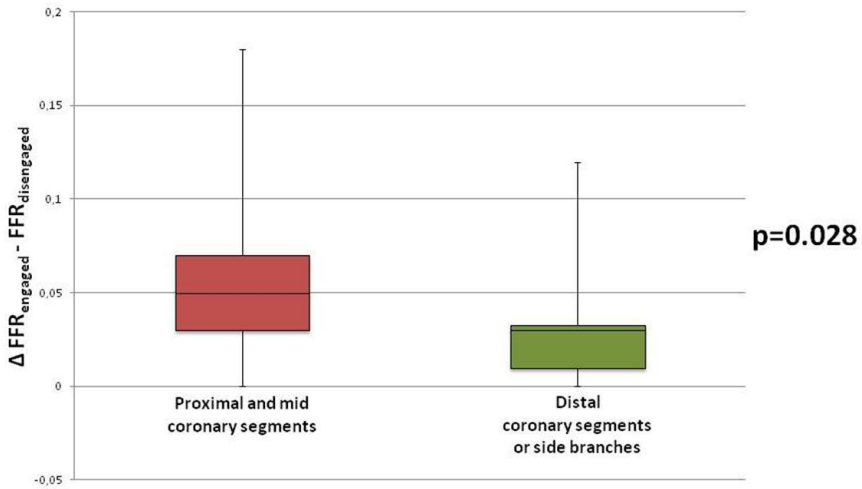

Figure 16: $\Delta FFR_{engaged}$–$FFR_{disengaged}$ of stenoses related to large amount of myocardium (proximal and mid coronary segments) vs. stenoses related to small amount of myocardium (distal coronary segments or side branches).

Conclusions: GC disengagement is associated with a slight albeit non-significant decrease in FFR values overall. Yet, GC disengagement resulted into a shift of FFR values from above to below the clinical-decision making threshold of 0.80 in 1 out of 5 measurements. Therefore it might be advisable to reassess FFR after disengaging the GC in case of FFR values close to 0.80.

CHAPTER 12

Angiographic and hemodynamic modifications of Myocardial Bridge during supine bicycle exercise

Aim: The aim of this study is to evaluate the hemodynamic effect of physiological exercise during coronary angiogram with P_d/P_a, end diastolic P_d/P_a and FFR measurements in symptomatic patients with Myocardial Bridge (MB).

Methods: We included all consecutive patients between July 2014 and November 2016 with symptomatic MB without significant CAD. Coronary angiogram was performed with radial approach and supine bicycle set on the table. A pressure wire was placed downstream the MB. Systolic compression was assessed with QCA. Hemodynamic was continuously recorded during the protocol with P_d/P_a and end diastolic P_d/P_a at rest and during exercise. The exercise protocol did not use nitrates prior to exercise, it started at 50 watts and increased of 15 watts every 2 minutes. After exercise intracoronary nitrates was used and finally IC adenosine administration for FFR measurement. The aim of this study is to evaluate the hemodynamic effect of physiological exercise on angiography, P_d/P_a, end diastolic P_d/P_a and FFR.

Results: 9 symptomatic patients with an isolated MB were included. Patients reached in average 73%±10% of maximum heart rate. No complication occurs during this protocol. Compression during systole significantly increases in peak exercise compare to rest respectively 78%

versus 37% (p=0.003). However P_d/P_a and end diastolic P_d/P_a values did not significantly changed respectively 0.90 at rest versus 0.87 at peak exercise (p=0.21) and 0.85 versus 0.82 (p=0.35). During the protocol no significant difference was observe between rest, peak exercise P_d/P_a and after nitrates (p>0.05 for all). FFR was significantly lower compared to rest, peak exercise and after nitrates (p<0.05 for all). End diastolic P_d/P_a values did not differ significantly except after nitrates and when adding adenosine compared to rest, respectively 0.78±0.05, 0.77±0.05 and 0.85±0.06, p=0.038 and p=0.017). Post exercise FFR was significantly lower compared to rest P_d/P_a. Lowest values were observed with FFR with a significant decrease flow (p=0.02) while it is not the case when using end diastolic P_d/P_a (p=0.20) (Figure 17).

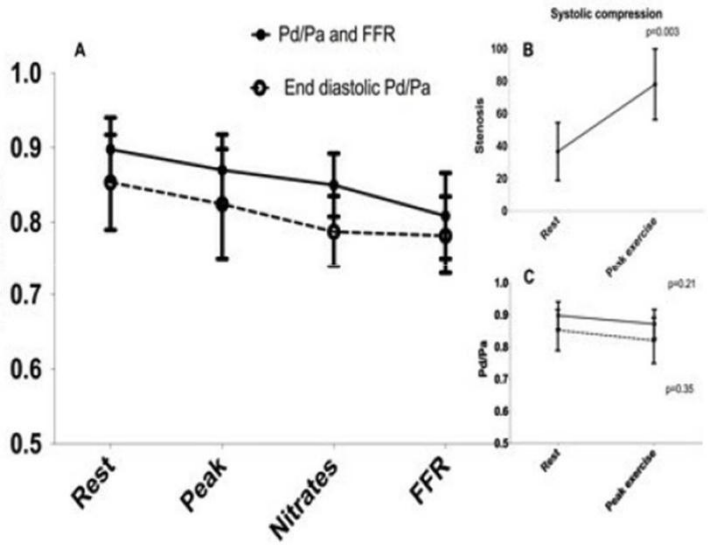

Figure 17: Changes in Pd/Pa, End diastolic Pd/Pa and FFR at rest, peak exercise after nitrates and after IC adenosine administration. FFR= fractional flow reserve; IC= intracoronary.

Conclusions: We reported invasive hemodynamic assessment of MB during physiological exercise conditions with supine bicycle. MB increase systolic compression during exercise with a preserved hemodynamic indices. Invasive hemodynamic evaluation of MB might be better assessed with FFR at rest.

CHAPTER 13

Fractional flow reserve to guide and to assess coronary artery bypass grafting

The aim of this review is to highlight the role of invasive functional evaluation in patients in whom CABG is indicated, and to examine the clinical evidence available in favour of FFR adoption in these patients, outline appropriate use, as well as point out potential pitfalls. FFR *after* CABG will also be reviewed, highlighting its correct interpretation and adoption when applied to both native coronary arteries and bypass grafts (Figure 18). Practice European guidelines support the use of FFR to complement coronary angiography with the highest degree of recommendation (Class IA) for the assessment of coronary stenosis before undertaking myocardial revascularization when previous non-invasive functional evaluation is unavailable or not conclusive. As a result, FFR has been adopted in routine clinical practice to guide clinicians decision as to whether or not perform a revascularization. Of note, due to the increasing confidence of the interventional cardiologists, FFR guidance is also being implemented to indicate or guide CABG. This is in anticipation of supportive clear-cut evidence, since recommendations for FFR adoption were based on randomized clinical trials investigating PCI strategies in which patients with typical indications for CABG were excluded (e.g. left main disease, valvular disease, and coronary anatomy unsuitable for PCI). Based on the critical appraisal of the literature, FFR can play an important role in risk stratification and determining management strategy of patients either

before or after CABG. The available data are mostly observational and seem to support the reliability and prognostic role of FFR in these patients. While waiting for the results of ongoing RCTs, FFR can be used to guide revascularization strategies, taking into account the divergent visions of the cardiac surgeons who aim for once-in-a-lifetime treatment of the patients, and that of the interventional cardiologists who have the option of deferring percutaneous revascularization to a later stage.

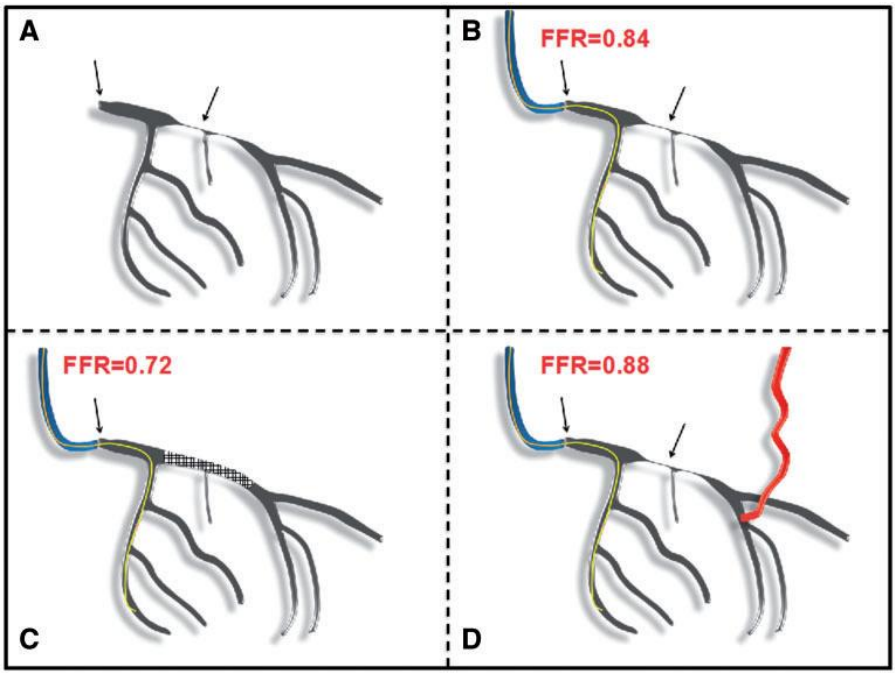

Figure 18: Schematic representation of a left coronary artery with sequential stenosis of the ostial left main (LM) and proximal left anterior descending (LAD) coronary artery (A, arrows). FFR of the LM measured with the pressure wire positioned in the left circumflex artery is 0.84 (B). If the proximal LAD was stented, FFR of the LM would lower to 0.72 as a consequence of the significant increase in the subtended myocardial mass (C). If a bypass graft would be implanted distal to the LAD stenosis, FFR of the LM would either remain the same or slightly increase, as a consequence of the fact that a large part of the left coronary artery territory is now being perfused by another vascular conduit (D). FFR, fractional flow reserve.

Chapter 14

Impact of fractional flow reserve on surgical coronary revascularization strategy

Background: FFR during angiography is associated with hemodynamic reclassification of coronary disease severity with significant impact on revascularization strategies. However, no prospective data exist on the impact of FFR on surgical coronary revascularization strategies.

Methods: GRAFFITI is a single-blinded, open-label, prospective 1:1 randomized controlled multi-center pilot trial comparing FFR-guided versus angiography-guided CABG surgery. Patients with a significantly diseased left anterior descending or left main stem and at least one more major coronary artery with angiographically intermediate stenosis were enrolled in the trial. First surgeons made a pure angiography-guided strategy, then patients were randomized to angiography-guided or to FFR-guided group. FFR was measured in all the intermediate stenoses in both groups, but disclosed to the surgeons only if patients were allotted to the FFR-guided strategy. Patients in the angiography-guided group were operated following the initial angiogram-based strategy. Patients in the FFR-guided group were operated according to the hemodynamic stenosis significance by FFR. In this latter group, surgeons had to detail the intended procedure before and after disclosing the FFR values.

Results: After randomization, 88 patients were included into the FFR-guided group. Among them disclosure of FFR has changed bypass strategy

in 55%. Comparing to initial angiogram-based surgical strategy, disclosing FFR lead to significant reduction in necessity of on-pump surgery (81% vs 69%, p=0.006; Figure 19A) and in total number of bypass grafts per patient (3[2;3] vs. 2[2;3], p=0.018) during the definitive surgical procedure. Of note, the number of procedures with >1 saphenous vein graft (SVG) was significantly reduced after FFR disclosure (43% vs. 31% after FFR disclosure, p=0.031; Figure 19B). Among the 64 vessels for which no revascularization was indicated based on the initial angiogram, 16 (25%) were finally bypassed based due to significant FFR. Among 108 lesions for which SVG implantation was indicated based on the initial angiogram, 25 (23%) were not bypassed after disclosing a preserved FFR value; while among 128 lesions for which arterial graft was indicated, 15 (12%) were eventually not bypassed (Figure 19C). At 1-year follow-up, outcomes were similar between patients with at least 1 change in strategy according to FFR and patient without any change in therapeutic decision.

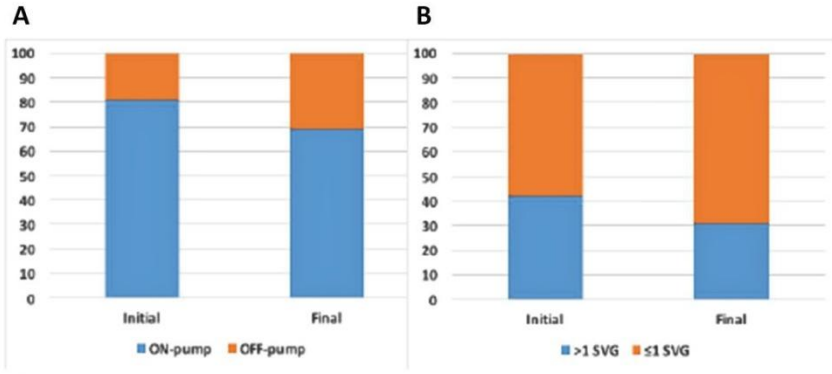

C

	Performed : nothing	Performed : vein	Performed : artery
Planed : nothing	**48**	**13**	**3**
Planed : vein	**25**	**78**	**5**
Planed : artery	**15**	**3**	**110**

Consistency : 236 = 79% ; **Upgrading : 21 = 7% ;** Downgrading : 43 = 14%

Figure 19: A) Changes in bypass strategy (on-pump vs. off-pump) after FFR values disclosure; B) Changes in number of SVGs implantation (>1 SVG vs. ≤1 SVG) after FFR values disclosure; C) Changes in number of SVGs and arterial grafts after the disclosure of preserved FFR values. FFR indicates fractional flow reserve; SVGs indicates saphenous vein grafts.

Conclusions: Change of procedural strategies after FFR assessment occurs in more than half of the cases, significantly simplifying the surgical protocol and without any untoward hazard on 1-year clinical outcome.

Chapter 15

Fractional Flow Reserve-Guided Revascularization in Patients With Aortic Stenosis

Background: FFR-guided revascularization strategies have been shown beneficial in patients with intermediate stenoses and multivessel CAD. The reliability and clinical usefulness of FFR has not been tested in patients with concomitant aortic stenosis (AS). Nevertheless, these are the very patients difficult to investigate with noninvasive functional testing and presenting with associated CAD in up to 50% of the cases.

Aim: We aimed to investigate the impact of FFR measured at the time of the diagnostic coronary angiography on percutaneous and surgical revascularization strategies and its related clinical outcome in patients with AS.

Methods: From 2002 to 2010, we retrospectively identified 106 patients with AS and significant CAD in which at least 1 intermediate lesion was either revascularized with an FFR value ≤ 0.80 or deferred with FFR > 0.8 (FFR-guided group). Then, from 694 contemporary patients in which the decision to revascularize was based on angiography only, we matched 212 as comparator (Angio-guided group).

Inclusion criteria were: presence of at least 1 intermediate stenosis (diameter stenosis: 50-70%) of a major coronary artery at the time of angiography; aortic valve area ≤ 1.5 cm^2 and/or aortic mean pressure gradient ≥ 20 mmHg. Severe AS was defined with a valve area ≤ 1 cm^2

and/or aortic mean pressure gradient ≥ 40 mmHg. All patients underwent left/right sided heart catheterization. Aortic valve area was calculated with the Gorlin formula. PCI and surgical interventions were left to the operator's discretion. CABG and aortic valve replacement (AVR) performed within 6 months from the diagnostic coronary angiography were referred to the index procedure.

Primary end point was the rate of major adverse cardiac events (MACE), defined as overall death, MI, and repeat revascularization up to 5 years. Secondary end points were all the individual end points included in MACE and AVR. Follow-up was obtained through telephone contacts or outpatient visits. Date of death was retrieved from Belgium national death registry. Informed consent to the use of personal data was obtained from each patient.

Results: The 2 groups were well matched with respect to clinical characteristics and AS severity did not differ between the groups. More patients in the FFR-guided group underwent PCI, while there was a trend towards more CABG in the Angio-guided group. Patients treated with PCI had lower AS severity as compared with patients treated with CABG (aortic valve area: 0.95 ± 0.29 vs. 0.76 ± 0.28, p <0.01; aortic mean gradient: 27 ± 15 vs. 41 ± 20; p < 0.01). At baseline angiogram, number of diseased vessels was similar in the 2 groups. After functional assessment with FFR, the number of diseased vessels was significantly downgraded within the FFR-guided group (p<0.01) and when compared to the Angio-guided group (p<0.01). In patients undergoing CABG, number of arterial grafts and anastomoses per patient was similar between the 2 groups, while significantly less venous conduits were used in the FFR-guided group, along

with less venous anastomoses. A trend towards less AVR was observed in the FFR-guided group. Clinical follow-up was available for all patients at a median time of 56 months. We found no difference in MACE up to 5 years, overall death, repeat revascularization and nonfatal MI between the 2 groups. Similar results were found in the subgroup of patients with severe AS. When stratified by initial treatment strategy, MACE rate was still not significantly different among FFR- and Angio-guided groups. Combined CABG and AVR was associated with the best clinical outcome and Medical Therapy with the worst, while intermediate outcomes were reported in patients initially treated with PCI or AVR only (Figure 20). AVR at follow-up was performed in 9% of patients in the FFR-guided group (time to AVR: 31 [22-43] months) vs. 6% in the Angio-guided group (time to AVR: 21 [7-54] months) (p= 0.28). At the latest follow-up available, cumulative AVR rate was still lower in the FFR-guided group (59 [55%] vs. 135 [63%]; p=0.16).

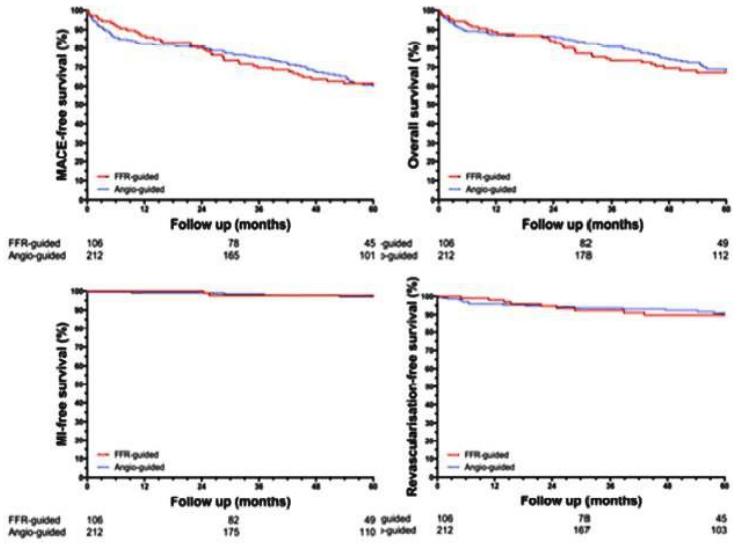

Figure 20: Kaplan-Meier curves for survival free from events in the FFR-guided and Angio-guided groups up to 5 years of follow-up: Survival free from MACE (upper left; p=0.98); Overall survival (upper right; p=0.68); Survival free from MI (lower left; p=0.83); Survival free

from revascularization (lower right; p=0.76). MACE, major adverse cardiac events; MI, myocardial infarction.

Conclusions: FFR guidance impacts the management of selected patients with moderate or severe AS and coronary artery disease by resulting into deferral of aortic valve replacement, more patients treated with PCI, and in patients treated with CABG, into less venous grafts and anastomoses without increasing adverse event rates up to 5 years.

Chapter 16

Clinical Outcome of Patients with Aortic Stenosis and Coronary Artery Disease Not Treated According to Current Recommendations

Background: Degenerative AS is the most common valvular heart disease in the developed countries and is associated with significant CAD in up to 50 % of the cases. When both conditions are present and symptoms occur, current guidelines recommend surgical treatment with combined AVR and CABG. Yet, due to frequent comorbidities in these patients, treatment might diverge from guideline recommendations.

Aim: In our study, we evaluated the real-world adoption of guideline recommendations in patients with combined moderate or severe aortic stenosis and significant coronary artery disease and assessed the impact of incomplete treatment strategies (i.e., diverging from classic AVR plus CABG) on the long-term clinical outcome.

Methods and results: From 2002 to 2010, we assessed death up to 5 years in 650 patients with moderate/severe aortic stenosis and at least one coronary lesion (>50 %): 23% weretreated conservatively (medical therapy, MT), 17% with percutaneous coronary intervention (PCI), 11% with AVR, and 49% with combined CABG and AVR. Number of vessels treated per patient was higher in the combined CABG and AVR group as compared to the PCI-only group. In the latter, drug-eluting stents (DES) were used in 29

% of the cases. Surgical pump and clamp time was significantly longer in the combined CABG and AVR than in the AVR-only group.

Clinical follow-up was available for all patients at a median time of 58 (21–60)months. Figure 21 shows the survival curves for the four treatment groups.

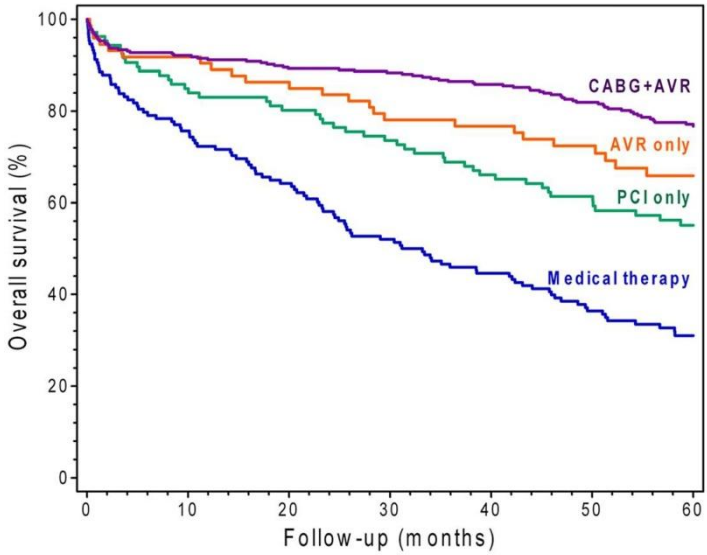

CABG+AVR	320	283	272	193
AVR only	74	63	55	36
PCI only	107	85	70	48
Medical therapy	149	95	66	35

Figure 21: Overall survival in the four groups (log-rank 106.006; p<0.01). CABG: coronary artery bypass graft; AVR: aortic valve replacement; PCI: percutaneous coronary intervention.

The adjusted Cox regression analysis confirmed the beneficial effect in terms of mortality of the CABG and AVR, AVR-only, and PCI-only group as compared to MT group (p <0.01). Other factors significantly associated with overall death were logistic EuroSCORE, atrial fibrillation, hyperlipidemia, and peripheral vascular disease. Direct comparison between PCI-only and AVR-only groups showed a trend toward better survival in the AVR-only

group (HR [95 % CI] 1.37 [0.85–2.2], p=0.19). As to the secondary endpoints, both AVR and revascularization at follow-up were significantly more frequent in the PCI group, followed by MT, with few or no events in the surgical groups. The time to AVR at follow-up was longer in the MT as compared to the PCI group (22 [19–37] vs. 11 [7–29]months, p=0.02). Kaplan-Meier curves showed improved survival in the MT group when AVR at follow-up was performed (p < 0.01), while a strong trend was observed in the PCI group (p=0.054) (Figure 22). At the adjusted Cox regression analysis corrected for confounders, AVR at follow-up confirmed its protective value in the MT group (HR [95 % CI] 0.39 [0.16–0.96], p=0.04), but not in the PCI group (HR [95 % CI] 0.65 [0.27–1.55], p=0.33). When patients with AVR at follow-up were excluded from the analysis, survival was still significantly higher in the PCI group (p <0.01) as compared with the MT group (Figure 23), even after adjusting for confounders in the Cox regression analysis (HR [95 % CI] 0.62 [0.41–0.94], p=0.024).

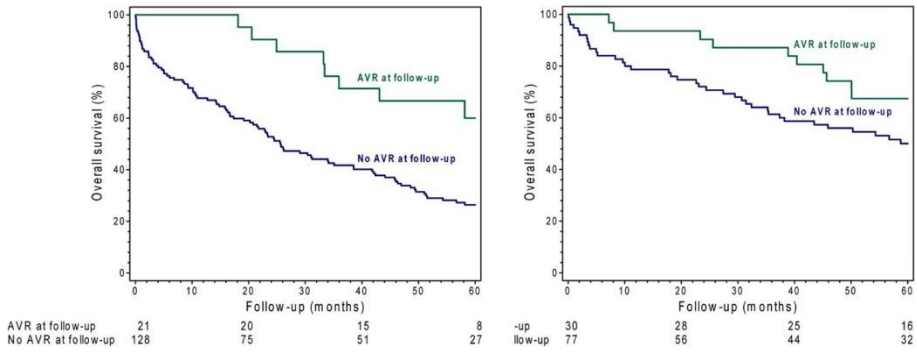

Figure 22: Impact of AVR performed at the follow-up on overall survival in the medical therapy (MT) group (log-rank 9.222; p < 0.01; on the *left*) and in the PCI group (log-rank 3.725; p=0.054; on the *right*).

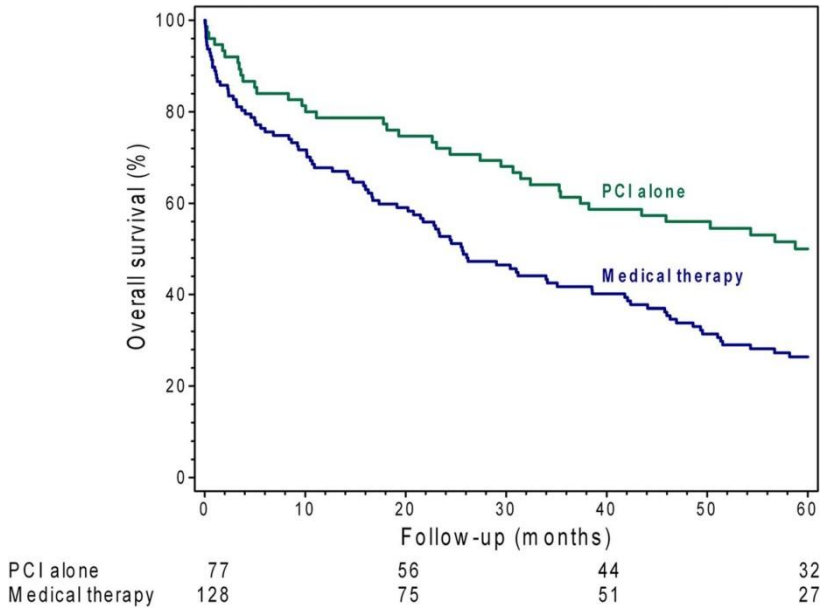

Figure 23: Overall survival in the medical therapy and PCI-alone groups after excluding patients undergoing AVR at the follow-up (log-rank 11.324; p<0.01).

Conclusions: In this real-world experience, only half of the symptomatic patients with moderate or severe AS and CAD initially underwent combined CABG and AVR as recommended by the guidelines. Our results confirm that this treatment strategy is associated with the best outcome at 5 years. Nevertheless, in patients in whom combined CABG and AVR was not performed, either PCI or AVR significantly improve survival at 5 years as compared to medical therapy. These findings might have important clinical implications especially in frail patients excluded even from TAVR but who might benefit from a percutaneous revascularization strategy.

Chapter 17

Impact of Right Atrial Pressure on Fractional Flow Reserve Measurements: Comparison of Fractional Flow Reserve and Myocardial Fractional Flow Reserve in 1,600 Coronary Stenoses

Background: FFR is defined as the ratio of maximal blood flow in the stenotic coronary artery to the maximal blood flow if the same artery were normal. Accordingly, FFR expresses to what extent a given stenosis limits the maximal achievable myocardial flow, and, as a corollary, to what extent myocardial flow can be improved by revascularization of the epicardial segment. This ratio of 2 flows can be derived from the ratio of their respective driving pressures during maximal hyperemia. In fact, the concept of FFR enables the assessment of the separate contribution of maximum coronary and collateral blood flow to myocardial blood flow, all expressed as a ratio to their normal values. The latter is called then myocardial FFR (FFR_{myo}), and for its calculation theoretically right atrial pressure should be included. Because in the majority of patients with coronary artery disease right atrial pressure is low, the latter is neglected in the calculation of FFR. Yet whether FFR measurement is still reliable across a wide range of hemodynamic conditions, such as in patients with heart failure, is not clear.

Aim: This study sought to assess the impact of a wide range of mean right atrial pressure (P_{ra}) on FFR measurements.

Methods and results: In 1,676 stenoses of 1,235 patients undergoing left-right heart catheterization for ischemic (642 [52%]) or valvular heart disease (593 [48%]), we compared the FFR values calculated without accounting for P_{ra} ($FFR=P_d/P_a$) to the corresponding myocardial fractional flow reserve (FFR_{myo}) values accounting for Pra ($FFR_{myo}= P_d - P_{ra}/P_a - P_{ra}$). The FFR and FFR_{myo} were measured and calculated for every coronary stenosis in the range between 30% and 90% diameter stenosis by visual estimate.

The average FFR value was 0.85 (interquartile range [IQR]: 0.78 to 0.91), and the average FFR_{myo} was 0.83 (IQR: 0.76 to 0.90). Correlation and agreement between the 2 parameters were excellent (r^2= 0.987; slope 1.096±0.003). The median difference between FFR and FFR_{myo} was 0.01 (IQR: 0.01 to 0.02) (Figure 24). In patients, with normal right atrial pressure (P_{ra}≤5 mmHg), the median difference between FFR and FFR_{myo} was minimal: 0.01 (IQR: 0.00 to 0.01). When grouping the patients into tertiles of P_{ra}, a statistically significant increase was observed in the difference between FFR and FFR_{myo} over the 3 groups: 0.01 (IQR: 0.00 to 0.01) versus 0.01 (IQR: 0.01 to 0.02) versus 0.02 (IQR: 0.01 to 0.03), respectively; p<0.001 (Figure 25).

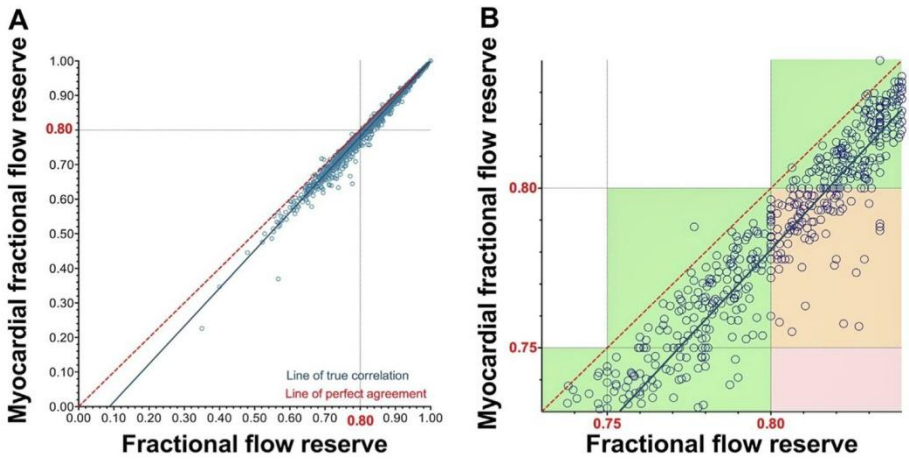

Figure 24: (A) The correlation and agreement between fractional flow reserve (FFR) and myocardial fractional flow reserve (FFR_{myo}) in the overall population. Note that there is minimal deviation between FFR and FFR_{myo} at the lower third of the entire range of FFR 0 to 1. (B) Despite the deviation between FFR and FFR_{myo}, the vast majority of the measurements have clinical agreement (green areas), a minor portion of FFR above 0.80 yields an FFR_{myo} ≤0.80 (orange area), and no FFR above 0.80 yields an FFR_{myo} ≤0.75 (pink area).

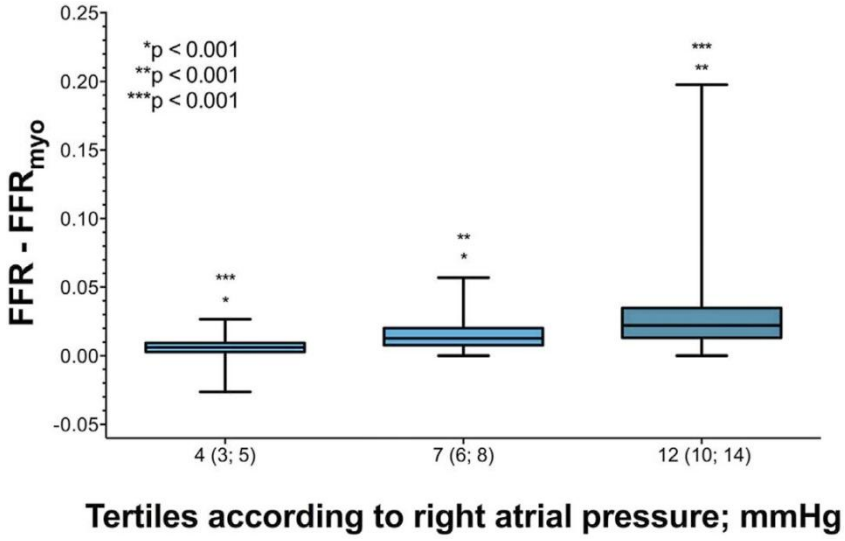

Figure 25: A significant constant increase was observed in the difference between fractional flow reserve (FFR) and myocardial fractional flow reserve (FFR_{myo}) over the tertiles by right atrial pressure. However, even in the highest tertile the mean difference remained clinically minimal.

The median difference between FFR and FFR_{myo} in lesions with FFR above 0.80 was 0.01 (IQR: 0.00 to 0.01). Out of 1,146 stenoses with an FFR >0.80, none had an FFR_{myo} ≤0.75, and 110 (9%) stenoses had an FFR_{myo} ≤0.80. In the latter group, the difference between FFR and FFR_{myo} was 0.02 (IQR: 0.02 to 0.03), yet with a P_{ra} statistically significantly higher than in the overall population (9 mm Hg [IQR: 7 to 12 mm Hg]; p < 0.001). Receiver operator characteristic analysis showed that an 0.80 FFR value has 83% sensitivity and 100% specificity in predicting an FFR_{myo} ≤0.80. Diagnostic accuracy

expressed as area under the curve was 0.913 (95% confidence interval: 0.896 to 0.931). The best cutoff value of FFR for predicting an FFR_{myo} ≤0.80 was found to be 0.82, with 96% sensitivity and 97% specificity. These findings remained unchanged when accounting for multiple lesions for some patients or when selecting at most 1 lesion per patient in a random fashion, justifying the negligible impact of any clustering effect.

We assessed 2 models of possible impact of P_{ra} on FFR measurements based on the available data set. In the first model, FFR_{myo} was calculated for the same patient population by applying 3 fixed values of potential P_{ra}: 5 mmHg, 10 mmHg, and 20 mmHg. A statistically significant increase was observed in the difference between FFR and FFR_{myo} over the 3 values, but it remained remarkably low (0.01 [IQR: 0.01 to 0.01] vs. 0.02 [IQR: 0.01 to 0.03] vs. 0.04 [IQR: 0.03 to 0.07], respectively; $p < 0.001$). In the 5 and 10 mmHg groups, values of FFR >0.80 never yielded an FFR_{myo} ≤0.75; whereas in the 20 mmHg group, this occurred in 4% of the cases. In addition, no FFR values >0.82, >0.83, or >0.87 would have yielded an FFR_{myo} ≤0.80 in the 3 groups, respectively (Figure 26). In the second model, we investigated in the same population what P_{ra} value could have a relevant impact on the following threshold values of FFR: 1) FFR >0.80 and FFR_{myo} ≤0.80; or 2) FFR >0.80 and FFR_{myo} ≤0.75. With a normal P_{ra}, FFR >0.80 never yields an FFR_{myo} ≤0.80 with FFR >0.82. With normal P_{ra} (≤5 mm Hg), FFR >0.80 never yields an FFR_{myo} ≤0.75. The latter might only occur when the FFR is close to the cutoff value of 0.80 or P_{ra} is particularly (even nonphysiological) high.

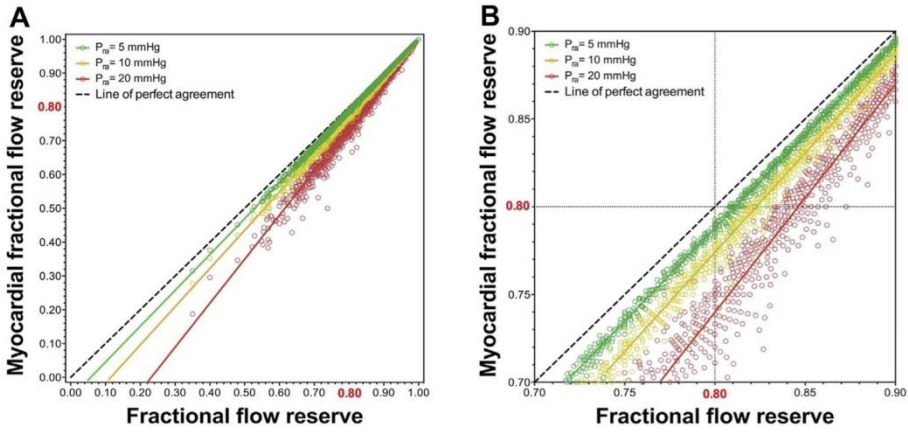

Figure 26: (A) Fractional flow reserve (FFR) and related myocardial fractional flow reserve (FFR_{myo}) values, calculated by applying 3 different potential P_{ra} values: 5, 10, and 20 mm Hg. A statistically significant increase was observed in the deviance from agreement between FFR and FFR_{myo} over the 3 groups. (B) No FFR values >0.82, >0.83, or >0.87 would have yielded an FFR_{myo} ≤0.80 in the 5, 10, or 20 mm Hg groups, respectively.

Conclusions: The difference between FFR and FFR_{myo} was minimal even in patients with markedly increased P_{ra}. FFR values above the gray zone (i.e., >0.80) did not yield values below the gray zone (i.e., ≤0.75) in any case, which suggests that the impact of right atrial pressure on FFR measurement is indeed negligible.

Chapter 18

Fractional flow reserve in patients with non-valvular left ventricular dysfunction

Background: In patients with LVD and CAD the indication for revascularization is controversial. FFR has been associated with improved clinical outcomes in patients with preserved left ventricular systolic function. Moreover, the use of FFR has been recently proven to be reliable in the presence of elevated right filling pressures in our single center experience. Nevertheless, its impact in patients with reduced ejection fraction has never been investigated.

Aim: to evaluated the impact of FFR on: a) reclassification of stenosis significance; b) indication to revascularization; c) revascularization strategy; d) long-term clinical follow-up.

Methods: From 2002 to 2010, we retrospectively identified 433 patients with non-valvular LVD and significant CAD in which at least 1 intermediate lesion was either revascularized with an FFR value ≤ 0.80 or deferred with FFR > 0.8 (FFR-guided group). Then, from 2399 contemporary patients in which the decision to revascularize was based on angiography only, we matched 866 as comparator (Angio-guided group). Inclusion criteria were: presence of at least 1 intermediate stenosis (diameter stenosis: 50-70%) of a major coronary artery at the time of angiography; left ventricular ejection fraction (LVEF) ≤ 50%. Exclusion criteria were: presence of cardiogenic shock at the time of the index procedure; moderate or severe valvular heart disease requiring surgical repair or replacement. The primary endpoint of

this study was the rate of major adverse cardiovascular and cerebrovascular events (MACCE), defined as all-cause death, MI, revascularization and stroke at 1 and 5 years of follow-up. Secondary endpoints were all the individual end points included in the primary endpoint, HF hospitalization and unplanned cardiac admission.

Results: After hemodynamic assessment, the number of stenotic vessels per patient was significantly downgraded within the FFR-guided group (from 2.0 ± 0.84 to 1.4 ± 0.98; p<0.01) and compared with the Angio-guided group (1.4 ± 0.98 vs. 2.02 ± 0.84; p<0.01). This was associated with a significantly lower revascularization rate as compared with the Angio-guided group (52% vs. 61%; p <0.01). PCI was performed more frequently in the FFR-guided group (36% vs. 28% in the angio-guided group; p<0.01); while CABG was more often the therapy of choice in the angio-guided group (32% vs. 16% in the FFR-guided group, p<0.01) (Figure 27).

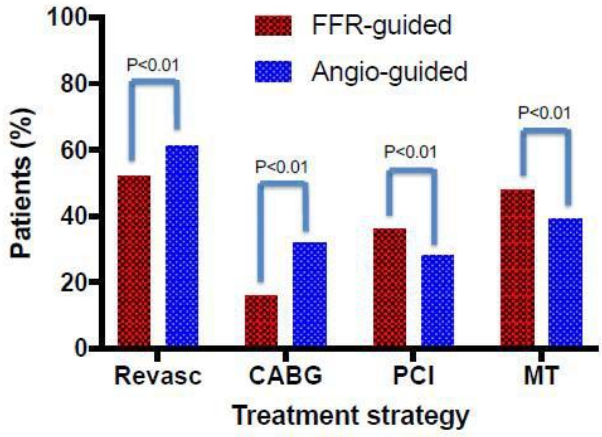

Figure 27: Difference in treatment strategies between the FFR- and the Angio-guided group. Revasc indicates revascularization. CABG, coronary artery bypass grafting; PCI, percutaneous coronary intervention; MT, medical therapy.

In patients undergoing CABG, there was significantly more off-pump (37% vs. 11%; p< 0.01); minimally invasive surgery (7% vs. 1%; p<0.01); lower rate of venous grafts per patient (1.02 ± 0.8 vs. 1.28 ± 0.7; p=0.01) in the FFR-guided group. At 1-year follow-up, we observed a significant lower rate of MACCE, all-cause death and stroke in the FFR-guided group (Figure 28). The difference in MACCE and mortality was confirmed up to 5 years. In both groups patients treated surgically had the worst outcome, with the majority of events occurring early after the index procedure. In patients treated medically, we observed lower MACCE and mortality rates in the FFR-guided group (Figure 29).

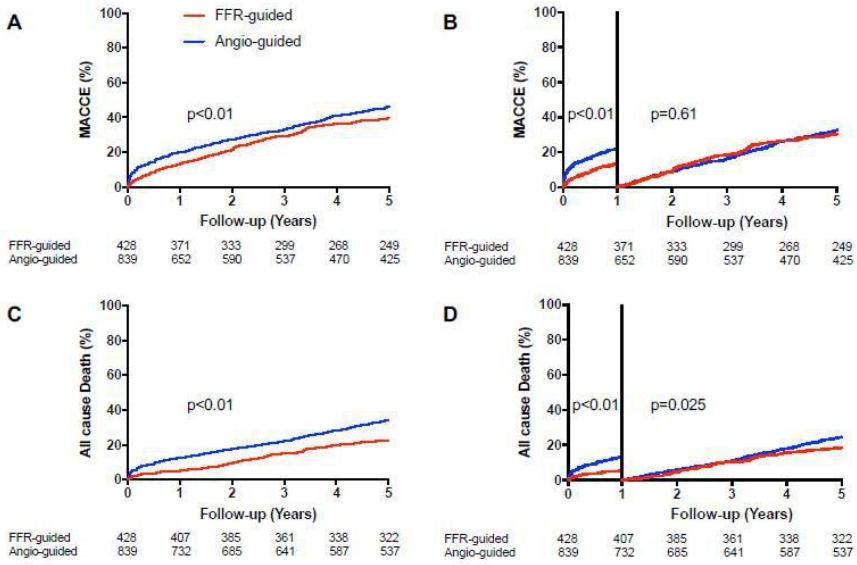

Figure 28: Kaplan–Meier curves reporting the cumulative incidence of major adverse cardiovascular and cerebrovascular events (MACCE) (A) and all cause Death (C); landmark analysis before and after 1-year timepoint for MACCE (B) and all cause Death (D).

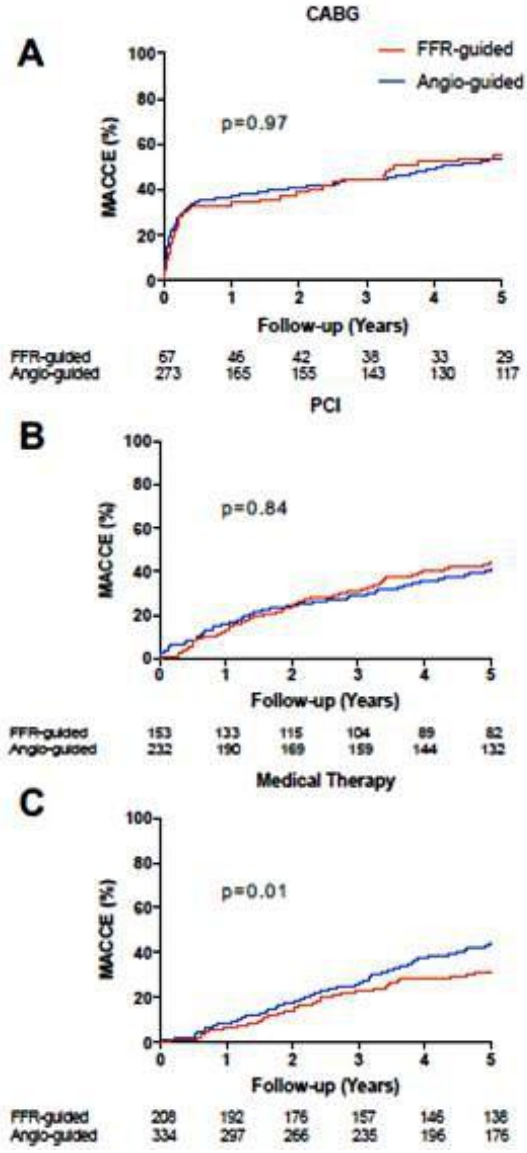

Figure 29: Kaplan–Meier curves reporting the cumulative incidence of major adverse cardiovascular and cerebrovascular events (MACCE) in patients treated with coronary artery bypass grafting (CABG) (A), Percutaneous coronary intervention (PCI) (B) or medical therapy (C).

Conclusions: In patients with non-valvular LVD and CAD, an FFR-guided revascularization strategy is associated with a lower rate of CABG and a higher rate of PCI and medical therapy. At 5-year follow-up, FFR was associated with lower MACCE and mortality rate and safer deferral of patients towards medical therapy as compared with an angio-guided strategy.

Part IV

Angiography-derived FFR technologies

Chapter 19

Diagnostic Accuracy of Fast Computational Approaches to Derive Fractional Flow Reserve From Diagnostic Coronary Angiography: The International Multicenter FAVOR Pilot Study

Background: numerous studies have documented favorable clinical outcomes for FFR-guided coronary interventions in patients with stable CAD. Despite the clear advantages and the Class I recommendations by the European Society of Cardiology Guidelines, the clinical adoption of FFR has been variable and slow. A tool that allows calculating FFR without the use of costly pressure wires and the administration of adenosine could increase the adoption of FFR.

Aim: we performed a prospective multicenter study to compare the diagnostic performance of these QFR computational models as compared with pressure wire-derived FFR.

Methods: The prospective, observational, multicenter FAVOR (Functional Assessment by Various Flow Reconstructions) pilot study investigated offline computation of QFR as compared with conventional pressure wire-based FFR as the standard reference. Exclusion criteria were contraindications to adenosine or adenosine triphosphate administration. Angiographic inclusion criteria were: 1) ≥ 1 lesion with 30% to 80% diameter stenosis by VE; and 2) FFR measurement deemed feasible by the operator. Exclusion criteria were: 1) ostial left main (LM) or ostial RCA lesion; and 2)

prior CABG of the interrogated vessels. The QFR computation was based on the underlying principles: 1) coronary pressure remains constant through normal epicardial coronary arteries; 2) the amount of pressure drop is determined by the stenosis geometry and the flow moving through the stenosis, described by the fluid dynamic equations; 3) the stenosis geometry can be characterized by the deviation of the diseased lumen sizing with respect to the reference sizing, i.e., the healthy lumen as if there was no stenosis, by 3D QCA; and 4) Coronary flow velocity is preserved distally relative to proximal flow velocity, and the mass flow rate in the main coronary arteries decreases with the tapering of the arteries due to the presence of side branches. Hence, the mass flow rate at each location along the interrogated vessel can be determined by the mean flow velocity and the reference sizing from 3D QCA.

The following 3 QFR computations were performed, based on the different mean hyperemic flow velocities:

1. The *fQFR pullback*: a fixed empiric HFV of 0.35 m/s that was derived from previous FFR studies was used for computation, and then a comparison with the pressure wire-based FFR was performed.

2. The *cQFR pullback*: frame count analysis was performed separately on the 2 diagnostic angiographic projections without pharmacologically induced hyperemia, and the modelled HFVs were derived by which the software computed 2 new QFR pullbacks. The analyst chose the QFR pullback based on best image quality (most well-defined contrast-flow) in the frame count analysis as the cQFR pullback to compare with the pressure wire-based FFR.

The computational FFR, denoted as quantitative flow ratio (QFR), can be obtained using 3 different flow models: 1) a fixed empiric hyperemic flow velocity (HFV), derived from previous FFR studies (fixed-flow QFR [fQFR]); 2) modelled HFV derived from coronary angiography without pharmacologically induced hyperemia (contrast-flow QFR [cQFR]), that is, the contrast flow was converted into the virtual hyperemic flow based on data derived from previous studies, and cQFR was computed as if adenosine was actually used; and 3) measured HFV derived from coronary angiography during adenosine-induced maximum hyperemia (adenosine-flow QFR [aQFR]).

3. The *aQFR pullback*: frame count analysis was performed separately on the 2 angiographic projections that were acquired during hyperemia, induced by intravenous administration of adenosine or adenosine triphosphate. The "real" HFVs were derived and the software calculated 2 new QFR pullbacks. The analyst chose the QFR pullback based on best image quality in the frame count analysis as the aQFR pullback to compare with the pressure wire-based FFR.

The QFR value at the position that matched the location of the pressure transducer on the pressure wire was used for comparison with the FFR value measured by the pressure wire. Representative examples of computation of QFR using different flow models are shown in Figure 30.

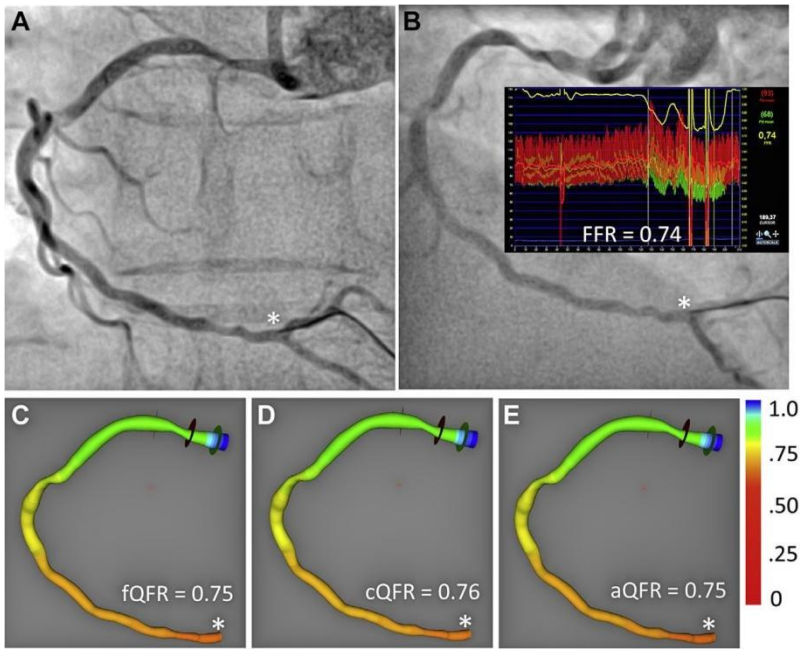

Figure 30: (A, B) Coronary angiography shows RCA with serial stenoses. The FFR measured by pressure wire at * was 0.74. (C) The computed fixed-flow QFR at * was 0.75. (D) The computed contrast-flow QFR was 0.76, and the mean flow velocity calculated on angiographic runs acquired without maximum hyperemia was 0.17 m/s. The modelled hyperemic flow velocity was 0.34 m/s. (E) The computed adenosine-flow QFR at * was 0.75, and the hyperemic flow velocity calculated on angiographic runs acquired during maximum hyperemia was 0.37 m/s. FFR= fractional flow reserve; aQFR= adenosine-flow QFR; cQFR= contrast-flow QFR; fQFR= fixed-flow QFR; QFR= quantitative flow ratio; RCA= right coronary artery.

Results: The QFR and FFR from 84 vessels in 73 patients with intermediate coronary lesions were compared. Mean angiographic DS% was 46.1 ± 8.9%; 27 vessels (32%) had FFR ≤ 0.80. Good agreement with FFR was observed for fQFR, cQFR, and aQFR, with mean differences of 0.003 ± 0.068 (p= 0.66), 0.001 ± 0.059 (p= 0.90), and -0.001 ± 0.065 (p= 0.90), respectively. The overall diagnostic accuracy for identifying an FFR of ≤0.80 was 80% (95% confidence interval [CI]: 71% to 89%), 86% (95% CI: 78% to 93%), and 87% (95% CI: 80% to 94%). The area under the receiver-operating characteristic

curve was higher for cQFR than fQFR (difference: 0.04; 95% CI: 0.01 to 0.08; p< 0.01), but did not differ significantly between cQFR and aQFR (difference: 0.01; 95% CI: -0.04 to 0.06; p= 0.65). Compared with DS%, both cQFR and aQFR increased the area under the receiver-operating characteristic curve by 0.20 (p < 0.01) and 0.19 (p < 0.01) (Figure 31). The positive likelihood ratio was 4.8, 8.4, and 8.9 for fQFR, cQFR, and aQFR, with negative likelihood ratio of 0.4, 0.3, and 0.2, respectively.

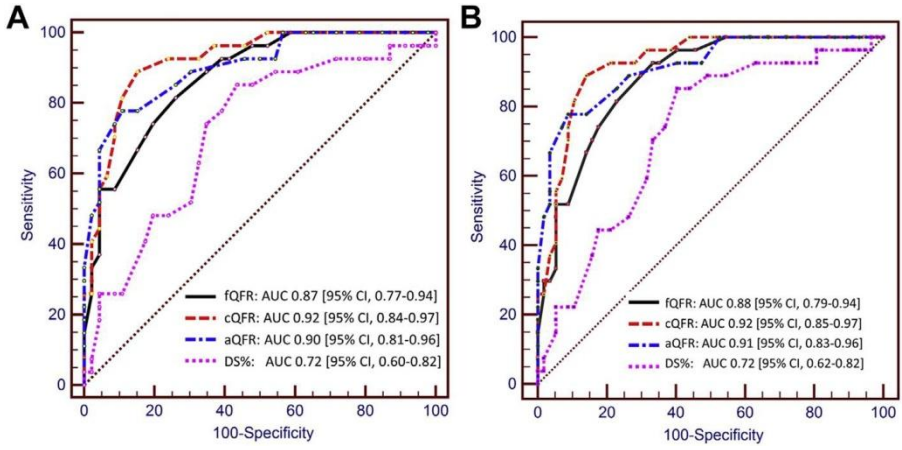

Figure 31: (A) Per patient. (B) Per vessel. The AUC was significantly higher for fQFR, cQFR, and aQFR, as compared with the anatomic parameter DS%. AUC= areas under the receiver-operator characteristics curve; DS%= percent diameter stenosis. Other abbreviations as in 29.

Conclusions: QFR computation improved the diagnostic accuracy of 3-dimensional quantitative coronary angiography-based identification of stenosis significance. The favorable results of cQFR that does not require pharmacologic hyperemia induction bears the potential of a wider adoption of FFR-based lesion assessment through a reduction in procedure time, risk, and costs.

Chapter 20

FFR_{angio}: theoretical basis

FFR_{angio} is a new angiography-derived FFR technology (developed by CathWorks, Ltd) which provides a 3-dimensional (3D) functional angiography mapping of the coronary tree with superimposed, color-coded, FFR values. Stated another way, FFR_{angio} displays a functional angiogram. This computational method is based on a rapid flow analysis after a classification of the dynamic characteristics of the vessels in conjunction with the patient's hemodynamic information, allowing to assess FFR using routine angiograms within a few minutes of automatic processing.

The primary element of FFR_{angio} is the proprietary 3D rebuild of the coronary tree from 2-dimensional (2D) images. This is accomplished automatically by reconstructing the geometry of the tree, including its centerlines and cross-sections at each point along them, as well as the exact topology. The reconstruction is based on the known geometry of ≥3 projections from single-plane angiograms and uses epipolar ray tracing (Figure 32A) together with mathematical constraints enforcing the tree's structure. The system is able to construct each vessel separately such that each region/ branch/lesion is not necessarily reconstructed from the same views, yet at the same time the tree topology is preserved and adheres to that reflected in all of the 2D images. A self-validation step follows whereby the 3D shape of the coronary arteries is projected back onto the 2D images used in its recovery, allowing for this verification loop to be inspected by the user. Finally, the 3D engine contains a compensation mechanism, whereby it uses all available projections at once to compensate for the different x/y/z

displacements apparent in the breathing and patient movements. In addition, panning of the table and C-arm is not recommended during the cine acquisition. Main vessels and side vessels (up to the first or second generation) must preserve the correct connectivity, stemming from the 2D projections (Figures 32B and 32C). Segment-node representation is maintained, whereas uneven motion displacements are compensated for using iterated-closest-point alignment. The coronary tree, represented by position and diameter values for all vessels, can then be surfaced using a triangular mesh and rendered to display a 3D coronary model (Figure 32D).

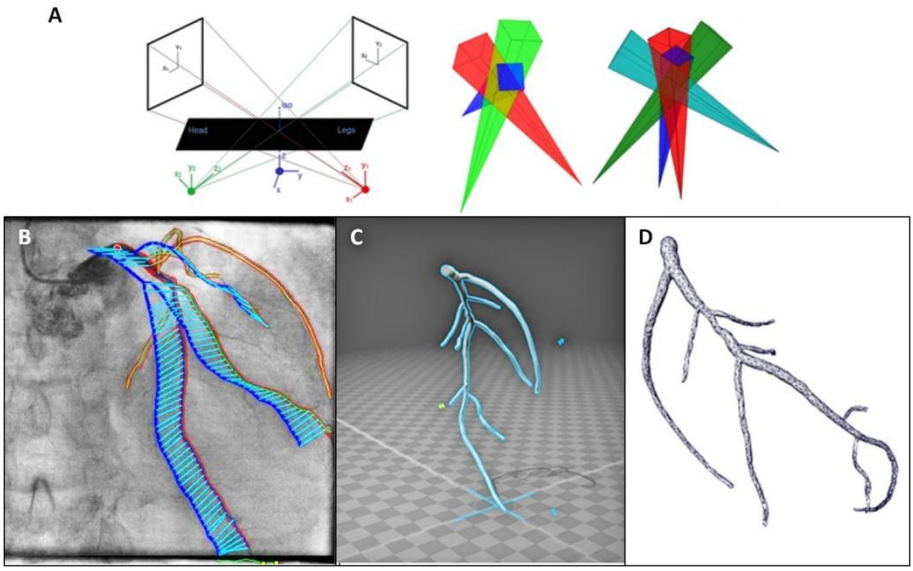

Figure 32: A) epipolar ray tracing; B) connectivity stemming from the 2D projections; C) 3D coronary model; D) triangular mesh.

Next, the system scans the entire reconstructed tree in 3D and analyzes each branch and each bifurcation (or trifurcation), looking for narrowed regions. Diameter stenosis is clinically defined as the proportion between the actual diameter of the measured vessel versus that of the healthy

vessel. An automatic stenosis analyzer, therefore, requires 3 components critical to the proper evaluation of the extent of the lesion. Because stenoses vary in length, location, and spread, it is necessary to look at each vessel at different scales. The first is at the segment level, where a segment is defined as the portion of a vessel that connects 2 junctions. The second scale is the branch level, looking at the entire vessel as a whole. Finally, as a third scale, the junction level is where a parent branch bifurcates (or trifurcates) into secondary or tertiary branches. At each level, a tailored process starts with an accurate detection of vessel walls, followed by determination of the reference diameter. It then evaluates the magnitude of flow resistance because each narrowing is added to the tree. A hemodynamic evaluation follows, where the contribution of each narrowing to the total resistance to flow is taken into account, and a subsequent lumped model is built. The contribution to the control of flow of certain vessels depends on their impact on overall resistance. The resistance of a vessel can be readily estimated from its length and diameter, applying Poiseuille law, and neglecting entrance effects and peculiarities of rheology. Applying various models to infer resistance, based on Poiseuille forces, Bernoulli forces, and the resistance model described in the study by Kirkeeide, all yield equivalent accuracies of the FFR_{angio} values.

The extent of the model is such that it includes a stenosis and spreads distally as far as the resolution of the imaging modality allows. The number of bifurcations is limited by the resolution to which vascular width can be determined from the images (>0.5 mm), and the availability of a larger number of measurable bifurcations is a potential advantage for a more complete reconstruction of the detailed vascular resistance. The accumulated volume of the coronary vessels and total coronary length,

calculated from a reconstruction of its geometry, enables an estimation of normal supply derived from the microcirculatory bed resistance.

The solution of the lumped model based on the inlet and outlet boundary conditions allows to evaluate ratios of flow rate for stenosed versus healthy coronary trees. A color-mapped mesh is then generated and displays the FFR values at every location, as long as thevessel diameter is not limited by image resolution.

Chapter 21

Fractional Flow Reserve Derived From Routine Coronary Angiograms

Background: Pressure wire-based FFR has become the standard of reference for decision making regarding coronary revascularization. Deriving FFR from routine angiograms could facilitate the uptake of FFR-based clinical decisions. Several angiography-derived FFR methods have recently been introduced. These methods are based on computational fluid dynamic simulations. FFR_{angio} is a novel technology providing a functional angiography mapping of the coronaries in 3D based on a rapid flow analysis of a dynamically derived lumped model that can assess FFR using routine angiograms and hemodynamic data.

Aim: to evaluate in an off-line analysis the diagnostic accuracy of FFR_{angio} compared with invasive FFR.

Methods: theoretical aspects of the FFR_{angio} have been extensively described in chapter 20. Eighty-eight patients with stable angina were included in this first in man study. FFR measurements were performed for clinical reasons in ≥ 1 coronary artery. Patients with left main stenoses, ostial stenosis, in-stent restenosis at the target vessel, and previous bypass surgery were excluded (7.7%). At least 2 angiographic projections of the vessel to be measured were acquired at 15 frames/s. The exact inclination of the radiographic tube was left to the operator's discretion. Care was taken to fill the artery as completely as possible with contrast medium and

to image the entire coronary tree at each view. The FFR_{angio} computations were performed offline from Digital Imaging and Communications in Medicine (DICOM) format files by operators not present in the catheterization laboratory and blinded to the invasive FFR results. Each series of DICOM cine sequences was loaded and processed along with the patient's mean aortic pressure obtained at the time the angiogram was acquired. Invasive FFR measurements were performed in duplicate with 6-F GCs, a pressure monitoring wire, and intracoronary adenosine (100– 200 μg). Care was taken to document the exact anatomical position of the sensor. To test interobserver variability and the possible influence of human factors on the results of FFR_{angio}, 2 independent operators analyzed all angiograms.

Results: A total of 101 lesions were analyzed, 30% of which had FFR values between 0.70 and 0.90. FFR_{angio} was calculated and compared to invasive FFR measurements at the exact location of the sensor (Figure 33A). A high degree of concordance was found between 2 measurements of FFR_{angio} performed by 2 different operators (interclass correlation coefficient of 0.97; $p < 0.001$). Figure 33B shows linear regression analyses for the 2 independent observers. We found that invasive FFR was a robust predictor of FFR_{angio}, with 86.8% of the variability of FFR_{angio} explained by the invasive FFR values; the β coefficient of invasive FFR was 0.855 (95% confidence interval [CI]: 0.789 to 0.922) and the intercept was 0.124 (95% CI: 0.068 to 0.179). The estimated bias was 0.004 ± 0.042 and did not differ significantly from zero. The 95% limits of agreement were -0.1 to 0.1. We used 0.8 as the cutoff value for FFR_{angio}, and found that the sensitivity, specificity, and diagnostic accuracy were 88%, 98%, and 94%, respectively.

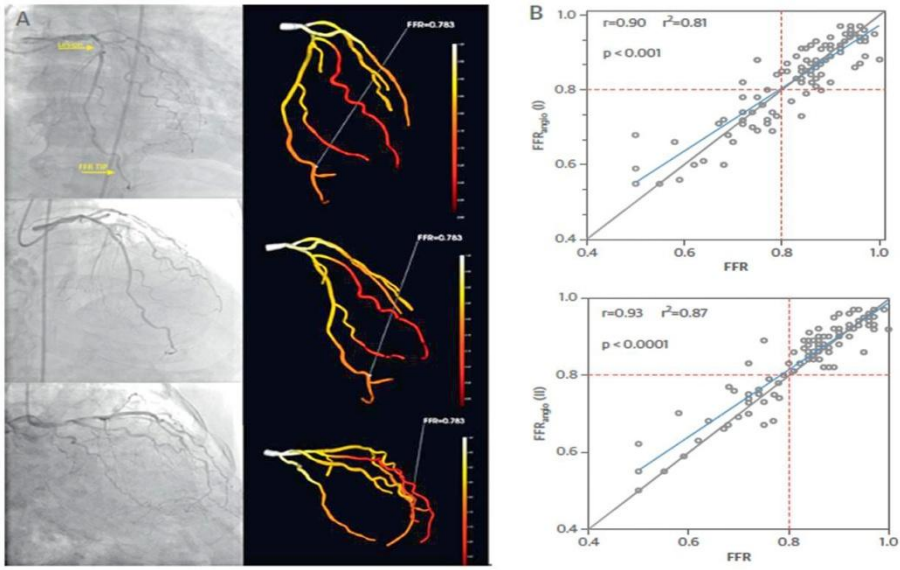

Figure 33: A case demonstrating a significant lesion in the left coronary tree (A). Correlation between invasive FFR and FFR_{angio} is represented by 2 different operators (B). FFR= fractional flow reserve; FFR_{angio}= angiography-derived FFR.

Conclusions: This first-in-human study indicated high reproducibility and diagnostic accuracy of FFR_{angio} compared with invasive FFR. The data were obtained in patients with characteristics encountered in most PCI trials and included relatively well-delineated lesions associated with a large range of FFR values. If the short turnaround time needed to obtain the FFR_{angio} value and the diagnostic accuracy are confirmed in larger studies, FFR_{angio} may foster a wider adoption of FFR-based decision making for revascularization in patients with CAD.

Chapter 22

Validation Study of Image-Based Fractional Flow Reserve During Coronary Angiography

Background: FFR is the gold standard for hemodynamic assessment of coronary intermediate stenoses but remains underused because of its invasive nature. Several image-based FFR methodologies exist that are based on computational fluid dynamics simulation. FFR_{angio} uses routine angiograms to generate a complete 3-dimensional coronary tree with color-coded FFR values at any epicardial location, without the need of a pressure wire or hyperemic stimulus or the need of computational fluid dynamics (CFD) simulation.

Aim: to assess the diagnostic performance and interobserver reproducibility of FFR_{angio} in patients with stable coronary artery disease.

Methods: theoretical aspects of the FFR_{angio} was described in chapter 20. Coronary angiography and invasive FFR measurements protocols as well as the offline FFR_{angio} computation were illustrated in chapter 21. To test interobserver variability, and the possible influence of human factors on the results of FFR_{angio}, 2 independent operators analyzed all angiograms. The mean values were compared with the FFR measurements obtained with the invasive pressure wire, at the exact location of the sensor.

Results: A total of 199 patients were enrolled for the study, but analysis was performed only in 184 of them (123 men, 203 stenoses) because of protocol violation in 8 cases (eg, post coronary bypass surgery, aorto-ostial stenosis, and in-stent restenosis lesions) and inadequate quality of the angiogram in 7 patients. Lesions were distributed as follows: 118 in the left anterior descending, 30 in the left circumflex, 39 in right coronary arteries, 5 in intermediate branches, 2 in the diagonal branch, and 9 in the obtuse

marginal branch. Sixty-seven percent of the invasive FFR values were between 0.70 and 0.90, and 35% between 0.75 and 0.85. The average intraclass correlation coefficient for the 2 measurements of FFR_{angio} conducted by 2 different operators blinded to each other and blinded to the results of invasive FFR was 0.962 with a 95% confidence interval from 0.95 to 0.971 (P<0.001; Figure 34). Figure 35 shows the correlation between the mean FFR_{angio} value as the dependent variable and the wire-based FFR as the predictor variable and the corresponding Bland–Altman plots. The estimated bias was 0.007, indicating that FFR_{angio} values do not systematically underestimate or overestimate invasive FFR values. The 95% limits of agreement were −0.096 to 0.112. Visual estimation of the Bland-Altman plot indicates that the differences between the 2 methods, and the scatter around the bias line, are stable as the average increases.

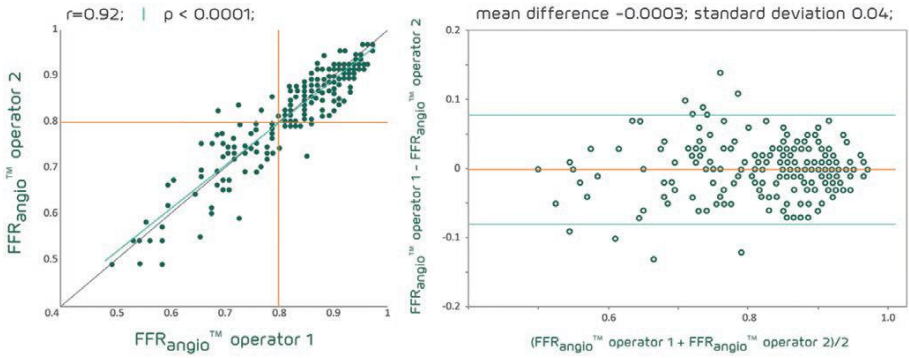

Figure 34: Correlation (scatter plot) of the FFR_{angio} values obtained by 2 blinded operators (*left*), with the corresponding Bland–Altman plot (*right*). The intraclass correlation (consistency of agreement) was found to be 0.962 (95% confidence interval, 0.950–0.971).

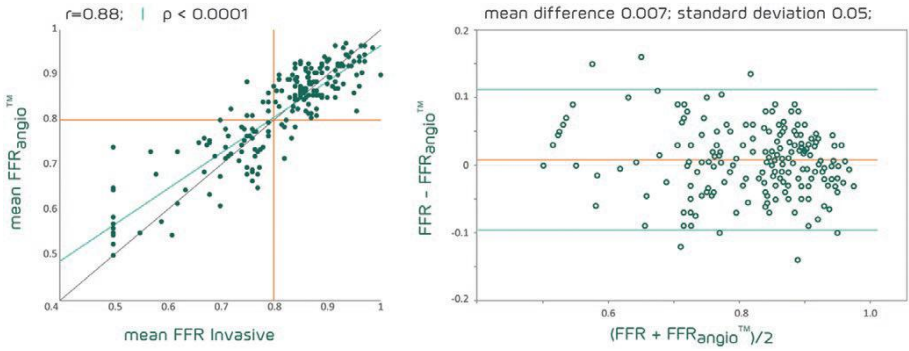

Figure 35: Correlation between invasive fractional flow reserve (FFR) and FFR_{angio} (*left*) and the corresponding Bland–Altman plot (*right*). FFR_{angio} values are the mean of 2 independent analyses performed by different observers. Invasive FFR values are the mean of 2 measurements done by the same operator.

Using 0.8 as a cutoff value for FFR_{angio} and invasive FFR, the sensitivity, specificity, diagnostic accuracy, positive likelihood ratio, and negative likelihood ratio for FFR_{angio} were 88%, 95%, 93%, 22, and 0.12, respectively. Figure 36 shows the plots of invasive FFR values compared with FFR_{angio}, diameter stenosis by visual estimate, and diameter stenosis by quantitative coronary angiography. The corresponding areas under the respective ROC curves are 0.97, 0.57, and 0.61.

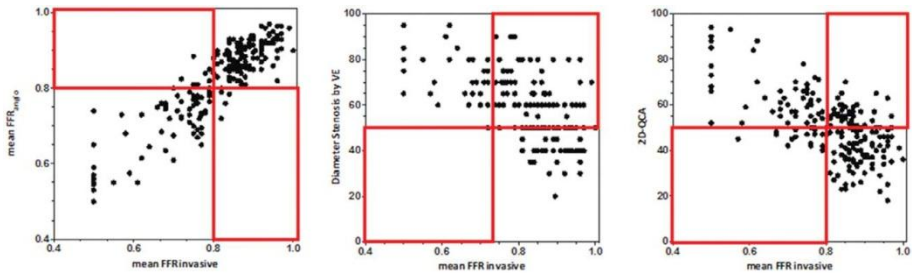

Figure 36: Plots of invasive fractional flow reserve (FFR) values compared with FFR_{angio}, diameter stenosis by visual estimate, and diameter stenosis by quantitative coronary angiography. The red borders indicate the values misclassified by FFR_{angio}, diameter stenosis by visual estimate, and diameter stenosis by quantitative coronary angiography, respectively.

Conclusions: The FFR_{angio} shows a high concordance with invasive FFR and can be obtained within minutes in the setting of a regular coronary angiogram. If confirmed in a larger study, FFR_{angio} appears as an easy means of integrating anatomy and physiology with high spatial resolution in the catheterization laboratory. This, in turn, may facilitate the adoption of FFR-based clinical decision making regarding coronary revascularization.

Part V

Platelet and microvascular function

Chapter 23

Effects of Prasugrel Versus Clopidogrel on Coronary Microvascular Function in Patients Undergoing Elective PCI

Background: Microvascular impairment has been reported in patients on clopidogrel undergoing elective PCI. The related potential mechanisms might include the high residual platelet reactivity (PR) observed in a substantial proportion of these patients pretreated with clopidogrel at the time of PCI. Alternatively, microvascular constriction could occur possibly as consequence of transient endothelial dysfunction related to impaired platelet response to clopidogrel.

Aim: to evaluate whether prasugrel might exert a protective effect on microcirculation during elective PCI in patients with stable CAD scheduled for elective PCI.

Methods: The prospective randomized double-blind controlled PROMICRO-2 (PROtecting MICROcirculation during coronary angioplasty) trial enrolled thienopyridine-naive patients with stable CAD referred to elective PCI of an isolated, functionally significant (FFR <0.80) lesion located in the proximal twothirds of a major coronary artery. Patients were randomized to either prasugrel (60 mg) or clopidogrel (600 mg) at least 12 h before PCI. All patients received a 500-mg loading dose of aspirin the day before the procedure. CFR, IMR, and FFR were measured in each patient before and

after PCI. High-sensitivity troponin T (hs-TnT) was assessed in blood samples before, and 8 and 24 h after PCI.

Results: At baseline, FFR, CFR, and IMR were similar in the 2 study groups. Patients in the prasugrel group showed significantly lower post-PCI IMR values compared with those in the clopidogrel group. Compared with baseline, IMR increased post-PCI in the clopidogrel group (p= 0.009), but not in the prasugrel group (p= 0.299). Repeated measures 2-way analysis of variance (ANOVA) showed a significant interaction between treatment (i.e., prasugrel vs. clopidogrel) and time in determining IMR values (p= 0.047). Consistently, post-PCI CFR was significantly higher in the prasugrel compared with the clopidogrel group. Compared with baseline, CFR remained unchanged post-PCI in the clopidogrel group (p= 0.563), whereas increased in the prasugrel group (p= 0.036). Repeated-measures 2-way ANOVA showed a nonsignificant interaction between treatment (i.e., prasugrel vs. clopidogrel) and time in determining CFR values (p= 0.053). Baseline Hs-TnT was 4.8 (IQR: 3.2 to 10.1) ng/ml in the prasugrel group versus 5.1 (IQR: 3.0 to 12.8) ng/ml in the clopidogrel group (p= 0.845). Post-PCI Hs-TnT was 12.8 (IQR: 7.7 to 23.6) ng/ml in the prasugrel group versus 25.6 (11.8 to 50.6) ng/ml in the clopidogrel group (p= 0.032). Repeated-measures 2-way ANOVA showed a significant interaction between treatmentand time in determining log-transformed Hs-TnT values (p= 0.044). Periprocedural Hs-TnT increase (i.e., difference between baseline and highest post-procedural values) was significantly lower in the prasugrel group compared with the clopidogrel group (6.6 [2.5 to 9.7] ng/ml vs. 15.8 [5.9 to 38.0] ng/ml; p= 0.034).

Conclusions: the results of the PROMICRO-2 trial suggest that more intensive antiplatelet regimens might offer additional benefit compared with clopidogrel also in the setting of elective PCI.

Chapter 24

Platelet Reactivity and Coronary Microvascular Impairment After Percutaneous Revascularization in Stable Patients Receiving Clopidogrel or Prasugrel

Background: Currently recommended antiplatelet therapy for patients with stable CAD undergoing elective PCI is unable to provide effective platelet inhibition in all patients. Despite pretreatment with aspirin and clopidogrel, a large proportion of these patients show high residual PR at the time of PCI. Coronary vessel manipulation especially during complex PCI is an additional trigger for transient increase in PR. Prasugrel provides more potent platelet inhibition than clopidogrel, though it is unknown whether it might also prevent PCI-related platelet activation.

Aim: In stable patients undergoing elective PCI, we compared: (1) the effects of prasugrel vs. clopidogrel on peri-procedural variations of PR; (2) the correlation of platelet inhibition potency with PCI-induced coronary microvascular impairment.

Methods: forty thienopyridine-naive patients were randomly assigned to a loading dose of either prasugrel 60 mg (n=20) or clopidogrel 600 mg (n=20) at least 12 hours before PCI. At the time of PCI, we assessed adenosine diphosphate (ADP)-induced PR with the Multiplate Analyzer, and IMR in the treated coronary, both at baseline and post-procedure.

Results: Patients in the prasugrel group showed significantly lower ADP-induced PR both at baseline (16.0±8.7 vs. 33.9±18.0 AU, $p<0.001$) and post-

PCI (16.2±9.0 vs. 39.0±18.6 AU, p<0.001) as compared with the clopidogrel group. While a significant peri-procedural increase in PR was observed in the clopidogrel group (p=0.008), PR was not significantly different before and after PCI in the prasugrel group (p=0.822) (Figure 37). Repeated measures 2-way ANOVA showed a significant interaction between treatment and time in determining PR values (p=0.022). Periprocedural variation (defined as the difference between after and before PCI) of PR (ΔPR) was 5.1±7.6 AU in the clopidogrel group and 0.3±4.9 in the prasugrel group (p=0.014).

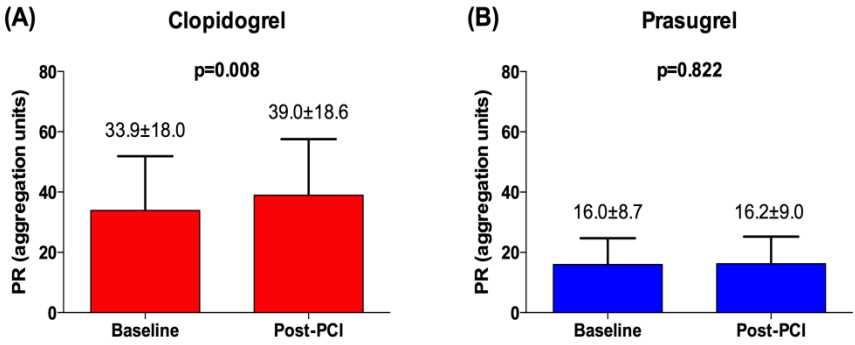

Figure 37: Platelet reactivity. Adenosine diphosphate-induced platelet reactivity (PR) at baseline and post-PCI. Panel A: patients treated with clopidogrel. Panel B: patients treated with prasugrel. Data shown as mean and standard deviation.

A significant correlation was observed between baseline and post-PCI IMR, both in the overall population (r=0.689, p<0.0001) and in the two study groups separately (clopidogrel: r=0.623, p=0.003; prasugrel: r=0.751, p<0.0001). The change between baseline and post-PCI IMR was not significantly different between the two study groups, neither when considering the net numerical difference (6±9 in the clopidogrel group vs. 2±7 in the prasugrel group; p=0.118), nor when considering the percent

difference (38±52% in the clopidogrel group vs. 42±98% in the prasugrel group; p=0.871). Considering the whole study population altogether, a significant correlation was found between IMR and PR both at baseline (r=0.458, p=0.003) and post-PCI (r=0.487, p=0.001) (Figure 38 panel A and B). A total of 24 patients showed a periprocedural increase in PR (15 in the clopidogrel group and 9 in the prasugrel group). In these patients, IMR post-PCI was significantly higher compared with patients who did not show a periprocedural increase in PR (24.6±10.9 vs. 17.3±8.7, p=0.029) (Figure 38, panel C). In patients with periprocedural increase in PR, a significant correlation was found between ΔPR and ΔIMR (r=0.453, p=0.026) (Figure 38, panel D).

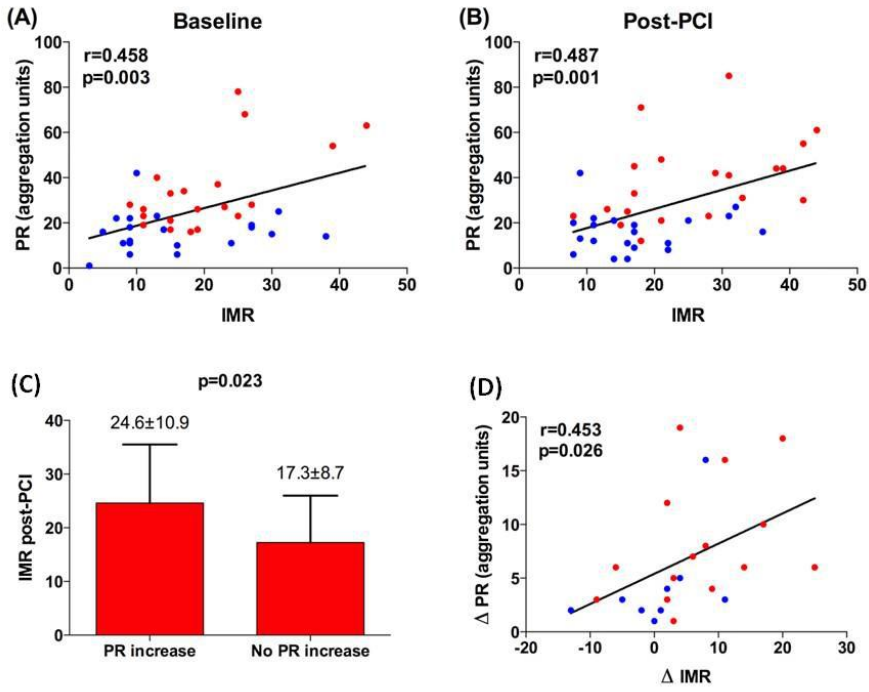

Figure 38: **Microvascular function and platelet reactivity.** Correlation between IMR and adenosine diphosphate-induced PR. Panel A: baseline. Panel B: post- PCI. Red dots indicate

patients in the clopidogrel group; blue dots indicate patients in the prasugrel group. **Periprocedural variations of platelet reactivity and microvascular function.** Panel C: IMR post-PCI in patients with and without periprocedural increase in adenosine diphosphate-induced PR. Data shown as mean and standard deviation. Panel D: correlation between variations of PR (ΔPR) and variations of IMR (ΔIMR) in patients with periprocedural increase in PR. Red dots indicate patients in the clopidogrel group; blue dots indicate patients in the prasugrel group. PCI: percutaneous coronary intervention; IMR: index of microvascular resistance; PR: platelet reactivity;

Conclusions: a loading dose of prasugrel compared with clopidogrel is able to attenuate PCI-related increase in PR in patients with stable CAD undergoing PCI, which might contribute to the beneficial effect of this drug on peri-procedural coronary microvascular function.

Chapter 25

Platelet reactivity in patients carrying the e-NOS G894T polymorphism after a loading dose of aspirin plus clopidogrel

Background: Nitric oxide (NO) plays an important role in the modulation of PR through platelet recruitment, activation and aggregation. G894T single nucleotide polymorphism of eNOS gene results in the substitution of glutamic acid at codon 298 by aspartic acid. This substitution in the protein sequence is responsible of lower enzyme activity, i.e. lower NO production, and it has been associated with coronary spasm, atherosclerosis, MI, and stroke. Whether these adverse clinical events might be partly attributed to the modulation of platelet reactivity exerted by eNOS is still unknown.

Aim: to assess the effect of G894T polymorphism on residual PR and on the risk of PMI in patients with stable CAD undergoing PCI and loaded with aspirin and clopidogrel at least 12 hours before, with a mean value of 8±2 hours.

Methods: A total of 632 patients with stable CAD undergoing elective PCI from October 2009 to December 2010 were retrospectively included. Exclusion criteria were upstream use of glycoprotein IIb/IIIa inhibitors, platelet count <70x10^9 /L, high bleeding risk (active internal bleeding, history of hemorrhagic stroke, intracranial neoplasm, arterial-venous malformation or aneurysm, ischemic stroke in the previous 3 months), surgery in the previous 3 months, and severe renal failure (serum creatinine

>2 mg/dl). All patients received at least 12 hours before PCI a dose of 500 mg of aspirin and 600 mg of clopidogrel. To assess genotype with the TaqMan single nucleotide polymorphism Genotyping Assay (Applied Biosystems) and the platelet reactivity with VerifyNow test (Accumetrics) blood samples were collected from each patient at the moment of arterial puncture before angiography, whereas to evaluate the PMI, defined as an increase in TnT above the 99th percentile of a normal reference population [upper reference limit (URL)], further blood samples were collected at 24 hours after PCI (Figure 39).

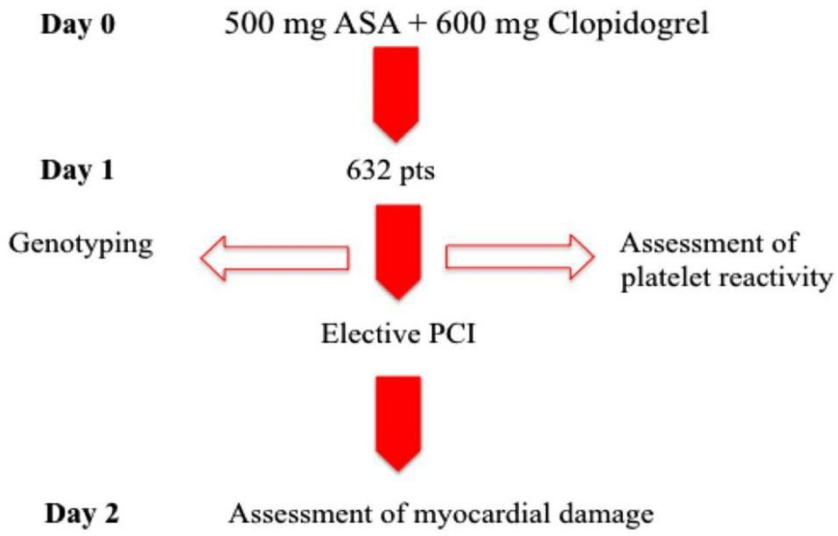

Figure 39: Study design. ASA is aspirin. Pts is patients. PCI is percutaneous coronary intervention.

Results: The observed genotype distribution for G894T, in Hardy-Weinberg equilibrium (p=0.56), was in the overall population as follows: homozygote G894G, n=263 (42%); heterozygote G894T, n=274 (43%); homozygote T894T, n=95 (15%). Analysis was conducted according to the dominant

model comparing Non Carriers (G894G: n=263 [42%]) versus Carriers of the 894T allele (G894T+T894T: n=369 pts [58%]). We did not observe significant differences in clinical characteristics between the two groups, with the exception of previous PCI that was more frequent in Carriers (159 [43%] vs. 89 [34%] in Non Carriers, p=0.02). Platelet reactivity values expressed as aspirin reactivity unit (ARU), P2Y12 reactivity unit (PRU) and platelet percentage inhibition were not different between groups as well as the HPR rate.

Conclusions: we found neither increased PR nor a suboptimal response to dual antiplatelet therapy in CAD patients undergoing elective PCI and carrying the 894T genetic variant. Our findings clearly suggest that PR does not contribute to the association between the G894T polymorphism and the unfavourable cardiovascular outcome.

Chapter 26

Correlation between serum uric acid levels and residual platelet reactivity in patients undergoing PCI

Background: Uric acid has been demonstrated within atherosclerotic plaque, where it may predispose to thrombus formation by increasing platelet adhesiveness and by altering the normal platelet reactivity. Recurrent ischemic events and increased risk of stent thrombosis were reported in patients undergoing PCI in the presence of high residual PR despite treatment with dual DAPT with aspirin and P2Y12 inhibitors (e.g. Clopidogrel). The Novara Atherosclerosis Study (NAS) group has recently demonstrated that in patients on chronic DAPT after an ACS or an elective PCI, the serum uric acid levels (sUA) do not influence the response to platelet function at 30-90 days post-discharge. Yet, a large heterogeneity in platelet inhibition has been demonstrated just at the time of the PCI.

Aim: to investigate whether sUA levels might have an impact on the rate of high PR.

Methods: We investigated the association between sUA and high PR in 185 patients with stable angina undergoing elective PCI. Blood samples were collected the day before PCI for sUA, and immediately after sheath insertion for platelet reactivity by VerifyNow P2Y12 assay (Accumetrics, San Diego, California) that was expressed as P2Y12 reaction units (PRU). High PR was defined as PRU ≥240. Hyper-uricemia was defined as sUA > 5.9 mg/dL. Patients were uniformly loaded with 500 mg ASA and 600 mg clopidogrel at

least 12 hours before PCI. Troponin T was measured before and 24 hours after percutaneous revascularization to assess PCI related myocardial damage (PMI=defined as 10 times TnT elevation).

Results: Mean age of the patients was 68 ± 10 years, 72% (134/188 patients) were males. Renal failure (GFR< 60 ml/min) was present in 26% (48/188) of the patients (mean GFR 71 ± 28.3 ml/min). The incidence of High PR was 39% (73/188 patients), while hyperuricemia was detected in 56% (103/188) of the patients. Patients with elevated sUA showed a higher incidence of renal failure than patients without elevated sUA (p=0,034). No significant differences were observed for gender, smoking habits, diabetes, and age. No correlation was found between sUA and PRU (r= 0.135; p= 0.084). PMI was detected in 6% (12/185) patients, with no significant difference between patients with and without elevated sUA (p=0,312).

Conclusions: Our findings confirm and further extend the results from the NAS group demonstrating no association between sUA and high PR in patients undergoing PCI even in the peri-procedural phase. Moreover, we found that the association of high PR and elevated sUA does not predict PMI.

Chapter 27

PROcedure related microvascular ACTIVation in long lEsions treated with bioresorbable vascular scaffold versus everolimus-eluting stent implantation (PROACTIVE trial)

Background: Significant platelet activation has been observed with long stented coronary segments, despite ongoing anti-platelet therapy. This has been associated with peri-procedural microvascular impairment and myonecrosis probably secondary to distal embolization. Compared with DES, Bioresorbable vascular scaffolds (BVS) has different interaction with the vessel wall, mostly due to the fact that scaffold is made of poly-L-lactic acid (PLLA), with lower stiffness as compared with metallic stents. In addition, BVS is not associated with an increased compliance at the inflow segment, but conversely tended to decrease compliance at the outflow segment, therefore resulting into a potentially lower degree of compliance mismatch. It is not yet clear what might be the relative impact of the expected lower compliance vascular mismatch of BVS on microvascular function especially in relation to platelet inhibition during and after PCI. Given the inherent flexibility, we hypothesized that BVS Absorb™ might be associated with less platelet activation, thrombus formation and downstream microvascular impairment as compared with metallic EES Xience™ in stable patients undergoing PCI of long coronary stenoses.

Aim: In long lesions treated either with everolimus-eluting bioresorbable vascular scaffold (BVS) or everolimus-eluting stent (EES), we sought to

investigate (a) procedure-related microvascular impairment, and (b) the relationship of platelet activation with microvascular function and related myonecrosis.

Methods: The PROACTIVE study was a prospective randomized (1:1) open-label superiority controlled trial in which 66 patients with stable coronary artery disease and long lesions (e.g. lesions to be treated with stent ≥ 25 mm long) were enrolled. Exclusion criteria were: a) ACS; b) contraindication to DAPT; c) bifurcations with a side branch > 2.0 mm; d) need for rotational atherectomy; e) atrial fibrillation and treatment with oral anticoagulants. Primary endpoint was the difference between groups in changes of pressure-derived corrected index of microvascular resistance (cIMR) after PCI. CFR, FFR and peri-procedural myonecrosis by hs-cTnT were also evaluated. Platelet reactivity was assessed by high-sensitivity adenosine diphosphate (hs-ADP)-induced platelet reactivity with the Multiplate Analyzer™ before, after PCI, then at 24 hours and at 30 days follow up.

Results: 66 patients were enrolled in this trial: 33 randomized to BVS Absorb™, and 33 to EES Xience Xpedition™ or Xience Alpine™ implantation. Baseline clinical characteristics were not different between the 2 groups. No in-hospital major adverse events occurred. No differences between the two groups in terms of number of vessel diseased, vessels and Syntax segments treated as well as complexity of the lesions defined according to the ACC/AHA classification of coronary lesions were observed. Semi-compliant balloons were more frequently used in patients treated with EES implantation, although there were no significant differences between the two group in terms of lesion preparation, as well as for maximum and minimum stent/scaffold diameter, number of stent/scaffolds implanted per

patient and total stent/scaffold length. As expected by recommendations, post-dilatation was more frequently performed in patients treated with BVS implantation, with associated longer procedure time in these patients. However, in the stent/scaffold optimization, no difference between the two groups have been observed regarding use of semi-compliant and non-compliant balloon, maximal diameter balloon, maximal pressure and total time of balloon inflation. No significant between groups differences were observed in FFR, CFR and cIMR both before and after-PCI. Yet, a significant difference in cIMR was observed within the BVS group after PCI versus baseline (19 ± 8 vs. 24 ± 12, p= 0.04), but not in the EES group (21 ± 9 vs. 21 ± 13, p= 0.84 (Figure 40). A significant difference in the primary endpoint of ΔcIMR was observed between the 2 groups (EES group -0,3 ± 13,6 vs. BVS group -4,7 ± 13,2; p= 0,04) (Figure 41).

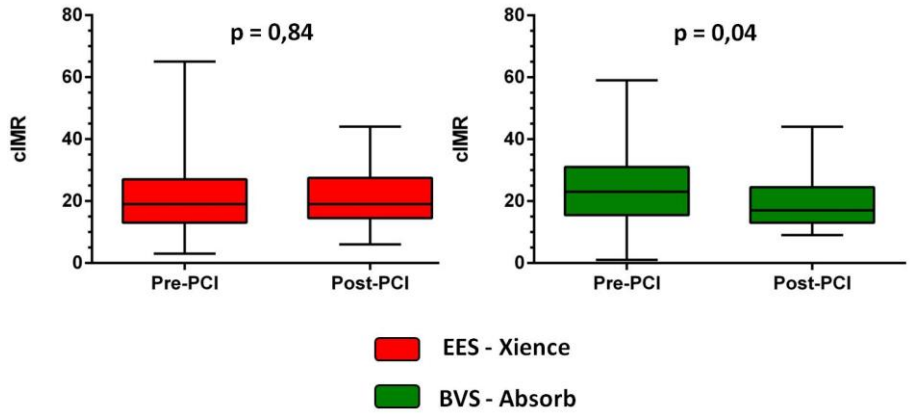

Figure 40: Changes in cIMR after PCI in the two group. Left panel: patients treated with EES - Xience; right panel: patients treated with BVS – Absorb. cIMR: corrected index of microvascular resistance.

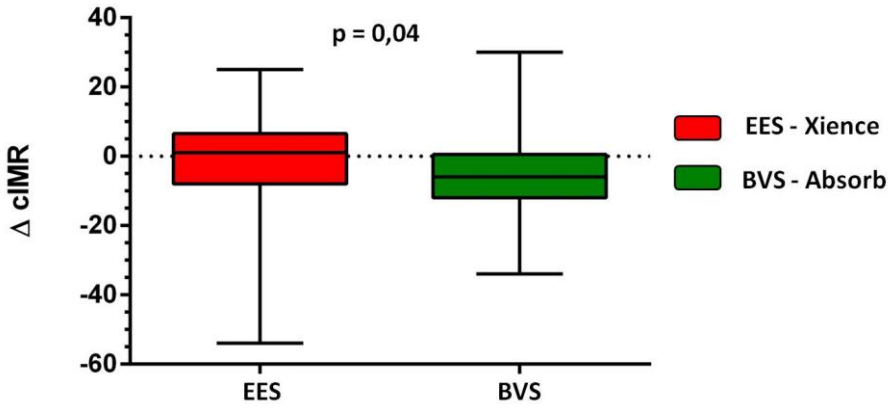

Figure 41: Difference between the two groups in ΔcIMR. Significant difference between the two groups in the primary endpoint, in favor of the BVS group. ΔcIMR: delta corrected index of microvascular resistance.

A significant reduction of hs-ADP was observed after PCI in both EES (hs-ADP: pre-PCI 18,4 ± 9,3 AU vs post-PCI 6,7 ± 4,8 AU; p < 0,0001) and BVS group (hs-ADP: pre-PCI 21,6 ± 11,1 AU vs post-PCI 13,8 ± 7,2 AU; p < 0,0001) without any difference between the two groups at baseline, post-PCI and at 30 days follow-up. Also no consistent trends of hs-ADP values across the three main time of measurements up to 30 days follow-up has been detected (ANOVA for trend p= 0,29). Hs-cTnT significantly increased in both groups after PCI (EES: hs-cTnT pre-PCI 11,4 ± 13,3 ng/L vs hs-cTnT post-PCI 84,9 ± 195,2 ng/L; p<0,0001. BRS: hs-cTnT pre-PCI 10,7 ± 16,1 ng/L vs hs-cTnT post-PCI 104,2 ± 182 ng/L; p<0,0001), without difference at baseline and after PCI between the two groups. Also no significant difference in terms of Δhs-cTnT between EES and BVS group has been observed (Δhs-cTnT EES group 73,4 ± 195,1 vs Δhs-cTnT BRS group 93,4 ± 185,3; p= 0,38).

Conclusions: In long lesions, BVS implantation is associated with a significant reduction in cIMR as compared with EES. The limited acute

impact of BVS on the microcirculation effect is associated with an optimal peri-procedural and short-term platelet inhibition, without significant difference in peri-procedural myonecrosis as compared with patients treated with EES.

Part VI

Percutaneous coronary interventions in bifurcation lesions: from bench tests to clinical outcome

Chapter 28

Single String Technique for stenting of complex coronary bifurcation stenoses

Background: For more complex bifurcations pathologies, in which an important side branch (SB) is involved or stenosed over a longer segment (more than 5 mm, starting at its ostium), the single stent strategy may not provide optimal results with adequate downstream flow in both territories. A wide variety of techniques using 2 regular stents hasbeen described and evaluated including T-, culotte, crush, minicrush, T- and protrusion stenting, but the best choice remains unclear. The main limitations of each of these techniques are due to superimposition of multiple metal layers and frequent stent strut malapposition.

Aim: The study aims to evaluate the clinical applicability of the single-string bifurcation stenting technique, developed to optimise PCI of complex bifurcation stenoses with respect to maximal wall coverage and to minimise multiple strut layers.

Methods: Single string is a novel double-stent bifurcation stenting method previously described (JACC Cardiovasc Interv. 2015), where first the SB stent is deployed with one single stent cell protruding into the main branch (MB). Second, the MB stent is deployed across this protruding stent cell. The procedure is completed by final kissing balloon dilation (Figure 42). Patients with true bifurcation lesions, involving at least 1 of the MB segments plus the SB, with SB stenosis extending for ≥ 5 mm, were selected

for single string procedure. The PCI procedure was performed according to the standardized protocol and procedural steps as described. Various stent brands were used: selection criterion was to have uniformly large cells of a minimum of 4.4-mm maximal cell expansion diameter.

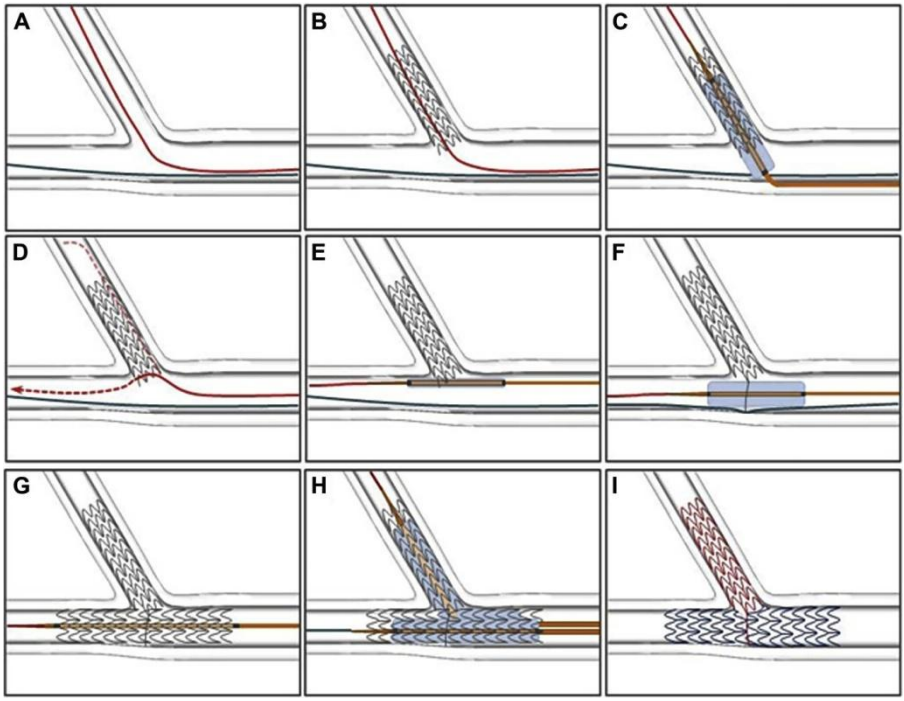

Figure 42: Guidewires are indicated as 'master-gw' (*highlighted in red*) and 'fellow-gw' (*highlighted in blue*). Master-gw is advanced into the SB, and the fellow-gw into the MB **(A)**. Stent is deployed in the SB with careful positioning of its proximal edge at the rim of the ostium, resulting in a single string of stent strut protruding into the MB **(B)**. The stent is proximally optimized **(C)**. The master-gw is pulled back and readvanced through the protruding single string cell into the MB **(D)**. Single string cell is opened up with a balloon **(E,F)**. MB stent is positioned and deployed through the single-string cell, over the master-gw **(G)**. Master-gw is advanced into the SB, crossing the most distal cell of the MB stent in the SB ostium, and fellow-gw is positioned into the MB. Sequential final kissing balloon dilation is performed as appropriate **(H)**. Final result is indicated in **(I)**. gw = guidewire; MB = main-branch; SB = side-branch.

Results: In this study, the single-string technique was applied in 35 consecutive patients with complex bifurcation stenoses with indication for

intended double stenting. Thirty-four lesions (94%) were located in the LAD, while 1 lesion (6%) was in the left circumflex. SB was significantly stenosed in 33 cases (94%), while 17 (49%) lesions were classified as true Medina 1,1,1 lesion. All procedures were performed successfully. For the procedure, 2.6±0.6 guidewires and 4.9±1.7 balloons were used. Duration was 105+32 minutes, while 294±84 mL contrast media was injected. A good angiographic result was achieved in all cases with a final residual diameter stenosis of 11±8% in the MB and 13±9% in the SB, measured by QCA. Results of extensive procedural optical coherence tomography (OCT) imaging will be available. During follow-up of 15±9 months, one major adverse cardiac event (early SB occlusion in a clopidogrel non-responder patient) was observed (3%).

Conclusions: The single-string bifurcation stenting technique is shown to be feasible for the treatment of complex bifurcation lesions with favourable long-term results.

Chapter 29

Reversed single string technique for coronary bifurcation stenting - First report of case demonstrations in vitro

Background: in a non-negligible proportion of bifurcation lesions, stenting of the SB becomes necessary at the end of PCI due to marked carina shift or dissection. The potential solutions that are currently available for securing the SB in such cases (for instance T-stenting, T-and-Protrusion, Reversed Crush, or Reversed Culotte) are all having limitations in terms of superimposition of multiple metallic layers, incomplete ostial coverage, or frequent stent strut malapposition. Single String technique appears to offer the best compromise between perfect strut coverage of the whole bifurcation area with minimal overlap of one single string of strut.

Aim: Based on the principle of Single String technique we sought to introduce a potential novel bail out strategy for provisional T stenting, when the result in the SB is suboptimal and requires stenting. In this proof-of-concept report, we describe the procedural steps of the Reversed Single String technique, illustrated with in vitro procedures.

Methods: The presented Reversed Single String stenting procedures were performed using guidewires (Balance Middleweight, Abott vascular, IL), semi-compliant balloons (Sprinter legend, Medtronic, Dublin, Ireland), and Ultimaster™ drug-eluting stents (Terumo Corporation, Tokyo, Japan) in size of 2.5 mm and 3.0 mm. Procedures were started with state-of-the-art provisional T-stenting technique: (1) a 3.0 mm stent was deployed in the

MB, then (2) proximal MB was optimized with a 3.5 mm 3 8 mm non-compliant balloons (Emerge, Boston Scientific, Galway, Ireland), and (3) finalized with kissing balloon dilation, using 3.0 mm and 2.5 mm balloons in the MB and the SB, respectively. Simulating real life scenarios, performing Reversed Single String technique can be indicated at this point, if the result in the SB is suboptimal (Fig. 43A). For educational reasons we call the two guidewires (gw), we use as “master-gw” (being in the MB—highlighted in red in Fig. 43) and “fellow-gw” (being in the SB—highlighted in blue in Fig. 43). (1) As first step, over the “fellow-gw” a 2.5 mm stent was deployed (12 bars) with careful positioning of its proximal edge at the proximal rim of the SB ostium. That resulted in no more than a single string of stent strut protruding into the MB (Fig. 43B). (2) Proximal optimization was done by reinflation of the stent delivery balloon at higher pressures (16 bars) after partial pullback (Fig. 43C). (3) Next the “fellow-gw” is slowly pulled back until it falls into the protruding cell, through which it was advanced into the distal MB (Fig. 43D). (4) The protruding cell was opened up to reasonable size with a 2.5 mm balloon, or a 1.5 mm balloon when needed (Fig. 43E). (5) “Master-gw” was pulled back and positioned in the SB. (6) Kissing balloon dilation was performed using 3.0 mm and 2.5 mm balloons in the MB and the SB, respectively (Fig. 43F). Finalized with proximal MB optimization with a 3.5 mm 3 8 mm non-compliant balloon. Schematic illustration of the final result is shown in Fig. 43G–I.

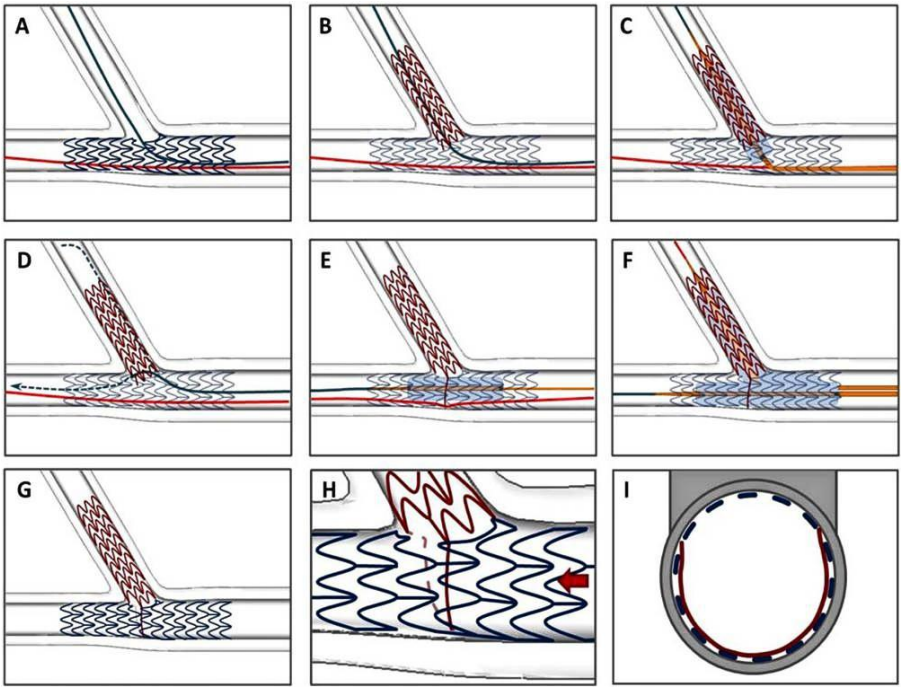

Figure 43: Schematic image depicting the steps of the Reverse Single String bifurcation stenting technique. See detailed description in the main text.

Optical frequency domain imaging (OFDI) imaging was done in each case. Note that OFDI pullback was considered as final step, meaning no further action was taken based on its results. For descriptive purposes, analysis of the imaging data was performed by dividing each bifurcation into six different areas, as shown in Fig. 44. Malapposition of stent struts was calculated and graded as (1) incomplete apposition (malapposition >0 µm), (2) marked malapposition (malapposition >200 µm), and (3) floating struts (malapposition >500 µm). 3D reconstruction was visually evaluated to describe potential strut fracture or strut expansion.

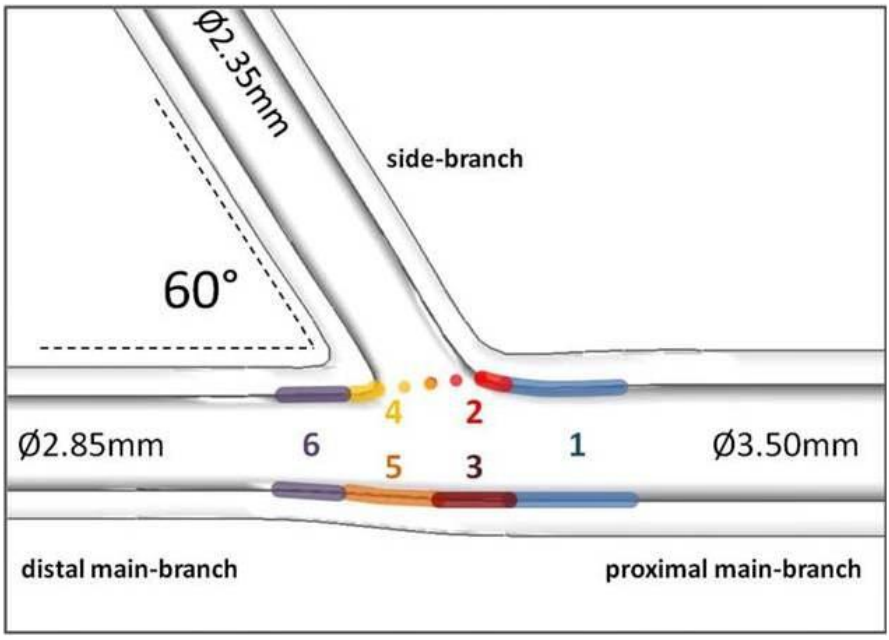

Figure 44: Silicone phantoms, used for in vitro testing. For didactical reasons bifurcation was divided into six sectors, when evaluating OFDI images. These sectors were as follows: proximal MB (1, blue), proximal bifurcation ostial half (2, light red), proximal bifurcation abostial half (3, dark red), distal bifurcation ostial half (4, yellow), distal bifurcation abostial half (5, orange), distal main branch (6, purple).

Results: All three in vitro procedures were successfully performed according to the protocol, with excellent result by fluoroscopy (Figure 45A). OFDI analyses were completed in each case. Procedure duration was 30, 25, and 22 minutes in Cases #1 to #3, respectively. Fluoroscopy time was 1.9, 2.4, and 1.8 minutes in Cases #1 to #3, respectively. In all three cases the initially chosen workhorse guidewires allowed to complete the procedure and one additional, small sized balloon was needed for predilating the string cell and for predilating the SB ostium before final kissing dilation.

OFDI was performed in all three cases (Case #1, #2, and #3). Struts were fully apposed in 79.0, 89.0, and 75.9% overall, respectively. When focusing

on the bifurcation areas alone (areas #2–5, as shown on Fig. 45), malapposition occurred in 1.5, 1.8, 17.0%, and floating struts were observed in 2.2, 0.0, 0.0% in the bifurcation areas of Cases #1, #2 and # 3, respectively. Malapposition was most frequently seen in the distal ostial area, namely where a neo-carina might have been created (area #4; 1.4, 0.0, 32.0% of Cases #1, #2, and # 3 respectively), less frequently observed in the proximal ostial area (area #2; 0.0, 0.0, 5.7% of Cases #1, #2, and # 3, respectively) and rarely found in other segments. No marked malapposition was observed in the side branch neither in the distal main branch (area #6).

3D reconstruction allowed exact evaluation of strut structure. Visual analysis did not reveal any strut rupture (Fig. 45B, left panel). Detailed visual inspection of the 3D reconstructed images suggests no marked loss in wall coverage (strut to wall surface ratio in all phantoms) in the ostial SB area, where the stent strut structure is mostly affected by the forces in the string strut (Fig. 45B, right panel).

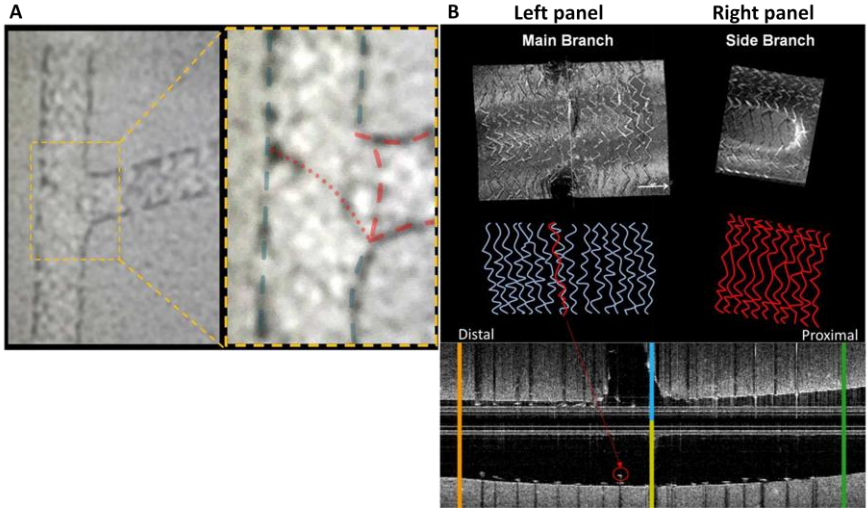

Figure 45: A) X-Ray. High-resolution fluoroscopic image offers excellent opportunity to evaluate the final result. B) 3D reconstructed OFDI. Pullback image in the main branch is shown in the left panel. In the right panel, pullback image in the ostial side branch is shown. In the lower schematic panels, the main branch stent is indicated in light blue, the side branch stent is indicated in red. The longitudinal pullback image is shown in the lower panel with the string strut within the red circle. See further explanation in the main text.

Conclusions: Although most provisional T stenting cases can be completed with one single main branch stent, there is a non-negligible portion of cases where the side branch eventually requires stenting. In this proof-of-concept report, Reversed Single String bifurcation technique was shown to be feasible, offering a potential bail out solution for such clinical scenarios. Clinical effectiveness remains to be confirmed in real clinical conditions.

Chapter 30

Resorbable magnesium scaffold in coronary bifurcations - report of in vitro experiments

Background: As coronary bifurcations represent 10-15% of all PCIs, it is crucial to understand whether and to what extent bioresorbable scaffolds are applicable in these rather common complex lesions. Due to marked variability in terms of distribution of atherosclerosic plaque, in terms of main branch and side branch calibers and in terms of their angulation, there is necessarily a significant discrepancy between the pure tubular shape of a stent and individual bifurcation anatomy. All currently widely accepted single- and double-stent techniques aim to address these variations, sometimes requiring a massive deformation of the original strut structure. While the behavior and performance of conventional metallic stents have been thoroughly investigated in vitro, as well as in vivo, our knowledge is still limited about bioresorbable vascular scaffolds, especially new technologies such as the resorbable magnesium scaffold (RMS) (Magmaris; Biotronik AG, Bülach, Switzerland).

Aim: The aim of the present work is to evaluate extensively in an *in vitro* setting the behavior of RMS in various non-bifurcation and bifurcation anatomies using standard interventional techniques.

Methods: Performance was evaluated in vitro with focus on vessel *tortuosity* and on *bifurcations*. All the tests were performed using 3.50x25 mm RMS in 3D printed, pure saline-filled silicone vessel phantoms.

Procedures were performed under conventional fluoroscopic guidance. Results were evaluated by (1) fluoroscopy, (2) OCT and (3) micro-computed tomography (μCT), in terms of scaffold conformability, strut apposition, structural deformation and strut fracture. Procedural performance (i.e. cross-ability of a guidewire or a balloon to the side branch) was described subjectively by the operator. In order to test the performance of RMS in *tortuous anatomies*, procedures were performed in a 90° bent silicone vessel model with 3.50 mm inner diameter. First, the RMS was implanted within the curve at a dilatation pressure of 12 atm. Secondly, the entire length of the scaffold was post-dilated with a 3.50x15 mm non-compliant balloon at 12 atm with multiple inflations. For *bifurcations*, procedures were performed in two types of uniform silicone bifurcation models, where proximal MB, distal MB and SB were 3.50/3.00/2.50 mm in diameter (Model #1), and 4.00 mm/3.50 mm/3.00 mm in diameter (Model #2), respectively. Angulation between distal MB and SB was uniformly 60°. Procedures were performed in five different ways, (1) MB stenting with SB opening and proximal optimization; for (2) MB stenting with final kissing and proximal optimization; for (3) T-and-protrusion technique; for (4) string technique. All tests were performed using 3.50x25 mm RMS.

Results: All procedures were successfully performed according to the protocol, as described above. No unexpected difficulty was described at any of the procedures. RMSs were advanced easily through markedly bent anatomies, as well as to MB and to side branches. Operators did not describe any unexpected difficulty of guide wire or balloon crossing to the jailed SB. Subjectively the performance of the RMSs was comparable to experiences with conventional permanent metallic stents.

In *tortuous vessels* (n=3) altogether 1470 scaffold struts were analyzed in 138 OCT frames. After initial scaffolding, the malapposition rates were 1.0%, 1.7% and 3.2% over the three cases. Post-dilation led to marked reduction, resulting in malapposition rates of as low as 0.0%, 0.4% and 0.4%, respectively. Note, that no strut with marked malapposition was observed at any phases. Malapposition was mainly seen in the middle portion of the stent, namely where the bending of the vessel is the most pronounced. Visual evaluation of the µCT images suggests that circular cross-section has been preserved along the bend. No relevant flattening tendency has been observed at any points of the bend, as illustrated on the example case depicted in Figure 46.

Figure 46: Bench setting for tortuose vessel. Fluoroscopy (*left*) and 3D-reconstructed µCT image (*right*) for visual evaluation of RMSs' performance.

In *bifurcations* cases the overall malapposition rate at OCT was 4.3%, occurring predominantly in the carinal area. No malapposition was seen at the proximal MB confirming proper conformability of RMS. µCT analysis has shown that final kissing dilation resulted in fully stretched struts in cases, where performed with 3.5 and 3.0 mm balloons (Figure 47). Accordingly in one case a broken connector (T-and-protrusion) and in another case, a broken strut (String technique) were identified (Figure 48).

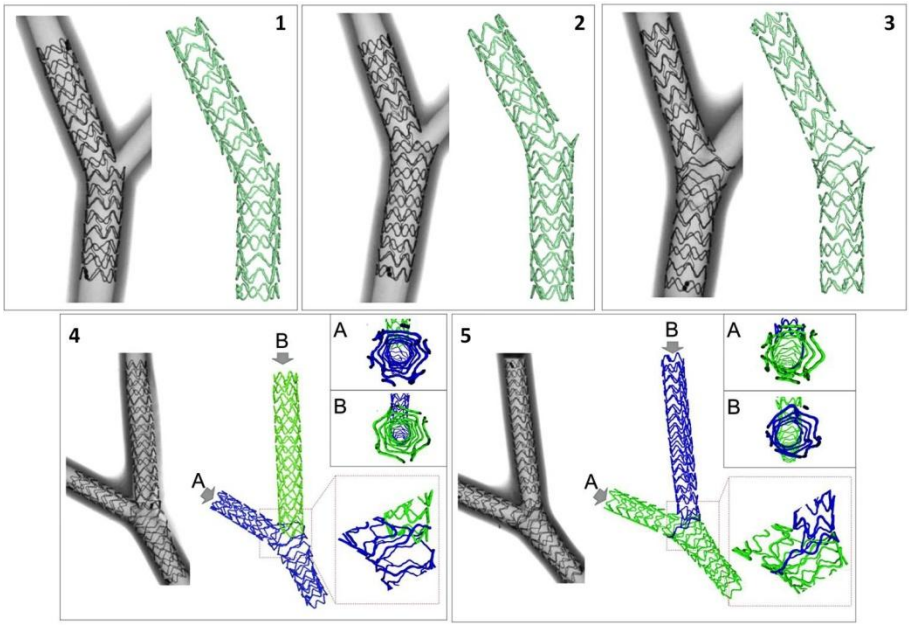

Figure 47: Bench setting for bifurcation PCI. 1) Main branch scaffolding with side branch opening alone – small side branch. 2) Main branch scaffolding and final kissing dilation – small side branch. 3) Main branch scaffolding and final kissing dilation – large side branch. 4) T-and-Protrusion technique – large side branch. A and B panels indicate longitudinal luminal views from distal main branch and distal side branch, respectively. 5) Single string technique – large side branch. A and B panels indicate longitudinal luminal views from distal main branch and distal side branch, respectively. In all the panels: Fluoroscopy (left) and 3D-reconstructed µCT image (right) for visual evaluation of RMSs' performance.

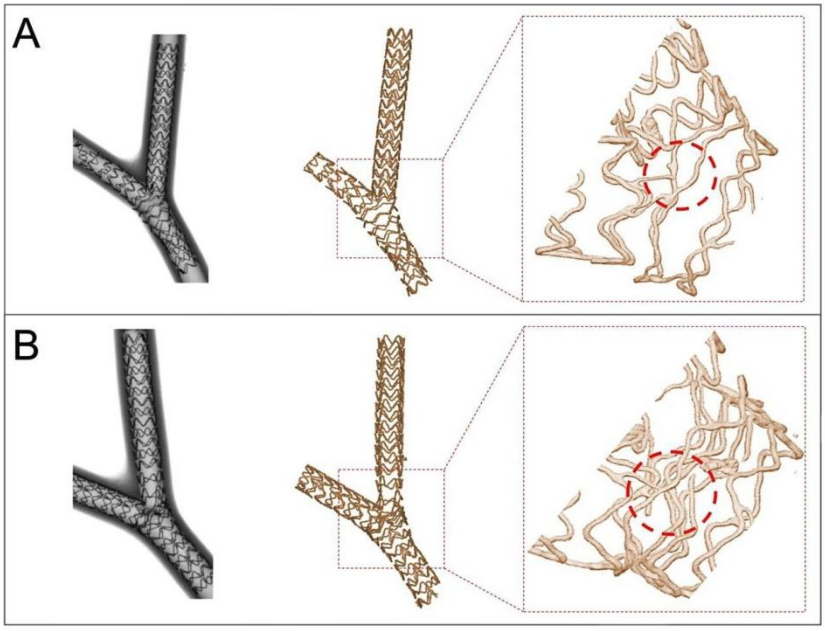

Figura 48: Scaffold fractures. Fluoroscopy (left) and 3D-reconstructed µCT images (right) of a T-and-Protrusion case (A) and a Single string technique case (B), where careful µCT analysis identified a connector fracture and a strut fracture, respectively.

Conclusions: Latest generation resorbable magnesium scaffolds can structurally cope with bifurcations in various in vitro models. Still, for cases (i.e. large diameter step down, large side branches, etc.) and techniques (culotte, string, etc.) where massive overexpansion of the scaffold (i.e. the lumen or any cell) is needed, RMS might not be the proper device due to a definite risk of strut fracture. This investigation may justify future clinical evaluation of the device in complex coronary anatomies using standardized procedural techniques.

Chapter 31

Mid-term outcomes after percutaneous interventions in coronary bifurcations

Background: Despite the major progress in stent technologies and adjunctive pharmacotherapies, the treatment of bifurcations is still challenging, as it is associated with worse outcomes when compared with non-bifurcation lesions. Although the single stent strategy is associated with a reduced risk of untoward events and is currently recommended, the double stent strategy may be required to guarantee the patency of both the main vessel and SB. In addition, it is unclear whether the clinical outcomes of PCI in bifurcations can be modulated by the choice of adjunctive P2Y12 inhibitor, the optimal DAPT, as well as the selection of the stent platform.

Aim: to investigate the major clinical, anatomic and procedural determinants of mid-term clinical outcomes in all comer patient population undergoing PCI in bifurcations.

Methods: The P2BiTO (P2Y12 inhibitor utilization in Bifurcation and Chronic Total Occlusion percutaneous coronary intervention with biologically active stents) registry was a retrospective multicenter registry in which 17 major coronary intervention centers in Europe and abroad participated, with the endorsement of the EuroBifurcation Club. Data were collected on consecutive patients who underwent PCI with “biologically active”, either DES or BVS, on a coronary bifurcation between January 2012 and December 2014. Inclusion criteria were: (1) patients aged ≥18 years with a diagnosis of

stable CAD or ACS; (2) PCI of a bifurcating lesion (all Medina types) with single or multiple “biologically active” stents (DES or BVS) at participating centers; and (3) main vessel diameter ≥2.5 mm and SB diameter ≥2.0 mm. Exclusion criteria were: (a) Patients who refused informed consent or with a life expectancy of ≤12 months; (b) pregnant or nursing mothers; women of child-bearing age will be asked if they are pregnant or think that they may be pregnant; (c) contraindication or suspected intolerance to anticoagulant (heparin, bivalirudin) or oral antiplatelet therapy (aspirin, clopidogrel, prasugrel, ticagrelor); (d) absence of bifurcation lesion or unwillingness to treat with PCI any of them. A loading dose of clopidogrel (600 mg), prasugrel (60 mg), or ticagrelor (180 mg) was administered before or immediately after PCI, unless patients were already on chronic maintenance therapy, followed by a maintenance dose of clopidogrel (75 mg od), prasugrel (10 mg od), or ticagrelor (90 mg bid).

The primary endpoint of the study was the cumulative occurrence of Major Adverse Cardiac Cerebrovascular Events (MACCE), defined as a composite of death (cardiac and noncardiac), nonfatal myocardial infarction (MI), stent thrombosis and stroke during the follow-up; the secondary endpoints were the single occurrence of death, MI, stent thrombosis and stroke.

Results: Among the 5,036 patients who underwent DES- or BVS-PCI on a coronary bifurcation, 639 (12.7%) in-hospital adverse events were reported: death in 53 cases (1.1%), periprocedural MI in 584 (11.6%), stroke in 28 (0.55%) and stent thrombosis in 50 cases (1.0%). Follow-up was available in 4,506 patients (89%). At a 18 months median (IQR 11-28) follow-up, the primary endpoint occurred in 453 (10%) patients: death in 235 cases (5.2%),

MI in 156 (3.5%), stroke in 75 (1.7%) and stent thrombosis in 110 cases (2.4%) (Fig. 49).

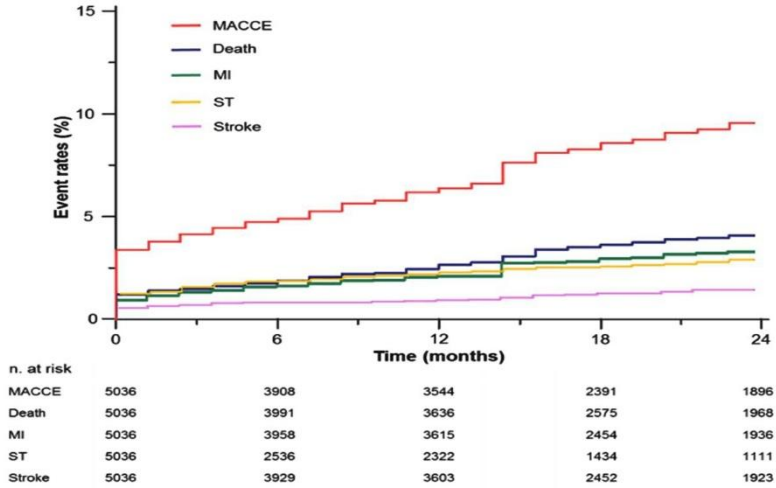

Figure 49: Cumulative incidence proportion of the primary and secondary endpoints. MACCE= major adverse cardiac and cerebrovascular events, MI= myocardial infarction.

Patients who experienced MACCE at follow-up were older, with a higher prevalence of diabetes, hypertension, prior MI, CABG and stroke, low (≤30%) LVEF and were more frequently admitted for an ACS. Also the latter higher prevalence of in-stent restenosis, more extensive CAD, longer lesions in both MB and SB, and a higher Syntax score; they more frequently received a BVS as compared with a DES, double stenting, an additional stent in bail-out, a higher total stent length and more frequently discontinued DAPT prematurely. The treatment of a left main and a planned strategy of double stenting as compared with planned single stent, showed only a trend towards an increased risk of the primary endpoint, but were significantly associated with increased mortality.

When analyzing the relevance of clinical presentation and angiographic morphology, ACS was a major risk factor for MACCE regardless the presence of a “true” Medina lesion (Fig. 50), while when taking into account the SB stenosis length, patients with stable CAD and SB lesion < 9 mm showed the lowest risk of MACCE (Fig. 51).

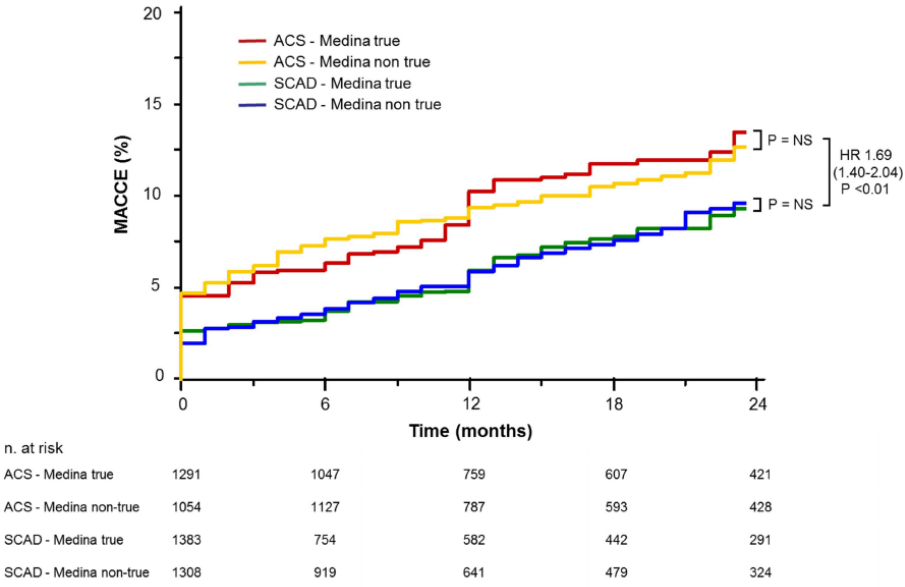

Figure 50: Cumulative incidence proportion of major adverse cardiac and cerebrovascular events (MACCE) stratified according to clinical presentation and Medina classification.

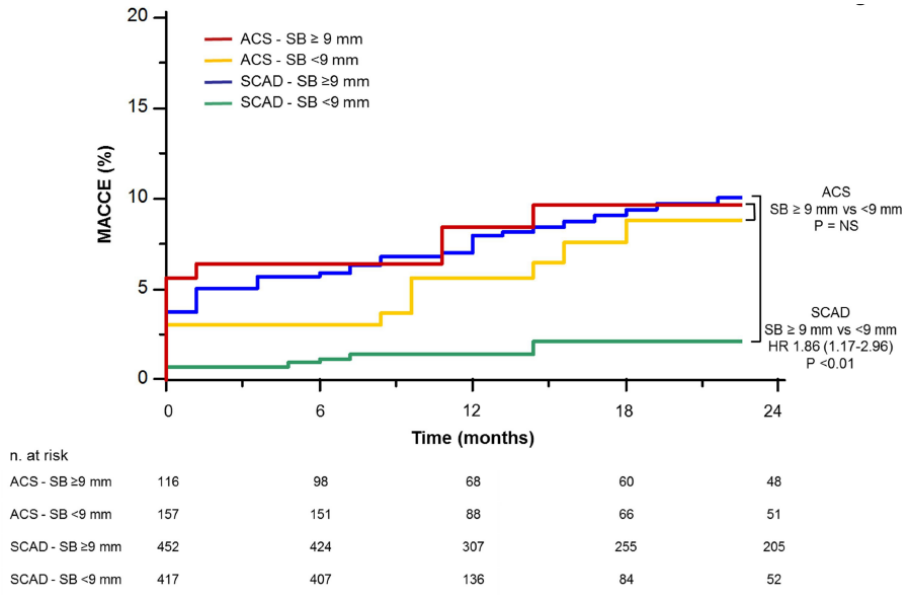

Figure 51: Cumulative incidence proportion of major adverse cardiac and cerebrovascular events (MACCE) stratified according to the lesion length of the side branch (SB) lesion.

As for stent strategy, a single "provisional" stent was used in 4,284 patients (85.1%), double stenting in 525 cases (10,4%), as planned. An additional stent was deployed as "bail-out" in 227 patients (4.5%), in the setting of a provisional stent strategy in 194 (4.3%), after double stenting in 33 (5.9%, P<0.05) cases. Main reasons for bail-out stenting were dissection of MB or SB (85, 37%), plaque shift (93, 41%), unsatisfactory result (34, 15%) or geographical miss (15, 7%). As for mid-term outcomes, while among patients receiving a planned strategy there was a trend favoring single as compared with double stenting, placement of an adjunctive stent in bail-out in the setting of a single provisional approach was associated with a higher incidence of MACCE than double stenting without any other stent in bail-out (Fig. 52). The Cox proportional hazard regression analysis documented that LVD, older age, a longer SB lesion length, the presence of

ACS at admission, bail-out stenting and diabetes were independent risk factors for MACCE.

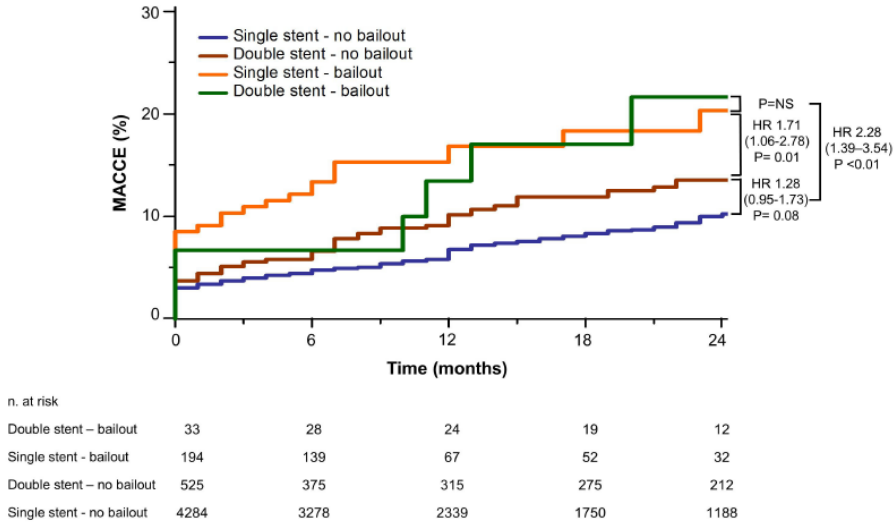

Figure 52: Cumulative incidence proportion of major adverse cardiac and cerebrovascular events (MACCE) stratified according to stent strategy.

Conclusions: In patients undergoing PCI of a coronary bifurcation with currently available drug and stent technology, clinical variables, such as older age, diabetes, clinical presentation with an ACS and reduced LVEF are independent predictors of mid-term untoward events. Moreover, treatment strategy must be carefully planned, as length of the SB lesion and “bail-out” stenting are independent predictors of adverse events.

Part VII

Discussion and conclusions

Discussion

Part I. From pressure derived-FFR to Absolute Flow and Microvascular Resistance

Since its first description[7-9], FFR is considered the standard of reference for evaluation of the ischemic potential of coronary stenoses and the expected benefit from revascularization[12-15,38,39]. Because FFR-based decisions are important for patients' outcomes, and given the need for rigor and reproducibility in reading the tracings by core laboratories, the highest technical quality of FFR measurements is desirable. We therefore proposed a standardization document (chapter 2) for acquiring, recording, interpreting, and archiving the pressure tracings for daily practice and for the purpose of clinical research involving a core laboratory. We believe that the benefit of FFR-guided revascularization strategies can be optimized when FFR measurement and analysis are performed in a rigorous and standardized manner[40]. In this work we aimed also at standardize the dosage of hyperemic agents. Administration of intravenous adenosine provides reliably stable maximal hyperemia, maintainable for minutes, when indicated. Therefore, in daily practice, it is to be applied when IC administration is difficult (e.g., in case of ostial stenosis) or when pullback measurements have to be performed (e.g., for the evaluation of serial stenosis), at the recommended dose is 140 μg/kg of body weight/min. Maximal hyperemia can be similarly induced by IC administration of adenosine. The degree of vasodilation is very similar and the FFR values are comparable to those obtained with IV. The test/retest repeatability tends to be better with IC than with IV administration of adenosine. We performed a

dose-response study (chapter 3) to establish the dosage of IC adenosine associated with minimal side effects and above which no further increase in flow can be expected. The analysis have shown that 100 µg in the right coronary artery and 200 µg in the left coronary artery reliably and reproducibly achieve >95% of maximum hyperemia without any significant side effects. The hyperemic effect of these doses is clinically indistinguishable from higher dosages, but with a lower rate of atrio-ventricular block; thus, there is no reason to use higher dosages[41].

In a complete accidental manner we have discovered, and subsequently tested, that even IC infusion of saline at room temperature is able to induce hyperemia. While performing measurements of minimal microvascular resistance in patients with mild atherosclerosis, we observed the occurrence or the increase of a pressure gradient between the coronary ostium and the distal part of the coronary artery few seconds after the start of the IC infusion of saline, even before the start of adenosine infusion. In order to prove this, we performed in 24 patients intracoronary doppler flow velocity measurements at rest, after IC adenosine, and during increasing infusion rates (5, 10, 15, and 20 mL/min) of saline at room temperature through the RayFlow™ catheter, a dedicated catheter for coronary thermodilution with 4 lateral side holes (chapter 4). We have also observed that the IC saline infusion does not affect blood pressure, systolic, or diastolic left ventricular function. The mechanisms by which the administration of saline through the side holes of the catheter in proximal epicardial segments induces vasodilation of downstream resistance arteries remain speculative and are probably multifactorial. We think that the stimulation of the proximal part of the coronary artery by the 4 small jets of saline at ≈34°C hitting the vascular wall appears central to the hyperemic

effect. Indeed, this phenomenon was weak and inconsistent when saline was given through the distal opening of an infusion catheter. Endothelial production of nitric oxide (NO) can be triggered by mechanical deformation resulting from shear forces or pulsatile strain caused by blood flow[42] and NO-dependent mechanisms contribute in a positive feedforward control to hyperemia during exercise in animals[43,44]. Endothelial cells can also release other vasoactive compounds, such as prostanoids, endothelin, and endothelium-derived hyperpolarizing factor[45,46]. Yet, their exact role on human microvasculature remains largely unknown, as is their stimulation by mechanical forces or changes in temperature. The fact that adding IV adenosine infusion to saline infusion through the RayFlow™ catheter does not increase coronary flow suggests that the pathway to induce coronary hyperemia is similar, or that saline infusion overrides many different pathways through which coronary vasodilation occurs. Finally, hyperemia seems to be strictly localized to the coronary artery in which saline is infused, as we did not observe any crosstalk between different myocardial beds.

These findings have definitively opened a new scenario in terms of microcirculatory assessment of flow and resistences using the RayFlow™ catheter, avoiding any specific pharmacological microvascular vasodilator, like adenosine. We therefore carried out a first-in-man study on 135 patients in order to test the feasibility, safety, and reproducibility of the continuous thermodilution method for the absolute coronary blood Flow and microvascular Resistance (chapter 6). The feasibility of the method was described 10 years ago, but the technique has been hampered by the absence of an appropriate monorail infusion catheter, the need for additional intravenous adenosine, and the absence of suitable software.

Now, all 3 issues have been solved: the RayFlow™ catheter allows the appropriate infusion of saline, there is no need for additional adenosine because the saline infusion induces hyperemia, and dedicated software for calculating Q and R online has been developed. Therefore, the procedure has become easy, taking ≈5 minutes including the 60 seconds of infusion of saline at room temperature, once the GC, the pressure/temperature wire, the RayFlow™ catheter, and the pump with saline are all set. The safety was confirmed by the absence of any significant complications (only 8% of the patients experienced transient bradycardia and concomitant atrioventricular block) and the duplicate measurements in a subgroup of 80 patients showed an high test-retest reproducibility[36].

Part II. Fractional flow reserve and natural history of stable coronary artery disease

FFR was initially validated against composite information from sequentially performed noninvasive tests[10,11,47]. It was shown that, below the value of 0.75, epicardial stenoses were associated with 100% positive predictive value for stress-inducible myocardial ischemia, whereas an FFR value >0.80 has a negative predictive value of >95%[10]. The DEFER trial indicated that PCI of coronary stenoses with FFR values >0.75 did not improve clinical outcome in comparison with patients deferred to optimal medical therapy (OMT)[38]. However in a minority of patients, an FFR value between 0.75 and 0.80 was found to be associated with typical exercise-induced angina and reversible flow maldistributions[47]. Therefore, in the era of DES, the threshold of 0.80 was adopted in subsequent studies[13,39] and in clinical practice, as well. FFR values between 0.75 and 0.80 have been referred to

as the FFR gray zone, alluding to some uncertainty regarding the degree of ischemia present related to the stenosis being interrogated. Based on this lack of evidences, we aimed at investigate the MACE (death, MI, and any revascularization) up to 5 years of 1459 patients with single-segment disease and an FFR value within the gray zone or within the 2 neighboring FFR strata (0.70–0.75 and 0.81–0.85), treated with PCI vs. OMT (chapter 7). In patients undergoing OMT, a progressive increase in MACE rate was observed when going from the highest FFR stratum of 0.81 to 0.85 to the lowest FFR stratum of 0.70 to 0.75. Even within the range of 0.70 to 0.85, the lower the FFR value, the higher the event rate. This result not only confirms the value of the 0.80 threshold, but also narrows the gray zone for clinical decision making: stenoses with an FFR <0.80 deserve revascularization, whereas stenoses with an FFR >0.80 are better treated with OMT, even though this dichotomy should obviously be nuanced by the morphological characteristics of the stenosis and the clinical context of the patient. These data are in line with the recent meta-analysis of Johnson et al. indicating a linear relationship between FFR values and clinical outcome[48]. Consistently, among 607 patients of the FAME 2 trial with documented stable CAD and in whom no revascularization was performed, we compared the respective values of angiographic diameter stenosis and FFR in predicting natural history (chapter 9). The primary end point, defined as vessel-oriented clinical end point (VOCE) at 2 years, was a composite of prospectively adjudicated cardiac death, vessel-related myocardial infarction, vessel-related urgent, and not urgent revascularization. The stenoses were divided into 4 groups according to FFR and %DS values: positive concordance (FFR≤0.80; DS≥50%), negative concordance (FFR>0.80; DS<50%), positive mismatch (FFR≤0.80; DS<50%), and negative

mismatch (FFR>0.80; DS≥50%). There was no significant difference in VOCE between the positive concordance and positive mismatch groups (p= 0.149) and no significant difference in rate of VOCE between the negative mismatch and negative concordance groups (p= 0.067)[49]. The data indicate that the FFR value predicts the natural history significantly better than DS, suggesting that "physiology trumps anatomy"[50]. In addition, among the stenoses with mismatch between DS and FFR, >50% had a low FFR in the presence of an angiographically mild stenosis. This relatively high rate of discordance (mismatch) between anatomy and physiology is actually not surprising because it relates to many different factors. First, there are a number of specific reasons, such as inaccuracy of border detection, foreshortening of the stenotic segment, superimposition of side branches, asymmetry of the stenotic segment, and inaccuracies of the pressure measurements. Second, cutoff values of both DS and FFR are surrounded by a grey zone. However, the most important reason for the disconnect between anatomy and physiology relates to the myocardial mass that depends on the stenosis and vasodilatory capacity of the vascular bed. The reference diameter partially accounts for the myocardial mass. This is the reason that the optimal cutoff value for DS decreases when the diameter of the vessel increases, typically in left main and proximal left anterior descending artery[5,51]. We think that FFR measurements should no longer be limited to angiographically intermediate stenosis but should be contemplated in stenoses that are mild or severe by visual evaluation.

On the way of the *risk continuum* between FFR and outcomes, we retrospectively explored the natural history of 414 intermediate stenoses from 331 patients with consecutive FFR measurements at least 6 months apart (chapter 10). We found that FFR regresses at a slow rate (median

ΔFFR= 0.007 per year). As a consequence, only 1 out of 4 lesions had a significant FFR worsening over a two-year period. The slow decline in FFR in our cohort was paralleled with a slow increase in stenosis severity measured by QCA. Despite the similar slow deterioration in both FFR and %DS, these metrics should not be used interchangeably to gauge clinical information. This is reflected in the very weak, albeit statistically significant, correlation of their rates of change in our cohort. "Baseline FFR", but not angiographic indices, is an independent predictor of significant longitudinal atherosclerosis progression, predicting which lesions will require revascularization[52].

Part III. Fractional flow reserve in special clinical settings

FFR has many useful features: 1) a unique and validated cut-off value set at 0.80[13-15]; 2) a reliable hyperemic response of the microcirculation once maximal hyperemia is induced[41]; 3) a complete independence from all hemodynamic changes (blood pressure, heart rate, and contractility)[53,54]. Still there are some potential technical pitfalls and drawback setting that we decided to better investigate. During FFR measurements, the mere presence of the GC in the coronary ostium induces some degree of stenosis, which depends on the relative size of the GC and the coronary ostium. This results into a not fully hyperemic flow across the ostium, with an artificial decrease of the mean aortic pressure (P_a) and a final overestimation of FFR value. In the DISENGAGE registry (chapter 11) we observed that GC disengagement is associated with: (a) slight albeit non-significant decrease in FFR values overall, mainly due to an increase of the mean P_a value rather than changes in the mean P_d value; (b) a shift from above to below the

clinical-decision making threshold of 0.80 in 1 out of 5 FFR measurements (in the range of 0.81-0.85 stratum), with a significant impact on treatment strategy; (3) a significant difference from the intrinsic variability of repeated FFR measurements in 50% of the stenoses (cut-off test-retest repeatability 0.02); and (4) a significant impact of the epicardial stenoses location on the FFR measurements (proximal and mid segments vs distal segments and side branches). Accordingly, for a proper FFR assessment, GC disengagement during hyperemic state has a crucial impact in order to guarantee the maximum flow across the coronary ostium.

Also a "dynamic epicardial stenosis", like the myocardial bridge (MB), might be a misleading setting in terms of functional assessment. Indeed in 9 symptomatic patients with MB and without significant CAD we aimed to evaluate the hemodynamic effect of physiological exercise (supine bicycle set during coronary angiography) on P_d/P_a, end-diastolic P_d/P_a and FFR. According to our results, invasive hemodynamic evaluation of MB might be better assessed with FFR at rest (chapter 12).

Due to the increasing confidence of the interventional cardiologists, FFR guidance is also being implemented to indicate or guide CABG. However recommendations for FFR adoption were based on RCTs investigating PCI strategies in which patients with typical indications for CABG were excluded (e.g. LM disease, valvular disease, and coronary anatomy unsuitable for PCI). In a sub-analysis of the GRAFFITI trial, a single-blinded, open-label, prospective 1:1 randomized controlled multi-center pilot trial comparing FFR-guided versus angiography-guided CABG, among the 88 patients randomized to FFR-guided strategy, the disclosure of FFR has changed bypass strategy in 55% of the patients, significantly simplifying the surgical

protocol. At 1-year follow-up, outcomes were similar between patients with at least 1 change in strategy according to FFR and patient without any change in therapeutic decision (chapter 14). Our results confirm that FFR can play an important role in risk stratification and determining management strategy of patients either before or after CABG, without any untoward hazard on 1-year clinical outcome.

Other settings in which FFR assessment is becoming more attractive, and for which there is a lack of evidence from RCTs are: valvular heart disesases, especially AS, and patients with LVD and/or HF. In patients with AS myocardial ischemia can be related to several factors than the mere epicardial stenosis. Some relate to left ventricular hypertrophy, others to the hemodynamic alterations associated with aortic valve disease. Therefore even in the presence of normal epicardial conductance, ischemia could be present in some AS patients. By matching 106 patients with AS and CAD treated according to FFR values, with 212 contemporary control patients with AS in which revascularization was decided on angiography only, we have founded a downgrading of the CAD severity in the FFR-guided group and resulted into more PCI. FFR evaluation in patients undergoing surgery was also associated with less venous grafts and anastomoses, yet without higher event rates up to 5 years of follow-up (chapter 15 and 16).

In 1,676 stenoses from patients affected by various degrees of HF of different etiologies we investigated whether incorporating the value of right atrial pressure into the FFR formula has any clinical impact on FFR measurement. Although these patients had a P_{ra} often markedly above the normal range, the agreement between measured FFR and calculated FFR_{myo} was excellent, with a difference as minimal as 0.01. In a small fraction of

patients (9%), the FFR value went from >0.80 to an FFR_{myo} value of ≤0.80, with an individual difference of no more than 0.03 and in no case did an FFR value >0.80 yield an FFR_{myo} <0.75 (chapter 17). This observed difference between the 2 values is still within the range of test–retest repeatability of FFR measurements. Considering the negligible impact of right atrial pressure on FFR measurement we subsequently evaluated, in patients with non-valvular LVD and CAD, the impact of FFR on: reclassification of stenosis significance; indication to revascularization; revascularization strategy; long-term clinical follow-up. After hemodynamic assessment, the number of stenotic vessels per patient was significantly downgraded within the FFR-guided group (433 patients), with a significantly lower revascularization rate as compared with the angio-guided group (866 patients). PCI was performed more frequently in the FFR-guided group (36% vs. 28% in the angio-guided group; p<0.01); while CABG was more often the therapy of choice in the angio-guided group (32% vs. 16% in the FFR-guided group, p<0.01). At 5-year follow-up, FFR was associated with lower MACCE and mortality rates and safer deferral of patients towards medical therapy as compared with an angio-guided strategy (chapter 18). Accordingly, FFR has the ability to discriminate patients who can benefit the most from surgical revascularization and to safely refer or defer other patients to less invasive treatment (PCI or OMT). In fact, the beneficial effect of FFR on clinical outcomes seems more evident in patients with severely reduced systolic function (EF ≤35%), likely presenting with many comorbidities and higher surgical risk.

Part IV. Angiography-derived FFR technologies

Despite its clear advantages, the clinical adoption of FFR has been variable and slow for several reasons widely discussed in the introduction paragraph[18,19]. A tool that allows calculating FFR without the use of costly pressure wires and the administration of adenosine could increase the adoption of FFR. Several image-based FFR methodologies have recently been introduced. Computational fluid dynamics (CFD) simulation applied to cardiac computed tomographic images and to flat detector angiograms for the evaluation of noninvasive FFR have been proposed[55-59]. However, the computational complexity of such simulations requires manual interaction and considerable processing time, which limits the application of these approaches in clinical practice. During the last 3 years we have carried out validation studies of FFR_{angio} and QFR, two new angiography derived-FFR technologies, not based on CFD, that are gaining interest in interventional cardiology practice. QFR (developed by Medis Medical Imaging System, Leiden, the Netherlands), based on a patient-specific flow by frame count analysis, showed a good agreement with the invasive standard FFR measurements, which was particularly favorable with QFR derived from contrast-flow (cQFR) and adenosine-flow models (aQFR). The diagnostic accuracy of all 3 QFR approaches for predicting an FFR of ≤0.80 was relatively high, ranging from 80% for QFR by the fixed-flow model (fQFR), to 86% and 87% for cQFR and aQFR models. Nevertheless, the diagnostic accuracy of the simplified fQFR computation is suboptimal, with a positive likelihood ratio of 4.8 which implies that this approach is not of sufficient diagnostic value to be clinically useful. In contrast, the transport time of the contrast medium can be used for a patient-specific estimation of coronary flow, which might improve FFR computation, as previously shown[60].

However, aQFR unexpectedly did not further improve the FFR estimation, compared with cQFR. Of note, good correlation and agreement between cQFR and aQFR was observed. FFR_{angio} (developed by CathWorks, Ltd) provides a 3D functional angiography mapping of the coronary tree with superimposed, color-coded, FFR values. Stated another way, FFR_{angio} displays a functional angiogram. This computational method is based on a rapid flow analysis after a classification of the dynamic characteristics of the vessels in conjunction with the patient's hemodynamic information, allowing to assess FFR using routine angiograms within a few minutes of automatic processing. All stenoses are converted into resistances in a lumped model, whereas scaling laws[61-63] are used to estimate the microcirculatory bed resistance. In our validation study FFR_{angio} achieved a diagnostic accuracy of 93%. Importantly, the fact that 67% of the lesions analyzed had invasive FFR values of 0.70 to 0.90, and 35% of the lesions had invasive FFR values between 0.75 and 0.85, that is, adjacent to the cutoff value, proves a high diagnostic accuracy for the entire clinically relevant range and not only in extreme cases. Moreover, a low interobserver variability was demonstrated for the FFR_{angio} system. To achieve a routine adoption of FFR_{angio} and QFR in the daily practice in cahtlab, at least 3 conditions should be met. First, data acquisition should minimally disrupt routine angiography. Both technologies only requires the acquisition of 2 to 3 conventional radiographic projections, in which the lesions can be clearly delineated. Care should be taken to visualize the entire coronary tree on the screen and to optimize filling. There is no need for vasodilation, nor any approximation of coronary flow. The images should be of high resolution, with a frame rate of at least 10 frames per second; all these parameters are routinely available in modern catheterization suites. Second, the processing

time should be as short as possible. In both validation studies performed, this aspect could not be quantified because the FFR_{angio} and QFR processing were performed offline to ensure the blinding of the operators. Third, the process should be as much operator independent as possible. The present versions of the FFR_{angio} and QFR technologies require minimal user guidance in the flow calculation process. This is translated into a low interoperator variability. In addition, it seems desirable to provide the physician with a full physiological roadmap, rather than only single-vessel segments. Once such a complete physiological roadmap is derived from the classical angiogram and simultaneously displayed next to it, anatomy and function can be easily integrated into the clinical decision-making process.

Part V. Platelet and microvascular function

An increased platelet reactivity (PR) associated with variable degree of coronary microvascular impairment has been reported after elective PCI, despite pretreatment with aspirin and clopidogrel[64,65]. Coronary vessel manipulation especially during complex PCI is an additional trigger for transient increase in PR[66], which could favor a thrombotic milieu portending distal embolization[67]. Considering the strong platelet inhibition of prasugrel, we compared in the PROMICRO 2 trial the effects of prasugrel vs. clopidogrel on PR and the PCI-induced coronary microvascular impairment. We observed a significant peri-procedural increase in PR in the clopidogrel group (p=0.008), but not in the prasugrel group (p=0.822), with a significant correlation between IMR and PR both at baseline (r=0.458, p=0.003) and post-PCI (r=0.487, p=0.001) (chapter 23 and 24). Our result (1) corroborate the suboptimal platelet inhibition of clopidogrel in a

substantial proportion of patients, with subsequent increased risk of ischemic events[64,65] and (2) suggest that a correlation exists between residual PR and coronary microvascular resistance. Therefore, the protective effect of a loading dose of prasugrel provide more potent platelet inhibition, which may be of particular benefit when extensive intracoronary manipulation in some PCI setting is expected. However, clopidogrel is still the antiplatelet agent of choice in patients with stable CAD undergoing elective PCI. Several studies have also demonstrated that the increased PR is proportional to the extent of vascular damage induced by the coronary intervention and to the length of the stent implanted, translating into PMI[66,68,69]. In PROACTIVE trial we compared the BVS Absorb™ with EES Xience™ in the setting of long coronary lesions, in order to evaluate if BVS implantation may acutely affect the coronary microvasculature with potential effect on the related platelet activation and peri-procedural myonecrosis. We found a significant reduction of cIMR after PCI in the BVS group but not in the EES group (p= 0,04), therefore meeting the primary endpoint of significant between groups difference in ΔcIMR, in favor of the BVS group (p= 0,04). In addition, we observed a significant PR reduction after PCI with both EES and BVS implantation, without differences between the two groups at baseline, post-PCI and at 30 days follow-up. Also no difference in PR over time up to 30 days follow-up has been detected. Last, peri-procedural myonecrosis after PCI of long coronary lesions was important with both BVS and EES, without significant variations in terms of Δhs-cTnT between the two groups. In designing the present randomised trial, the assumption was made that the metallic DES is associated with an increased compliance at the two contiguous segments of the stent implanted, generating a compliance mismatch. This translates into

important ring vortices at the in-flow of the stent and rapid variations of wall shear stress that might potentially induce platelet activation and thrombus formation[70]. The significant reduction of cIMR after BVS implantation might seem at odds with the available data in the literature suggesting increased thrombogenicity. To achieve a similar radial strength to that of an 80 µm metallic stent, the PLLA backbone of the 150 µm everolimus-eluting BVS is designed to have both thicker and wider struts [71-73]. This translates on one hand into a significantly increased surface of contact between the BVS and vessel wall compared to second and third generation DES[74-76], but on the other hand, the increased strut thickness and width have been associated with more thrombogenicity in animal models[77], also explaining the increased thrombogenicity of BVS in comparison with EES[78,79]. How does our finding reconcile with these evidences? We can assume that the lower microvascular impairment after BVS implantation is due to two main reasons: (1) as compared with EES implantation, the scaffold deployment is associated with a greater retention of athero-thrombotic debris from the coronary plaques preventing their embolization distally in the microcirculation; (2) The potential increased thrombogenicity of BVS is compensated by a lower compliance mismatch, with a final neutral impact on the microvasculature. BVS implantation is not associated with an increase in compliance at the inflow segment, but conversely tended to decrease compliance at the outflow segment, therefore resulting into a potentially lower degree of compliance mismatch[70]. The significant reduction in platelet reactivity with both BVS and EES is another interesting finding of the PROACTIVE trial. The significant reduction of hs-ADP in both groups, in fact, without differences at baseline, post-PCI and 30 days follow-up, confirm the results of previous

studies supporting that in patients with adequate response to DAPT, thrombogenicity of BVS Absorb™ is not affected by on-treatment platelet reactivity but is mainly due to a suboptimal vessel sizing and procedural technique at the time of its implantation[80,81]. In our trial the discrepancy between the reduction of cIMR and the significant increase of hs-cTnT after BVS implantation could be explained by the fact that, although the BVS implantation is associated with an high retention of atherothrombotic debris, because of thicker wider struts as compared with DES, is also related to an important rate of small side branches occlusion. Our results are in line with a post-hoc analysis of the ABSORB II trial, where no differences in the incidence of cardiac biomarker rise and PMI were found between the two groups [82].

Part VI. Percutaneous coronary interventions in bifurcation lesions: from bench tests to clinical outcome

According to different calculations and observations, nearly 10% to 15% of all PCI procedures involve a clinically relevant bifurcation stenosis[83,84]. Although provisional T-stenting represents a good solution for simpler anatomies[85], the proper treatment of more complex coronary bifurcation lesions remains a challenge. This is mainly due to their anatomic variation in terms of diameters, angulations, and the involvement by atherosclerotic disease. Various approaches have been developed for bifurcation stenting using conventional stent platforms. We evaluated in 35 patients the clinical applicability of the single-string bifurcation stenting technique, previously described by Kawasaki T et al[86], and further investigated by us in detailed vitro analysis[87]. All the cases were performed successfully, within a reasonable length of time and using the usual amount of contrast and

radiation exposure. Furthermore, postprocedural laboratory tests did not show clinically relevant periprocedural myocardial necrosis (chapter 28). It is important to emphasize that the single string technique is safe to perform because, in case of difficulties, the procedure can be immediately converted to the culotte technique (if the protrusion into the MB was unnecessarily long), the mini-crush technique (if the protrusion into the MB was too small), or T-stenting (if no protrusion into the MB was obtained at all). Also it appears to offer the best compromise between perfect strut coverage of the whole bifurcation area with minimal overlap of one single string of strut. Based on the principle of single string technique we sought to introduce a potential novel bail out strategy for provisional T-stenting, when the result in the SB is suboptimal and requires stenting. We therefore described, in 3 vitro silicone phantoms, the procedural steps of the Reversed Single String technique. As shown, procedure can be performed within a reasonable time, with acceptable radiation exposure and without need for much additional equipment. Analysis of the cases showed excellent final result with a malapposition rate lower than 15% in the area of the bifurcation. Although such in vitro case report does not allow direct comparison with other methods, the observed malapposition rate is promisingly low, when considering that other techniques have reported malapposition rates as high as 30–49%[88-92](chapter 29). We believe that Reversed Single String bifurcation technique could offer a potential bail out solution for such clinical scenarios.

While the behavior and performance of conventional metallic stents have been thoroughly investigated in vitro, as well as in vivo, our knowledge is still limited about bioresorbable vascular scaffolds, especially new technologies such as the resorbable magnesium scaffold (RMS). For the first

time we evaluated the RMS performance in vitro, focus on vessel tortuosity and bifurcations. All procedures were performed successfully with good result according to fluoroscopy, with an overall malapposition rate in bifurcation cases of 4.3%, detected by OCT, occurring predominantly in the carinal area. Considering that previous in vitro and in vivo studies, with limited sample sizes, investigating various bifurcation techniques reported malapposition rates in the region of bifurcation ranging between 30-45%, present data can be considered at least comparable, if not favourable[87,93]. No strut fractures or major deformations were revealed by OCT. No relevant malapposition was seen at the proximal MB confirming the proper conformability of the RMS, at least in the indicated range of diameters (chapter 30). To summarize, performance was comparable with previous in vitro and in vivo experiences with conventional metallic stents in the literature. This finding is also aligned with the limited animal data using RMS in bifurcations[94]. Despite such advances in stent technologies and adjunctive pharmacotherapies, the treatment of bifurcations is associated with worse outcomes when compared with simple coronary lesions[95]. Also other areas of incertitude in PCI of bifurcation lesions derive from the choice of adjunctive P2Y12 inhibitor, the optimal DAPT, as well as the selection of the stent platform. In the "P2Y12 inhibitor utilization in Bifurcation and Chronic Total Occlusion percutaneous coronary intervention with biologically active stents (P2BiTO) registry" we aimed to verify the relative implication of clinical presentation, angiographic characteristics and treatment strategies on mid-term outcomes in 5,036 patients who underwent PCI with either DES or BVS on coronary bifurcations. Older age, ACS at admission, diabetes, left ventricular dysfunction, SB lesion length ≥9 mm, bail-out stenting (beyond a planned

strategy of either single or double stenting) and use of BVS were independent risk factors for MACCE (chapter 31). Even considering the retrospective, observational design of this study, our findings emphasize the importance of a carefully planned strategy for complex bifurcation PCI in the "real world" clinical practice.

Conclusions

In this long lasting research journey we investigated: a) the prognistic role of FFR in functional evaluation of epicardial stenosis in different anatomical and clinical settings of patients with stable CAD, heart valve disease and LVD; b) the role of IMR, CFR and absolute coronary flow and microvascular resistances assessment with a new dedicated thermodilution catheter; c) the diagnostic performance of two new angiography-derived FFR technologies for a quantitative and functional assessment of CAD; d) the impact of antiplatelet agents and BVS Absorb™ implantantion on procedure-related microvascular impairment, platelet activation and the related myonecrosis; e) the safety and feasibility of new 2-stent bifurcation techniques and the clinical outcome of known bifurcations techniques. We believe that many answers have been provided by our extensive translational research. FFR remain the milestone in functional assessment of the ischemic burden related to coronary stenoses. Our findings corroborate the strong clinical outcome background of FFR, supporting FFR-guided revascularization strategies above angio-based decision making, and

therefore strongly discouraging any purely anatomy guided revascularization attempts in different clinical and anatomical settings. Absolute coronary blood flow (Q) and microvascular resistance (R) can be safely and reproducibly measured with continuous thermodilution, opening new opportunities for the study of the coronary microcirculation. FFR_{angio} and QFR provide both a comprehensive physiological assessment of the entire coronary tree within few minutes, enabling online FFR measurement during the angiographic procedure. This, in turn, may facilitate the adoption of FFR-based clinical decision making regarding coronary revascularization. Both prasugrel and BVS Abosrb™ have proven a beneficial acute effect on peri-procedural coronary microvascular function and platelet activation. Although BVS Absorb™ did not live up to its promise because of the higher events in the mid-term due to greater scaffold thrombosis, our findings are at least reassuring on the acute impact of these devices on the microcirculation. Lastly in PCI of bifurcation lesions, our feasibility results of in vitro tests, offer new solutions for both complex anatomy requiring 2-stent-technique and bailout technique in case of failure of the most consolidated provisional T-stenting.

List of abbreviations

CAD: coronary artery disease;

FFR: fractional flow reserve;

PCI: percutaneous coronary intervention;

CFR: coronary flow reserve;

IMR: index of microcirculatory resistance;

Tmn: mean transit time;

CABG: coronary artery bypass grafting;

LVD: left ventricular dysfunction;

HF: heart failure;

PMI: periprocedural myocardial infarction;

RMS: resorbable magnesium scaffold;

RCT: randomized clinical trial;

RCA: right coronary artery;

LCA: left coronary artery;

IC: intracoronary;

TTE: transthoracic echocardiography;

IV: intravenous;

MI: myocardial infarction;

VE: visual estimation;

QCA: quantitative coronary angiography;

RF: risk factors;

DS: diameter stenosis;

VOCE: vessel-oriented clinical end point;

GC: guiding catheter;

ACS: acute coronary syndrome;

STEMI: ST-segment elevation myocardial infarction;

NSTEMI: non-ST segment elevation myocardial infarction;

MB: Myocardial Bridge;

SVG: saphenous vein graft;

AS: aortic stenosis;

AVR: aortic valve replacement;

MACE: major adverse cardiac events;

MT: medical therapy;

DES: drug-eluting stent;

LVEF: left ventricular ejection fraction;

MACCE: major adverse cardiovascular and cerebrovascular events;

LM: left main;

QFR: quantitative flow ratio;

3D: 3-dimensional;

DICOM: Digital Imaging and Communications in Medicine;

CFD: computational fluid dynamic;

PR: platelet reactivity;

hs-TnT: High-sensitivity troponin T;

NO: Nitric oxide;

ARU: aspirin reactivity unit;

PRU: P2Y12 reactivity unit;

DAPT: dual antiplatelet therapy;

sUA: serum uric acid;

BVS: Bioresorbable vascular scaffold;

PLLA: poly-L-lactic acid;

EES: everolimus-eluting stent;

cIMR: corrected index of microvascular resistance;

hs-ADP: high-sensitivity adenosine diphosphate;

SB: side branch;

MB: main branch;

OCT: optical coherence tomography;

OFDI: Optical frequency domain imaging;

μCT: micro-computed tomography;

OMT: optimal medical therapy;

Bibliography

1. Sones FM Jr, Shirey EK. Cine coronary arteriography. Mod Concepts Cardiovasc Dis 1962;31:735–738.

2. Johnson NP, Kirkeeide RL, Gould KL. Coronary anatomy to predict physiology: fundamental limits. Circ Cardiovasc Imaging. 2013 Sep;6(5):817-32.

3. Gould KL, Johnson NP, Bateman TM, Beanlands RS, Bengel FM, Bober R, Camici PG, Cerqueira MD, Chow BJW, Di Carli MF, Dorbala S, Gewirtz H, Gropler RJ, Kaufmann PA, Knaapen P, Knuuti J, Merhige ME, Rentrop KP, Ruddy TD, Schelbert HR, Schindler TH, Schwaiger M, Sdringola S, Vitarello J, Williams KA, Gordon D, Dilsizian V, Narula J. Anatomic versus physiologic assessment of coronary artery disease: role of CFR, FFR, and PET imaging in revascularization decision making. J Am Coll Cardiol 2013;62:1639–1653.

4. Tonino PA, Fearon WF, De Bruyne B, Oldroyd KG, Leesar MA, Ver Lee PN, Maccarthy PA, Van't Veer M, Pijls NH. Angiographic versus functional severity of coronary artery stenoses in the FAME study fractional flow reserve versus angiography in multivessel evaluation. J Am Coll Cardiol. 2010 Jun 22;55(25):2816-21.

5. Toth G, Hamilos M, Pyxaras S, Mangiacapra F, Nelis O, De Vroey F, Di Serafino L, Muller O, Van Mieghem C, Wyffels E, Heyndrickx GR, Bartunek J, Vanderheyden M, Barbato E, Wijns W, De Bruyne B. Evolving concepts of angiogram: fractional flow reserve discordances in 4000 coronary stenoses. Eur Heart J. 2014 Oct 21;35(40):2831-8.

6. Kern MJ, Samady H. Current concepts of integrated coronary physiology in the catheterization laboratory. J Am Coll Cardiol. 2010 Jan 19;55(3):173-85.

7. Pijls NH, van Son JA, Kirkeeide RL, De Bruyne B, Gould KL. Experimental basis of determining maximum coronary, myocardial,

and collateral blood flow by pressure measurements for assessing functional stenosis severity before and after percutaneous transluminal coronary angioplasty. Circulation. 1993 Apr;87(4):1354-67.

8. De Bruyne B, Pijls NH, Paulus WJ, Vantrimpont PJ, Sys SU, Heyndrickx GR. Transstenotic coronary pressure gradient measurement in humans: in vitro and in vivo evaluation of a new pressure monitoring angioplasty guide wire. J Am Coll Cardiol. 1993 Jul;22(1):119-26.

9. De Bruyne B, Baudhuin T, Melin JA, Pijls NH, Sys SU, Bol A, Paulus WJ, Heyndrickx GR, Wijns W. Coronary flow reserve calculated from pressure measurements in humans. Validation with positron emission tomography. Circulation. 1994 Mar;89(3):1013-22.

10. Pijls NH, Van Gelder B, Van der Voort P, Peels K, Bracke FA, Bonnier HJ, el Gamal MI. Fractional flow reserve. A useful index to evaluate the influence of an epicardial coronary stenosis on myocardial blood flow. Circulation. 1995 Dec 1;92(11):3183-93.

11. Pijls NH, De Bruyne B, Peels K, Van Der Voort PH, Bonnier HJ, Bartunek J, Koolen JJ. Measurement of fractional flow reserve to assess the functional severity of coronary-artery stenoses. N Engl J Med. 1996 Jun 27;334(26):1703-8.

12. Zimmermann FM, Ferrara A, Johnson NP, van Nunen LX, Escaned J, Albertsson P, Erbel R, Legrand V, Gwon HC, Remkes WS, Stella PR, van Schaardenburgh P, Bech GJ, De Bruyne B, Pijls NH. Deferral vs. performance of percutaneous coronary intervention of functionally non-significant coronary stenosis: 15-year follow-up of the DEFER trial. Eur Heart J. 2015 Dec 1;36(45):3182-8.

13. De Bruyne B, Fearon WF, Pijls NH, Barbato E, Tonino P, Piroth Z, Jagic N, Mobius-Winckler S, Rioufol G, Witt N, Kala P, MacCarthy P, Engström T, Oldroyd K, Mavromatis K, Manoharan G, Verlee P, Frobert O, Curzen N, Johnson JB, Limacher A, Nüesch E, Jüni P; FAME 2 Trial Investigators. Fractional flow reserve-guided PCI for

stable coronary artery disease. N Engl J Med. 2014 Sep 25;371(13):1208-17.

14. van Nunen LX, Zimmermann FM, Tonino PA, Barbato E, Baumbach A, Engstrøm T, Klauss V, MacCarthy PA, Manoharan G, Oldroyd KG, Ver Lee PN, Van't Veer M, Fearon WF, De Bruyne B, Pijls NH; FAME Study Investigators. Fractional flow reserve versus angiography for guidance of PCI in patients with multivessel coronary artery disease (FAME): 5-year follow-up of a randomised controlled trial. Lancet. 2015 Nov 7;386(10006):1853-60.

15. Xaplanteris P, Fournier S, Pijls NHJ, Fearon WF, Barbato E, Tonino PAL, Engstrøm T, Kääb S, Dambrink JH, Rioufol G, Toth GG, Piroth Z, Witt N, Fröbert O, Kala P, Linke A, Jagic N, Mates M, Mavromatis K, Samady H, Irimpen A, Oldroyd K, Campo G, Rothenbühler M, Jüni P, De Bruyne B; FAME 2 Investigators. Five-Year Outcomes with PCI Guided by Fractional Flow Reserve. N Engl J Med. 2018 Jul 19;379(3):250-259.

16. Neumann FJ, Sousa-Uva M, Ahlsson A, Alfonso F, Banning AP, Benedetto U, Byrne RA, Collet JP, Falk V, Head SJ, Jüni P, Kastrati A, Koller A, Kristensen SD, Niebauer J, Richter DJ, Seferovic PM, Sibbing D, Stefanini GG, Windecker S, Yadav R, Zembala MO; ESC Scientific Document Group. 2018 ESC/EACTS Guidelines on myocardial revascularization. Eur Heart J. 2018 Aug 25.

17. Fihn SD, Gardin JM, Abrams J, Berra K, Blankenship JC, Dallas AP, Douglas PS, Foody JM, Gerber TC, Hinderliter AL, King SB 3rd, Kligfield PD, Krumholz HM, Kwong RY, Lim MJ, Linderbaum JA, Mack MJ, Munger MA, Prager RL, Sabik JF, Shaw LJ, Sikkema JD, Smith CR Jr, Smith SC Jr, Spertus JA, Williams SV. 2012 ACCF/AHA/ACP/AATS/PCNA/SCAI/STS Guideline for the Diagnosis and Management of Patients With Stable Ischemic Heart Disease: Executive Summary: A Report of the American College of Cardiology Foundation/American Heart Association Task Force on Practice Guidelines, and the American College of Physicians, American Association for Thoracic Surgery, Preventive Cardiovascular Nurses Association, Society for Cardiovascular Angiography and Interventions, and Society of Thoracic Surgeons. J Am Coll Cardiol. 2012 Dec 18;60(24):2564-603.

18. Toth GG, Toth B, Johnson NP, De Vroey F, Di Serafino L, Pyxaras S, Rusinaru D, Di Gioia G, Pellicano M, Barbato E, Van Mieghem C, Heyndrickx GR, De Bruyne B, Wijns W. Revascularization decisions in patients with stable angina and intermediate lesions: results of the international survey on interventional strategy. Circ Cardiovasc Interv. 2014 Dec;7(6):751-9.

19. Tebaldi M, Biscaglia S, Fineschi M, Musumeci G, Marchese A, Leone AM, Rossi ML, Stefanini G, Maione A, Menozzi A, Tarantino F, Lodolini V, Gallo F, Barbato E, Tarantini G, Campo G. Evolving Routine Standards in Invasive Hemodynamic Assessment of Coronary Stenosis: The Nationwide Italian SICI-GISE Cross-Sectional ERIS Study. JACC Cardiovasc Interv. 2018 Aug 13;11(15):1482-1491.

20. Murai T, Kanaji Y, Yonetsu T, Lee T, Matsuda J, Usui E, Araki M, Niida T, Isobe M, Kakuta T. Preprocedural fractional flow reserve and microvascular resistance predict increased hyperaemic coronary flow after elective percutaneous coronary intervention. Catheter Cardiovasc Interv. 2017 Feb 1;89(2):233-242.

21. Kern MJ, Dupouy P, Drury JH, Aguirre FV, Aptecar E, Bach RG, Caracciolo EA, Donohue TJ, Rande JL, Geschwind HJ, Mechem CJ, Kane G, Teiger E, Wolford TL. Role of coronary artery lumen enlargement in improving coronary blood flow after balloon angioplasty and stenting: a combined intravascular ultrasound Doppler flow and imaging study. J Am Coll Cardiol. 1997 Jun;29(7):1520-7.

22. Reis SE, Holubkov R, Lee JS, Sharaf B, Reichek N, Rogers WJ, Walsh EG, Fuisz AR, Kerensky R, Detre KM, Sopko G, Pepine CJ. Coronary flow velocity response to adenosine characterizes coronary microvascular function in women with chest pain and no obstructive coronary disease. Results from the pilot phase of the Women's Ischemia Syndrome Evaluation (WISE) study. J Am Coll Cardiol. 1999 May;33(6):1469-75.

23. Crea F, Camici PG, Bairey Merz CN. Coronary microvascular dysfunction: an update. Eur Heart J. 2014 May;35(17):1101-11.

24. Corcoran D, Young R, Adlam D, McConnachie A, Mangion K, Ripley D, Cairns D, Brown J, Bucciarelli-Ducci C, Baumbach A, Kharbanda R, Oldroyd KG, McCann GP, Greenwood JP, Berry C. Coronary microvascular dysfunction in patients with stable coronary artery disease: The CE-MARC 2 coronary physiology sub-study. Int J Cardiol. 2018 Sep 1;266:7-14.

25. Rösner A, Avenarius D, Malm S, Iqbal A, Baltabaeva A, Sutherland GR, Bijnens B, Myrmel T. Persistent dysfunction of viable myocardium after revascularization in chronic ischaemic heart disease: implications for dobutamine stress echocardiography with longitudinal systolic strain and strain rate measurements. Eur Heart J Cardiovasc Imaging. 2012 Sep;13(9):745-55.

26. Johnson NP, Kirkeeide RL, Gould KL. Is discordance of coronary flow reserve and fractional flow reserve due to methodology or clinically relevant coronary pathophysiology? JACC Cardiovasc Imaging. 2012 Feb;5(2):193-202.

27. Ahn SG, Suh J, Hung OY, Lee HS, Bouchi YH, Zeng W, Gandhi R, Eshtehardi P, Gogas BD, Samady H. Discordance Between Fractional Flow Reserve and Coronary Flow Reserve: Insights From Intracoronary Imaging and Physiological Assessment. JACC Cardiovasc Interv. 2017 May 22;10(10):999-1007.

28. Fearon WF, Balsam LB, Farouque HM, Caffarelli AD, Robbins RC, Fitzgerald PJ, Yock PG, Yeung AC. Novel index for invasively assessing the coronary microcirculation. Circulation. 2003 Jul 1;107(25):3129-32.

29. Yong AS, Layland J, Fearon WF, Ho M, Shah MG, Daniels D, Whitbourn R, Macisaac A, Kritharides L, Wilson A, Ng MK. Calculation of the index of microcirculatory resistance without coronary wedge pressure measurement in the presence of epicardial stenosis. JACC Cardiovasc Interv. 2013 Jan;6(1):53-8.

30. Fearon WF, Low AF, Yong AS, McGeoch R, Berry C, Shah MG, Ho MY, Kim HS, Loh JP, Oldroyd KG. Prognostic value of the Index of

Microcirculatory Resistance measured after primary percutaneous coronary intervention. Circulation. 2013 Jun 18;127(24):2436-41.

31. Melikian N, Vercauteren S, Fearon WF, Cuisset T, MacCarthy PA, Davidavicius G, Aarnoudse W, Bartunek J, Vanderheyden M, Wyffels E, Wijns W, Heyndrickx GR, Pijls NH, De Bruyne B. Quantitative assessment of coronary microvascular function in patients with and without epicardial atherosclerosis. EuroIntervention. 2010 Apr;5(8):939-45.

32. Lee JM, Layland J, Jung JH, Lee HJ, Echavarria-Pinto M, Watkins S, Yong AS, Doh JH, Nam CW, Shin ES, Koo BK, Ng MK, Escaned J, Fearon WF, Oldroyd KG. Integrated physiologic assessment of ischemic heart disease in real-world practice using index of microcirculatory resistance and fractional flow reserve: insights from the International Index of Microcirculatory Resistance Registry. Circ Cardiovasc Interv. 2015 Nov;8(11):e002857.

33. Fearon WF, Aarnoudse W, Pijls NH, De Bruyne B, Balsam LB, Cooke DT, Robbins RC, Fitzgerald PJ, Yeung AC, Yock PG. Microvascular resistance is not influenced by epicardial coronary artery stenosis severity: experimental validation. Circulation. 2004 May 18;109(19):2269-72.

34. Aarnoudse W, Fearon WF, Manoharan G, Geven M, van de Vosse F, Rutten M, De Bruyne B, Pijls NH. Epicardial stenosis severity does not affect minimal microcirculatory resistance. Circulation. 2004 Oct 12;110(15):2137-42.

35. Ng MK, Yeung AC, Fearon WF. Invasive assessment of the coronary microcirculation: superior reproducibility and less hemodynamic dependence of index of microcirculatory resistance compared with coronary flow reserve. Circulation. 2006 May 2;113(17):2054-61.

36. Xaplanteris P, Fournier S, Keulards DCJ, Adjedj J, Ciccarelli G, Milkas A, Pellicano M, Van't Veer M, Barbato E, Pijls NHJ, De Bruyne B. Catheter-Based Measurements of Absolute Coronary Blood Flow and Microvascular Resistance: Feasibility, Safety, and Reproducibility in Humans. Circ Cardiovasc Interv. 2018 Mar;11(3):e006194.

37. De Bruyne B, Adjedj J, Xaplanteris P, Ferrara A, Mo Y, Penicka M, Floré V, Pellicano M, Toth G, Barbato E, Duncker DJ, Pijls NH. Saline-Induced Coronary Hyperemia: Mechanisms and Effects on Left Ventricular Function. Circ Cardiovasc Interv. 2017 Apr;10(4). pii: e004719.

38. Pijls NH, van Schaardenburgh P, Manoharan G, Boersma E, Bech JW, van't Veer M, Bär F, Hoorntje J, Koolen J, Wijns W, De Bruyne B. Percutaneous coronary intervention of functionally nonsignificant stenosis: 5-year follow-up of the DEFER Study. J Am Coll Cardiol. 2007 May 29;49(21):2105-11.

39. Tonino PA, De Bruyne B, Pijls NH, Siebert U, Ikeno F, van' t Veer M, Klauss V, Manoharan G, Engstrøm T, Oldroyd KG, Ver Lee PN, MacCarthy PA, Fearon WF; FAME Study Investigators. Fractional flow reserve versus angiography for guiding percutaneous coronary intervention. N Engl J Med. 2009 Jan 15;360(3):213-24.

40. Toth GG, Johnson NP, Jeremias A, Pellicano M, Vranckx P, Fearon WF, Barbato E, Kern MJ, Pijls NH, De Bruyne B. Standardization of Fractional Flow Reserve Measurements. J Am Coll Cardiol. 2016 Aug 16;68(7):742-53.

41. Adjedj J, Toth GG, Johnson NP, Pellicano M, Ferrara A, Floré V, Di Gioia G, Barbato E, Muller O, De Bruyne B. Intracoronary Adenosine: Dose-Response Relationship With Hyperemia. JACC Cardiovasc Interv. 2015 Sep;8(11):1422-30.

42. Duncker DJ, Bache RJ. Regulation of coronary blood flow during exercise. Physiol Rev. 2008;88:1009–1086.

43. Parent R, Paré R, Lavallée M. Contribution of nitric oxide to dilation of resistance coronary vessels in conscious dogs. Am J Physiol. 1992;262(1 pt 2):H10–H16.

44. Altman JD, Kinn J, Duncker DJ, Bache RJ. Effect of inhibition of nitric oxide formation on coronary blood flow during exercise in the dog. Cardiovasc Res. 1994;28:119–124.

45. Duffy SJ, Castle SF, Harper RW, Meredith IT. Contribution of vasodilator prostanoids and nitric oxide to resting flow, metabolic vasodilation, and flow-mediated dilation in human coronary circulation. Circulation. 1999 Nov 9;100(19):1951-7.

46. Friedman PL, Brown EJ Jr, Gunther S, Alexander RW, Barry WH, Mudge GH Jr, Grossman W. Coronary vasoconstrictor effect of indomethacin in patients with coronary-artery disease. N Engl J Med. 1981 Nov 12;305(20):1171-5.

47. De Bruyne B, Pijls NH, Bartunek J, Kulecki K, Bech JW, De Winter H, Van Crombrugge P, Heyndrickx GR, Wijns W. Fractional flow reserve in patients with prior myocardial infarction. Circulation. 2001;104:157–162.

48. Johnson NP, Tóth GG, Lai D, Zhu H, Açar G, Agostoni P, Appelman Y, Arslan F, Barbato E, Chen SL, Di Serafino L, Domínguez-Franco AJ, Dupouy P, Esen AM, Esen OB, Hamilos M, Iwasaki K, Jensen LO, Jiménez-Navarro MF, Katritsis DG, Kocaman SA, Koo BK, López-Palop R, Lorin JD, Miller LH, Muller O, Nam CW, Oud N, Puymirat E, Rieber J, Rioufol G, Rodés-Cabau J, Sedlis SP, Takeishi Y, Tonino PA, Van Belle E, Verna E, Werner GS, Fearon WF, Pijls NH, De Bruyne B, Gould KL. Prognostic value of fractional flow reserve: linking physiologic severity to clinical outcomes. J Am Coll Cardiol. 2014 Oct 21;64(16):1641-54.

49. Ciccarelli G, Barbato E, Toth GG, Gahl B, Xaplanteris P, Fournier S, Milkas A, Bartunek J, Vanderheyden M, Pijls N, Tonino P, Fearon WF, Jüni P, De Bruyne B. Angiography Versus Hemodynamics to Predict the Natural History of Coronary Stenoses: Fractional Flow

Reserve Versus Angiography in Multivessel Evaluation 2 Substudy. Circulation. 2018 Apr 3;137(14):1475-1485.

50. Gould KL, Lipscomb K. Effects of coronary stenoses on coronary flow reserve and resistance. Am J Cardiol. 1974 Jul;34(1):48-55.

51. Park SJ, Kang SJ, Ahn JM, Shim EB, Kim YT, Yun SC, Song H, Lee JY, Kim WJ, Park DW, Lee SW, Kim YH, Lee CW, Mintz GS, Park SW. Visual-functional mismatch between coronary angiography and fractional flow reserve. JACC Cardiovasc Interv. 2012 Oct;5(10):1029-36.

52. Xaplanteris P, Ntalianis A, De Bruyne B, Strisciuglio T, Pellicano M, Ciccarelli G, Milkas A, Barbato E. Coronary lesion progression as assessed by fractional flow reserve (FFR) and angiography. EuroIntervention. 2018 May 15. pii: EIJ-D-17-00872.

53. Johnson NP, Johnson DT, Kirkeeide RL, Berry C, De Bruyne B, Fearon WF, Oldroyd KG, Pijls NHJ, Gould KL. Repeatability of Fractional Flow Reserve Despite Variations in Systemic and Coronary Hemodynamics. JACC Cardiovasc Interv. 2015 Jul;8(8):1018-1027.

54. Matsumura M, Johnson NP, Fearon WF, Mintz GS, Stone GW, Oldroyd KG, De Bruyne B, Pijls NHJ, Maehara A, Jeremias A. Accuracy of Fractional Flow Reserve Measurements in Clinical Practice: Observations From a Core Laboratory Analysis. JACC Cardiovasc Interv. 2017 Jul 24;10(14):1392-1401.

55. Morris PD, van de Vosse FN, Lawford PV, Hose DR, Gunn JP. “Virtual” (computed) fractional flow reserve: current challenges and limitations. JACC Cardiovasc Interv. 2015;8:1009–1017.

56. Tu S, Bourantas CV, Nørgaard BL, Kassab GS, Koo BK, Reiber JH. Image-based assessment of fractional flow reserve. EuroIntervention. 2015;11 Suppl V:V50-4.

57. Morris PD, Ryan D, Morton AC, Lycett R, Lawford PV, Hose DR, Gunn JP. Virtual fractional flow reserve from coronary angiography: modeling the significance of coronary lesions: results from the VIRTU-1 (VIRTUal Fractional Flow Reserve From Coronary Angiography) study. JACC Cardiovasc Interv. 2013;6:149–157.

58. Papafaklis MI, Muramatsu T, Ishibashi Y, Lakkas LS, Nakatani S, Bourantas CV, Ligthart J, Onuma Y, Echavarria-Pinto M, Tsirka G, Kotsia A, Nikas DN, Mogabgab O, van Geuns RJ, Naka KK, Fotiadis DI, Brilakis ES, Garcia-Garcia HM, Escaned J, Zijlstra F, Michalis LK, Serruys PW. Fast virtual functional assessment of intermediate coronary lesions using routine angiographic data and blood flow simulation in humans: comparison with pressure wire - fractional flow reserve. EuroIntervention. 2014;10:574–583.

59. Taylor CA, Fonte TA, Min JK. Computational fluid dynamics applied to cardiac computed tomography for noninvasive quantification of fractional flow reserve: scientific basis. J Am Coll Cardiol. 2013;61:2233–2241.

60. Tu S, Barbato E, Köszegi Z, Yang J, Sun Z, Holm NR, Tar B, Li Y, Rusinaru D, Wijns W, Reiber JH. Fractional Flow Reserve Calculation From 3-Dimensional Quantitative Coronary Angiography and TIMI Frame Count: A Fast Computer Model to Quantify the Functional Significance of Moderately Obstructed Coronary Arteries. JACC Cardiovasc Interv. 2014 Jul;7(7):768-77.

61. Huo Y, Kassab GS. Intraspecific scaling laws of vascular trees. J R Soc Interface. 2012;9:190–200.

62. Molloi S, Wong JT. Regional blood flow analysis and its relationship with arterial branch lengths and lumen volume in the coronary arterial tree. Phys Med Biol. 2007;52:1495–1503.

63. Takarada S, Zhang Z, Molloi S. An angiographic technique for coronary fractional flow reserve measurement: in vivo validation. Int J Cardiovasc Imaging. 2013;29:535–544.

64. Mangiacapra F, Patti G, Barbato E, Peace AJ, Ricottini E, Vizzi V, Gatto L, D'Ambrosio A, De Bruyne B, Wijns W, Di Sciascio G. A therapeutic window for platelet reactivity for patients undergoing elective percutaneous coronary intervention: results of the ARMYDA-PROVE (Antiplatelet therapy for Reduction of MYocardial Damage during Angioplasty-Platelet Reactivity for Outcome Validation Effort) study. JACC Cardiovasc Interv. 2012 Mar;5(3):281-9.

65. Tantry US, Bonello L, Aradi D, Price MJ, Jeong YH, Angiolillo DJ, Stone GW, Curzen N, Geisler T, Ten Berg J, Kirtane A, Siller-Matula J, Mahla E, Becker RC, Bhatt DL, Waksman R, Rao SV, Alexopoulos D, Marcucci R, Reny JL, Trenk D, Sibbing D, Gurbel PA; Working Group on On-Treatment Platelet Reactivity. Consensus and update on the definition of on-treatment platelet reactivity to adenosine diphosphate associated with ischemia and bleeding. J Am Coll Cardiol. 2013 Dec 17;62(24):2261-73.

66. Mangiacapra F, Bartunek J, Bijnens N, Peace AJ, Dierickx K, Bailleul E, Di Serafino L, Pyxaras SA, Fraeyman A, Meeus P, Rutten M, De Bruyne B, Wijns W, van de Vosse F, Barbato E. Periprocedural variations of platelet reactivity during elective percutaneous coronary intervention. J Thromb Haemost. 2012 Dec;10(12):2452-61.

67. Braunwald E, Angiolillo D, Bates E, Berger PB, Bhatt D, Cannon CP, Furman MI, Gurbel P, Michelson AD, Peterson E, Wiviott S. The problem of persistent platelet activation in acute coronary syndromes and following percutaneous coronary intervention. Clin Cardiol. 2008 Mar;31(3 Suppl 1):I17-20.

68. Mangiacapra F, De Bruyne B, Muller O, Trana C, Ntalianis A, Bartunek J, Heyndrickx G, Di Sciascio G, Wijns W, Barbato E. High residual platelet reactivity after clopidogrel: extent of coronary atherosclerosis and periprocedural myocardial infarction in patients with stable angina undergoing percutaneous coronary intervention. JACC Cardiovasc Interv. 2010 Jan;3(1):35-40.

69. Legrand V, Cuisset T, Chenu P, Vrolix M, Martinez C, Dens J, Gach O, Boland J, Claeys MJ, Magne J, Barbato E, Wijns W. Platelet reactivity and cardiovascular events after percutaneous coronary intervention in patients with stable coronary artery disease: the Stent Thrombosis In Belgium (STIB) trial. EuroIntervention. 2014 Jun;10(2):204-11.

70. Brugaletta S, Gogas BD, Garcia-Garcia HM, Farooq V, Girasis C, Heo JH, van Geuns RJ, de Bruyne B, Dudek D, Koolen J, Smits P, Veldhof S, Rapoza R, Onuma Y, Ormiston J, Serruys PW. Vascular compliance changes of the coronary vessel wall after bioresorbable vascular scaffold implantation in the treated and adjacent segments. Circ J. 2012;76(7):1616-23.

71. Serruys PW, Garcia-Garcia HM, Onuma Y. From metallic cages to transient bioresorbable scaffolds: change in paradigm of coronary revascularization in the upcoming decade? Eur Heart J. 2012 Jan;33(1):16-25b.

72. Oberhauser JP, Hossainy S, Rapoza RJ. Design principles and performance of bioresorbable polymeric vascular scaffolds. EuroIntervention. 2009 Dec 15;5 Suppl F:F15-22.

73. Bangalore S, Bezerra HG, Rizik DG, Armstrong EJ, Samuels B, Naidu SS, Grines CL, Foster MT, Choi JW, Bertolet BD, Shah AP, Torguson R, Avula SB, Wang JC, Zidar JP, Maksoud A, Kalyanasundaram A, Yakubov SJ, Chehab BM, Spaedy AJ, Potluri SP, Caputo RP, Kondur A, Merritt RF, Kaki A, Quesada R, Parikh MA, Toma C, Matar F, DeGregorio J, Nicholson W, Batchelor W, Gollapudi R, Korngold E, Sumar R, Chrysant GS, Li J, Gordon JB, Dave RM, Attizzani GF, Stys TP, Gigliotti OS, Murphy BE, Ellis SG, Waksman R. The State of the Absorb Bioresorbable Scaffold: Consensus From an Expert Panel. JACC Cardiovasc Interv. 2017 Dec 11;10(23):2349-2359.

74. Thondapu V, Tenekecioglu E, Poon EKW, Collet C, Torii R, Bourantas CV, Chin C, Sotomi Y, Jonker H, Dijkstra J, Revalor E, Gijsen F, Onuma Y, Ooi A, Barlis P, Serruys PW. Endothelial shear stress 5 years after implantation of a coronary bioresorbable scaffold. Eur Heart J. 2018 Feb 2. doi: 10.1093/eurheartj/ehx810.

75. Tenekecioglu E, Torii R, Bourantas C, Abdelghani M, Cavalcante R, Sotomi Y, Crake T, Su S, Santoso T, Onuma Y, Serruys PW. Assessment of the hemodynamic characteristics of Absorb BVS in a porcine coronary artery model. Int J Cardiol. 2017 Jan 15;227:467-473.

76. Bourantas CV, Papafaklis MI, Kotsia A, Farooq V, Muramatsu T, Gomez-Lara J, Zhang YJ, Iqbal J, Kalatzis FG, Naka KK, Fotiadis DI, Dorange C, Wang J, Rapoza R, Garcia-Garcia HM, Onuma Y, Michalis LK, Serruys PW. Effect of the endothelial shear stress patterns on neointimal proliferation following drug-eluting bioresorbable vascular scaffold implantation: an optical coherence tomography study. JACC Cardiovasc Interv. 2014 Mar;7(3):315-24.

77. Waksman R, Lipinski MJ, Acampado E, Cheng Q, Adams L, Torii S, Gai J, Torguson R, Hellinga DM, Westman PC, Joner M, Zumstein P, Kolodgie FD, Virmani R. Comparison of Acute Thrombogenicity for Metallic and Polymeric Bioabsorbable Scaffolds: Magmaris Versus Absorb in a Porcine Arteriovenous Shunt Model. Circ Cardiovasc Interv. 2017 Aug;10(8). pii: e004762.

78. Wykrzykowska JJ, Kraak RP, Hofma SH, van der Schaaf RJ, Arkenbout EK, IJsselmuiden AJ, Elias J, van Dongen IM, Tijssen RYG, Koch KT, Baan J Jr, Vis MM, de Winter RJ, Piek JJ, Tijssen JGP, Henriques JPS; AIDA Investigators. Bioresorbable Scaffolds versus Metallic Stents in Routine PCI. N Engl J Med. 2017 Jun 15;376(24):2319-2328.

79. Capodanno D, Gori T, Nef H, Latib A, Mehilli J, Lesiak M, Caramanno G, Naber C, Di Mario C, Colombo A, Capranzano P, Wiebe J, Araszkiewicz A, Geraci S, Pyxaras S, Mattesini A, Naganuma T, Münzel T, Tamburino C. Percutaneous coronary intervention with everolimus-eluting bioresorbable vascular scaffolds in routine clinical practice: early and midterm outcomes from the European multicentre GHOST-EU registry. EuroIntervention. 2015 Feb;10(10):1144-53.

80. Stone GW, Abizaid A, Onuma Y, Seth A, Gao R, Ormiston J, Kimura T, Chevalier B, Ben-Yehuda O, Dressler O, McAndrew T, Ellis SG, Kereiakes DJ, Serruys PW. Effect of Technique on Outcomes Following Bioresorbable Vascular Scaffold Implantation: Analysis From the ABSORB Trials. J Am Coll Cardiol. 2017 Dec 12;70(23):2863-2874.

81. Suwannasom P, Sotomi Y, Ishibashi Y, Cavalcante R, Albuquerque FN, Macaya C, Ormiston JA, Hill J, Lang IM, Egred M, Fajadet J, Lesiak M, Tijssen JG, Wykrzykowska JJ, de Winter RJ, Chevalier B, Serruys PW, Onuma Y. The Impact of Post-Procedural Asymmetry, Expansion, and Eccentricity of Bioresorbable Everolimus-Eluting Scaffold and Metallic Everolimus-Eluting Stent on Clinical Outcomes in the ABSORB II Trial. JACC Cardiovasc Interv. 2016 Jun 27;9(12):1231-42.

82. Ishibashi Y, Muramatsu T, Nakatani S, Sotomi Y, Suwannasom P, Grundeken MJ, Cho YK, Garcia-Garcia HM, van Boven AJ, Piek JJ, Sabaté M, Helqvist S, Baumbach A, McClean D, de Sousa Almeida M, Wasungu L, Miquel-Hebert K, Dudek D, Chevalier B, Onuma Y, Serruys PW. Incidence and Potential Mechanism(s) of Post-Procedural Rise of Cardiac Biomarker in Patients With Coronary Artery Narrowing After Implantation of an Everolimus-Eluting Bioresorbable Vascular Scaffold or Everolimus-Eluting Metallic Stent. JACC Cardiovasc Interv. 2015 Jul;8(8):1053-1063.

83. Y-Hassan S, Lindroos MC, Sylvén C. A Novel Descriptive, Intelligible and Ordered (DINO) classification of coronary bifurcation lesions. Review of current classifications. Circ J. 2011;75(2):299-305. Epub 2010 Dec 24.

84. Sawaya FJ, Lefèvre T, Chevalier B, Garot P, Hovasse T, Morice MC, Rab T, Louvard Y. Contemporary Approach to Coronary Bifurcation Lesion Treatment. JACC Cardiovasc Interv. 2016 Sep 26;9(18):1861-78.

85. Burzotta F, Lassen JF, Banning AP, Lefèvre T, Hildick-Smith D, Chieffo A, Darremont O, Pan M, Chatzizisis YS, Albiero R, Louvard Y, Stankovic G. Percutaneous coronary intervention in left main coronary artery disease: the 13th consensus document from the European Bifurcation Club. Burzotta F, Lassen JF, Banning AP, Lefèvre T, Hildick-Smith D, Chieffo A, Darremont O, Pan M, Chatzizisis YS, Albiero R, Louvard Y, Stankovic G. EuroIntervention. 2018 May 20;14(1):112-120.

86. Kawasaki T, Koga H, Serikawa T. Modified culotte stenting technique for bifurcation lesions: the cross-stenting technique. J Invasive Cardiol. 2010 May;22(5):243-6.

87. Toth GG, Pyxaras S, Mortier P, De Vroey F, Di Gioia G, Adjedj J, Pellicano M, Ferrara A, De Schryver T, Van Hoorebeke L, Verhegghe B, Barbato E, De Bruyne B, De Beule M, Wijns W. Single String Technique for Coronary Bifurcation Stenting: Detailed Technical Evaluation and Feasibility Analysis. JACC Cardiovasc Interv. 2015 Jun;8(7):949-59.

88. Attizzani GF, Capodanno D, Ohno Y, Tamburino C. Mechanisms, pathophysiology, and clinical aspects of incomplete stent apposition. J Am Coll Cardiol. 2014 Apr 15;63(14):1355-67.

89. Radu M, Jørgensen E, Kelbæk H, Helqvist S, Skovgaard L, Saunamäki K. Optical coherence tomography at follow-up after percutaneous coronary intervention: relationship between procedural dissections, stent strut malapposition and stent healing. EuroIntervention. 2011 Jul;7(3):353-61.

90. Kim JS, Ha J, Kim BK, Shin DH, Ko YG, Choi D, Jang Y, Hong MK. The relationship between post-stent strut apposition and follow-up strut coverage assessed by a contour plot optical coherence tomography analysis. JACC Cardiovasc Interv. 2014 Jun;7(6):641-51.

91. Foin N, Alegria-Barrero E, Torii R, Chan PH, Viceconte N, Davies JE, Di Mario C. Crush, culotte, T and protrusion: which 2-stent technique for treatment of true bifurcation lesions? - insights from in vitro experiments and micro-computed tomography. Circ J. 2013;77(1):73-80.

92. Hildick-Smith D, de Belder AJ, Cooter N, Curzen NP, Clayton TC, Oldroyd KG, Bennett L, Holmberg S, Cotton JM, Glennon PE, Thomas MR, Maccarthy PA, Baumbach A, Mulvihill NT, Henderson RA, Redwood SR, Starkey IR, Stables RH. Randomized trial of simple versus complex drug-eluting stenting for bifurcation lesions: the British Bifurcation Coronary Study: old, new, and evolving strategies. Circulation. 2010 Mar 16;121(10):1235-43.

93. Tyczynski P, Ferrante G, Moreno-Ambroj C, Kukreja N, Barlis P, Pieri E, De Silva R, Beatt K, Di Mario C. Simple versus complex approaches to treating coronary bifurcation lesions: direct assessment of stent strut apposition by optical coherence tomography. Rev Esp Cardiol. 2010 Aug;63(8):904-14.

94. Bennett J, Vanhaverbeke M, Vanden Driessche N, Hiltrop N, Adriaenssens T, Desmet W, Sinnaeve P, Dubois C. The drug-eluting resorbable magnesium vascular scaffold in complex coronary

bifurcations: insights from an in vivo multimodality imaging study. EuroIntervention. 2018 Apr 20;13(17):2036-2046.

95. Grundeken MJ, Wykrzykowska JJ, Ishibashi Y, Garg S, de Vries T, Garcia-Garcia HM, Onuma Y, de Winter RJ, Buszman P, Linke A, Ischinger T, Klauss V, Eberli F, Corti R, Wijns W, Morice MC, Di Mario C, Meier B, Jüni P, Yazdani A, Copt S, Windecker S, Serruys PW. First generation versus second generation drug-eluting stents for the treatment of bifurcations: 5-year follow-up of the LEADERS all-comers randomized trial. Catheter Cardiovasc Interv. 2016 Jun;87(7):E248-60.

Curriculum Vitae

PERSONAL INFORMATION

MARIANO PELLICANO

Riemstraat 22, bus 21, 2000 Antwerp (Belgium)

0039098132046 0032468202321 (Belgian) - 00393491661040 (Italian)

marianopellicano@libero.it

Skype contact: mariano.pellicano1

Date of birth 28/09/1981 Nationality Italian

Job applied for **Interventional Cardiologist**

CURRENT POSITIONS

January 2018 - Present

Resident Interventional Cardiology

Cardiovascular Center Aalst, OLV Hospital, Moorselbaan n 164, B 9300 Aalst, Belgium (Chief: Dr. Bernard De Bruyne).

November 2015 - Present

PhD Fellow in Cardiovascular Pathophysiology and Therapeutics (CardioPath)

Joint Academic Consortium

1) University of Naples Federico II, Italy;
2) Clinica Montevergine Mercogliano (AV), Italy;
3) **Cardiovascular Center Aalst, OLV Hospital, Aalst, Belgium;**
4) Inselspital, University Hospital, Bern, Switzerland.

WORK EXPERIENCE

January 2017 – December 2017

Clinical & Research Fellow in Interventional Cardiology

PhD Program in Cardiovascular Pathophysiology and Therapeutics Montevergine Clinic, Via Mario Malzoni, 5, 83013 Mercogliano AV, Italy (Chief: Dr. Tullio Tesorio).

January 2015 – October 2015

Master of Science in Diagnostic Cardiac Imaging

"Sapienza" University of Rome, Policlinico Umberto I, Rome, Italy - Cardiovascular Center Aalst, OLV Hospital, Aalst, Belgium, with the maximal score of 110/110 cum laude, with a thesis entitled: "*Optical Coherence Tomography Imaging during percutaneous coronary intervention impacts physician decision-making: single center experience of ILUMIEN I study*", Supervisors Prof. Carlo Gaudio ("Sapienza" University of Rome), Prof. William Wijns (Cardiovascular Center Aalst, OLV Hospital, Aalst Belgium) and Prof. Emanuele Barbato ("Federico II" University of Naples - Cardiovascular Center Aalst, OLV Hospital, Aalst Belgium);

September 2013 – December 2016

Clinical & Research Fellow in Interventional Cardiology

Cardiovascular Center Aalst, OLV Hospital, Moorselbaan n 164, B 9300 Aalst, Belgium (Chief: Dr. Bernard De Bruyne).

July 2009 – July 2012

Experience of general physician

(Italy)

Doctor's ambulance and first aid service

(Italy)

EDUCATION AND TRAINING

July 2009 – July 2014	**Residency in Cardiology** "Sapienza" University of Rome, Policlinico Umberto I (Viale del Policlinico 155 Rome) (Director Prof. Francesco Fedele), with the maximal score of 70/70 cum laude, with a thesis entitled: "*Ruolo della valutazione funzionale invasiva (riserva di flusso frazionale o FFR) in pazienti candidati a by-pass aorto-coronarico*", Supervisors Prof. Enrico Mangieri ("Sapienza" University of Rome) and Prof. Emanuele Barbato ("Federico II" University of Naples - Cardiovascular Center Aalst, OLV Clinic, Aalst (Belgium);
September 2011 - July 2013	**Practice and training in Interventional Cardiology Unit** "Sapienza" University of Rome, Policlinico Umberto I (Chief Prof. Enrico Mangieri).
August 2010 - August 2011	**Practice and training in Coronary Intensive Care Unit, echocardiography and Holter**
July 2009 - July 2010	**Practice and training in Clinical Cardiology, ergometry, Holter, basic echocardiography, stress echocardiography and tilt test**
August 2008 - October 2008	**Internship in Interventional Cardiology** Interventional Cardiology Unit, Hospital of São Josè do Rio Preto, Medical School of São Josè do Rio Preto (SP, Brasil) (Chief: Prof. Moacir Fernandes de Godoy);
April 2nd 2008 - June 30th 2008	**Internship evaluation for the National certification to the Medical Profession**
March 18th, 2008	**Medical degree cum laude** I Faculty of Medicine, "Sapienza" University of Rome, with a thesis entitled: "*Correlation between serum levels of PRO-BNP and Anti-tissue Transglutaminase Antibodies on the development of Left Ventricular Remodeling after Acute Myocardial Infarction*", Supervisor Prof. Francesco Barillà;
November 2004 - March 2008	**Elective Internship for graduation thesis** Coronary Intensive Care Unit (Chief Prof. Francesco Barillà) of the Department Heart and Great Vessels "Attilio Reale", Policlinico Umberto I, "Sapienza" University of Rome;

CERTIFICATIONS

February 14th, 2018	Certificate of training ICH-GCP (Novartis)
January 12th, 2018	Belgian cardiology board (RIZIV number 148733-65-730)
March 2013 – Present	Belgian medical board (VISA number 58265)
July 2013 – Present	East Flanders medical board (VISA number 48733)
July 17th, 2008	National (Italian) Certification for the medical profession
April 19th, 2005	Qualification of "BLSD performer", issued by Center of Training for Cardio-pulmonary Resuscitation (CPR), Chief Professor Igino Genuini, Department of Cardiovascular and Respiratory Sciences (Director Prof. Francesco Fedele).

AWARDS AND GRANT AWARDS

May 22nd, 2015	"Raffaele Mattioli" Award 2015, for young investigator grown to the Department Heart and Great Vessels "Attilio Reale", Policlinico Umberto I, "Sapienza" University of Rome;

REVIEWER FOR THE FOLLOWING JOURNALS

- European Heart Journal
- Catheterization and Cardiovascular Interventions
- European Heart Journal - Cardiovascular Imaging
- Eurointervention
- BMC Cardiovascular Disorders
- Journal of Cardiovascular Medicine
- Journal of Cardiovascular Translational Research
- Coronary Artery Disease
- Advances in Interventional Cardiology
- Clinical Medical Reviews and Case Reports
- International Journal of Clinical Cardiology
- Journal of Cardiovascular Medicine and Cardiology

MAIN RESEARCH PROJECTS

June 2018 - Present

Member of the Independent Clinical Event Committee/Safety Monitoring Board for the INCORPORATE trial

INtentional COronary Revascularization versus conservative therapy in Patients undergOing peripheral arTEry revascularization due to critical limb ischemia (INCORPORATE trial).

May 2018 - Present

Sub-investigator of the PIONEER III Trial

A Prospective Global Randomized Trial Assessing the Safety and Efficacy of the BuMA Supreme™ Biodegradable Drug Coated Coronary Stent System for Coronary Revascularization in Patients With Stable Coronary Artery Disease or Non-ST Segment Elevation Acute Coronary Syndromes

April 2018 - Present

Sub-investigator of the MASTER-DAPT Trial

Management of High Bleeding Risk Patients Post Bioresorbable Polymer Coated Stent Implantation With an Abbreviated Versus Prolonged DAPT Regimen

February 2018 - Present	Sub-investigator of the XIENCE 28 Global Study Prospective, single arm, multi-center, open label, non-randomized trial to evaluate the safety of 1-month dual antiplatelet therapy in subjects at high risk of bleeding (HBR) undergoing PCI with the approved XIENCE family.
July 2015 - Present	Sub-investigator of the POPular Genetics trial Cost-effectiveness of CYP2C19 genotype guided treatment with antiplatelet drugs in patients with ST-segment-elevation myocardial infarction undergoing immediate PCI with stent implantation: optimization of treatment" (POPular Genetis).
January 2015 – December 2016	Study Coordinator of the STRING registry Evaluation of a modified bifurcation stenting procedure technique.
May 2014 – April 2016	Study Coordinator of the GRAFFITI trial Graft Patency After FFR-guided versus Angio-guided CABG.
February 2014 – December 2016	Sub-investigator of the FFRangio Angiography based Fractional Flow Reserve (FFRangio) – Validation study.
December 2013 – April 2017	Co-investigator of the PROACTIVE trial PROcedure Related Platelet ACTIVation in Long Lesions Treated With Bioresorbable Vascular Scaffold Versus Xience Xpedition Implantation.
May 2010 – September 2013	Co-investigator of the SIGNIfY trial Study assessInG the morbidity–mortality beNefits of the If inhibitor ivabradine in patients with coronarY artery disease.
October 2008 – March 2009	Sub-investigator of the Multicenter, randomized, double-blind, parallel group study to evaluate the efficacy and safety of the association of Aliskiren / Amlodipine (300/5 mg and 300/10 mg) versus Aliskrien 300 mg in patients with essential hypertension not adequately controlled by Aliskiren 300 mg monotherapy".

Research areas of interest

- Coronary physiology (FFR, IMR) and imaging (OCT and 3D-QCA);
- Image-Based FFR during coronary catheterization;
- Platelet reactivity in patients with ACS and stable angina;
- Ventricular remodelling after ACS;
- Bioresorbable vascular scaffold;

MEMBERSHIPS

June 2018 - Present	Member of EAPCI Fellowship Committee 2018-2020
September 2014 – Present	Member of European Association of Percutaneous Cardiovascular Interventions (EAPCI)
April 2010 - Present	Member of Italian Society of Cardiology (SIC)

Mother tongue: Italian

Other language(s)	UNDERSTANDING		SPEAKING		WRITING
	Listening	Reading	Spoken interaction	Spoken production	
English	C1	C1	C1	C1	C1
Dutch	A2	A2	A2	A2	A2
Portuguese	A1	A1	A1	A1	A1

Levels: A1 and A2: Basic user - B1 and B2: Independent user - C1 and C2: Proficient user

Common European Framework of Reference for Languages

Computer skills: Excellent skills and knowledge of Internet use office suite

List of Publications

BOOK CHAPTERS

- *"Pressure-derived Fractional Flow Reserve (FFR)"*. Toth G.G., **Pellicano M**., De Bruyne B. Part IV, Chapter 30, Book "Coronary stenosis – Imaging, Structure and Physiology" – Second edition.

_ _ _ _ _ _ _ _ _ _ _ _ _ _ _ _ _ _ _ _

PEER-REVIEWED MANUSCRIPTS AND ABSTRACTS

- *"Second-generation drug-eluting stents versus bare-metal stents in saphenous vein grafts: is the choice more complicated than before?"*. **Pellicano M**, Azzano A, Barbato E. J Thorac Dis 2018 (in press).

- *"Mid-term outcomes after percutaneous interventions in coronary bifurcations"*. Zimarino M, Briguori C, MD, Amat-Santos IJ, Radico F, Barbato E, Chieffo A, Cirillo P, Costa R, Erglis A, Gamra H, Gil RJ, Kanic V, Kedev SA, Maddestra N, Nakamura S, **Pellicano M**, Petrov I, Strozzi M, Tesorio T, Vukcevic V, De Caterina R, Stankovic G, on behalf of the EuroBifurcation Club. Int J Cardiol. 2018 Dec (in press).

- *"Platelet Reactivity and Coronary Microvascular Impairment After Percutaneous Revascularization in Stable Patients Receiving Clopidogrel or Prasugrel".* Mangiacapra F, **Pellicano M**, Di Serafino L, Bressi E, Peace AJ, Di Gioia G, Morisco C, Bartunek J, Wijns W, De Bruyne B, Barbato E. Atherosclerosis. 2018 Aug 30;278:23-28.

- *"Impact of fractional flow reserve on surgical coronary revascularization strategy"*. Fournier S, Toth GG, De Bruyne B, Kala P, Ribichini FL, F Casselman F, Ramos R, Piroth Z, **Pellicano M**, C Van Mieghem C, Penicka M, Mates M, Van Praet F, Stockman B, Degriek I, Barbato E. European Heart Journal 2018, n Supplement nnn.

- *"Impact of fractional flow reserve on clinical management strategies in patients with heart failure and reduced ejection fraction"*. Di Gioia G, **Pellicano M**, Bartunek J, Xaplanteris P, Colaiori I, Fournier S, Fiordelisi A, Vanderheyden M, De Bruyne B, Barbato E. European Heart Journal 2018, n Supplement nnn.

- *"Non-uniform temporal evolution of FFR in intermediate coronary lesions: what matters?"*. Xaplanteris P, De Bruyne B, Strisciuglio T, **Pellicano M**, Fournier S, Ciccarelli G, Barbato E. EuroIntervention Supplement May 2018, Abstracts of EuroPCR Congress, Paris, 22-25 May 2018.

- *"From debulking to delivery: sequential use of rotational atherectomy and Guidezilla™ for complex saphenous vein grafts intervention"*. **Pellicano M**, Floré V, Barbato E, De Bruyne B. BMC Cardiovasc Disord. 2018 Jun 19;18(1):122.

- *"Coronary lesion progression as assessed by fractional flow reserve (FFR) and angiography"*. Xaplanteris P, Ntalianis A, De Bruyne B, Strisciuglio T, **Pellicano M**, Ciccarelli G, Milkas A, Barbato E. EuroIntervention. 2018 May 15. pii: EIJ-D-17-00872.

- *"Catheter-Based Measurements of Absolute Coronary Blood Flow and Microvascular Resistance. Feasibility, Safety, and Reproducibility in Humans"*. Xaplanteris P, Fournier S, Keulards DCJ, Adjedj J, Ciccarelli G, Milkas A, **Pellicano M**, van't Veer M, Barbato E, Pijls NHJ, De Bruyne B. Circ Cardiovasc Interv. 2018;11:e006194, originally published March 16, 2018.

- *"Edge effect after intracoronary beta radiation brachytherapy and bare metal stent implantation: the pathway for very late stent failure*". **Pellicano M**, Floré V, Ferrara A, Adjedj J, Barbato E, Wijns W. Minerva Cardioangiol. 2018 Feb;66(1):126-127.

- *"Angiography versus hemodynamic assessment to predict the natural history of coronary stenoses: a fractional flow reserve versus angiography in multivessel evaluation 2, (FAME 2)-substudy".* Ciccarelli G, Barbato E, Toth GG, **Pellicano M**, Xaplanteris P, Milkas A, S Fournier S, De Bruyne B. European Heart Journal 2017, 38 Supplement 415.

- *"Angiographic and hemodynamic modifications of Myocardial Bridge during supine bicycle exercise"*. Adjedj J, **Pellicano M**, Ferrara A, Xaplanteris P, Ciccarelli G, Viggiano A, Bartunek J, De Bruyne B, Barbato E. European Heart Journal 2017, 38 Supplement 383.

- *"Validation Study of Image-Based Fractional Flow Reserve During Coronary Angiography"*. **Pellicano M**, Lavi I, De Bruyne B, Vaknin-Assa H, Assali A, Valtzer O, Lotringer Y, Weisz G, Almagor Y, Xaplanteris P, Kirtane AJ, Codner P, Leon MB, Kornowski R. Circ Cardiovasc Interv. 2017 Sep;10(9).

- *"Visual and Quantitative Assessment of Coronary Stenoses at Angiography Versus Fractional Flow Reserve: The Impact of Risk Factors".* Adjedj J, Xaplanteris P, Toth G, Ferrara A, **Pellicano M**, Ciccarelli G, Floré V, Barbato E, De Bruyne B. Circ Cardiovasc Imaging. 2017 Jul;10(7). pii: e006243.

- *"Correlation between serum uric acid levels and residual platelet reactivity in patients undergoing PCI".* Ciccarelli G, Mangiacapra F, **Pellicano M**, Barbato E. Nutr Metab Cardiovasc Dis. 2017 May;27(5):470-471.

- *"Reversed single string technique for coronary bifurcation stenting-*

First report of case demonstrations in vitro". Adjedj J, Toth GG, **Pellicano M**, Wijns W. Catheter Cardiovasc Interv. 2017 May 16. doi: 10.1002/ccd.27113.

- *"Relative impact of clinical presentation, lesion complexity and planned strategy on 1-year outcomes after revascularisation with biologically active stents in the current management of coronary bifurcations: insights from the P2BiTO registry – bifurcation substudy".* Zimarino M, Briguori C, Amat-Santos IJ, Radico F, Barbato E, Chieffo A, Cirillo P, Costa R, Erglis A, Gamra H, Gil RJ, Kanic V, Kedev SA, Nakamura S, **Pellicano M**, Petrov I, Strozzi M, Tesorio T, Vukcevic V, Stankovic G. EuroIntervention Supplement May 2017, Abstracts of EuroPCR Congress, Paris, 16-19 May 2017.

- *"Detect FFR of epicardial stenosis with guiding catheter disengagement: DISENGAGE study"*. **Pellicano M**, Ciccarelli G, Xaplanteris P, Milkas A, Di Gioia G, Heyse A, Van Durme F, Vanderheyden M, Bartunek J, Van Mieghem C, Wijns W, De Bruyne B, Barbato E. EuroIntervention Supplement May 2017, Abstracts of EuroPCR Congress, Paris, 16-19 May 2017.

- *"Angiographic and haemodynamic modifications of myocardial bridge during supine bicycle exercise"*. Adjedj J, **Pellicano M**, Ferrara A, Xaplanteris P, Ciccarelli G, Bartunek J, De Bruyne B, Barbato E. EuroIntervention Supplement May 2017, Abstracts of EuroPCR Congress, Paris, 16-19 May 2017.

- *"STEMI and multivessel disease: predictors of non-culprit lesion revascularization"*. De Biase C, Di Gioia G, **Pellicano M**, Strisciuglio T, Barbato E. EuroIntervention Supplement May 2017, Abstracts of EuroPCR Congress, Paris, 16-19 May 2017.

- *"How do intermediate coronary lesions evolve over time? A morphological and functional retrospective, longitudinal study of 414 stenoses"*. Xaplanteris P, De Bruyne B, Strisciuglio T, Ciccarelli G, Milkas A, **Pellicano M**, Barbato E. EuroIntervention Supplement

May 2017, Abstracts of EuroPCR Congress, Paris, 16-19 May 2017.

- *"Online angiography-based FFR assessment during coronary catheterization"*. Kornowski R, Vaknin-Assa H, Assali A, **Pellicano M**, De Bruyne B. EuroIntervention Supplement May 2017, Abstracts of EuroPCR Congress, Paris, 16-19 May 2017.

- *"Angiography vs. haemodynamic assessment to predict the natural history of coronary stenoses: an FFR vs. angiography in multivessel evaluation 2 (FAME 2) substudy".* Ciccarelli G, Barbato E, Toth G, **Pellicano M**, Xaplanteris P, Milkas A, De Bruyne B. EuroIntervention Supplement May 2017, Abstracts of EuroPCR Congress, Paris, 16-19 May 2017.

- *"Saline-Induced Coronary Hyperemia: Mechanisms and Effects on Left Ventricular Function"*. De Bruyne B, Adjedj J, Xaplanteris P, Ferrara A, Mo Y, Penicka M, Floré V, **Pellicano M**, Toth G, Barbato E, Duncker DJ, Pijls NH. Circ Cardiovasc Interv. 2017 Apr;10(4).

- *"Correlation between serum uric acid levels and residual platelet reactivity in patients undergoing PCI"*. Ciccarelli G, Mangiacapra F, **Pellicano M**, Barbato E. Nutr Metab Cardiovasc Dis. 2017 Mar 4. pii: S0939-4753(17)30041-8.

- *"Platelet reactivity in patients carrying the e-NOS G894T polymorphism after a loading dose of aspirin plus clopidogrel"*. Strisciuglio T, Di Gioia G, Mangiacapra F, De Biase C, Delrue L, **Pellicano M**, Bartunek J, Vanderheyden M, Izzo R, Trimarco B, Wijns W, Barbato E. Thromb Res. 2017 Jan 27;151:72-73.

- *"Fractional flow reserve to guide and to assess coronary artery bypass grafting"*. **Pellicano M**, De Bruyne B, Toth GG, Casselman F, Wijns W, Barbato E. Eur Heart J. 2016 Dec 23.

- *"TCT-11 Diagnostic Accuracy of Fast Computational Approaches to Derive Fractional Flow Reserve from Diagnostic Coronary X-ray Angiography in the International Multicenter FAVOR (Functional Assessment by Various FlOw Reconstructions) Pilot Study"*. Tu S, Westra J, Yang J, von Birgelen C, Ferrara A, **Pellicano M**, Nef H, Tebaldi M, Murasato Y, Lansky A, Barbato E, van der Heijden L, Reiber J, Holm N, Wijns W. J Am Coll Cardiol. 2016 Nov 1;68(18S):B5.

- *"Fractional Flow Reserve Derived From Routine Coronary Angiograms"*. Kornowski R, Lavi I, **Pellicano M**, Xaplanteris P, Vaknin-Assa H, Assali A, Valtzer O, Lotringer Y, De Bruyne B. J Am Coll Cardiol. 2016 Nov 15;68(20):2235-2237.

- *"Diagnostic Accuracy of Fast Computational Approaches to Derive Fractional Flow Reserve From Diagnostic Coronary Angiography: The International Multicenter FAVOR Pilot Study"*. Tu S, Westra J, Yang J, von Birgelen C, Ferrara A, **Pellicano M**, Nef H, Tebaldi M, Murasato Y, Lansky A, Barbato E, van der Heijden LC, Reiber JH, Holm NR, Wijns W; FAVOR Pilot Trial Study Group. JACC Cardiovasc Interv. 2016 Oct 10;9(19):2024-2035.

- *"Plaque protrusion compromising bioresorbable coronary scaffold patency"*. Floré V, **Pellicano M**, Adjedj J, Ferrara A, Van Der Steen K, Bartunek J. EuroIntervention. 2016 Sep 18;12(7):873.

- *"Reduced coronary flow reserve in coronary arteries without stenosis: impact of various hemodynamic and clinical parameters"*. Toth GG, Adjedj J, **Pellicano M**, Di Gioia G, Barbato E, De Bruyne B. Best posters in diet and activity: getting the balance right. ESC congress, Rome August 27 - 31, 2016.

- *"Validation of a novel catheter for thermodilution-derived measurement of absolute coronary blood flow and microvascular resistances"*. Xaplanteris P, Adjedj J, Toth GG, Ferrara A, **Pellicano M**, Floré V, Ciccarelli G, Milkas A, Barbato E, De Bruyne B. ESC

congress, Rome August 27 - 31, 2016.

- *"Bailout stenting in coronary bifurcations is associated with increased risk of in-hospital and 1-year adverse outcomes: insights from the P2BiTO registry"*. Amat Santos IJ, Kedev SA, Zimarino M, Radico F, Briguori C, **Pellicano M**, Andrejs E, Gamra H, Kanic V, Gil RJ, Strozzi M, Tesorio T, Vukcevic V, Cirillo P, Stankovic G on behalf of The EuroBifurcation Club. ESC congress, Rome August 27 - 31, 2016.

- *"Saline-induced coronary hyperemia mechanisms and effects on left ventricular function"* B. De Bruyne B, Adjedj J, Xaplanteris P, Ferrara A, Mo Y, Penicka M, Flore V, **Pellicano M**, Toth GG, Johnson N, Barbato E, Pijls N. ESC congress, Rome August 27 - 31, 2016.

- *"Clinical significance and predictors of coronary lesion progression as assessed by fractional flow reserve (FFR)"*. Xaplanteris P, De Bruyne B, **Pellicano M**, Ciccarelli G, Milkas A, Barbato E. ESC congress, Rome August 27 - 31, 2016.

- *"Image-based FFRangio during coronary catheterization"*. **Pellicano M**, Kornowski R, Lavi I, Assali A, Vaknin-Assa H, Valtzer O, De Bruyne B. on behalf of FFRAngio. Best poster in e-cardiology. ESC congress, Rome August 27 - 31, 2016.

- *"Standardization of Fractional Flow Reserve Measurements"*. Toth GG, Johnson NP, Jeremias A, **Pellicano M**, Vranckx P, Fearon WF, Barbato E, Kern MJ, Pijls NH, De Bruyne B. J Am Coll Cardiol. 2016 Aug 16;68(7):742-53.

- *"Effects of Prasugrel Versus Clopidogrel on Coronary Microvascular Function in Patients Undergoing Elective PCI"*. Mangiacapra F, Di Gioia G, **Pellicano M**, Di Serafino L, Bressi E, Peace AJ, Bartunek J, Wijns W, De Bruyne B, Barbato E. J Am Coll Cardiol. 2016 Jul 12;68(2):235-7.

- *"Fractional Flow Reserve-Guided Revascularization in Patients With Aortic Stenosis"*. Di Gioia G, **Pellicano M**, Toth GG, Casselman F, Adjedj J, Van Praet F, Ferrara A, Stockman B, Degrieck I, Bartunek J, Trimarco B, Wijns W, De Bruyne B, Barbato E. Am J Cardiol. 2016 May 1;117(9):1511-5.

- *"Reversed single string technique for single bifurcation stenting: first case of in vitro case demonstration"*. Adjedj J, Toth GG, **Pellicano M**, Ferrara A, Barbato E, De Bruyne B, Wijns W. EuroIntervention Supplement May 2016, Abstracts of EuroPCR Congress, Paris, 17-20 May 2016.

- *"PROcedure Related Microvascular ACTIVation In Long LEsions Treated With Bioresorbable Vascular Scaffold Versus Everolimus Eluting Stent Implantation PROACTIVE trial"*. **Pellicano M**, Di Gioia G; Toth GG, Ferrara A, Adjedj J, Van Durme F, Heyse A, Vanderheyden M, Bartunek J; Wijns W; De Bruyne B; Barbato E. EuroIntervention Supplement May 2016, Abstracts of EuroPCR Congress, Paris, 17-20 May 2016.

- *"FFR compared with angiographic estimation of coronary artery disease: impact of diabetes"*. Adjedj J, Xaplanteris P, Floré V, **Pellicano M**, Ferrara A, Ciccarelli G, Barbato E, De Bruyne. EuroIntervention Supplement May 2016, Abstracts of EuroPCR Congress, Paris, 17-20 May 2016.

- *"Impact of Right Atrial Pressure on Fractional Flow Reserve Measurements: Comparison of Fractional Flow Reserve and Myocardial Fractional Flow Reserve in 1,600 Coronary Stenoses"*. Toth GG, De Bruyne B, Rusinaru D, Di Gioia G, Bartunek J, **Pellicano M**, Vanderheyden M, Adjedj J, Wijns W, Pijls NH, Barbato E. JACC Cardiovasc Interv. 2016 Mar 14;9(5):453-9.

- *"Clinical Outcome of Patients with Aortic Stenosis and Coronary*

Artery Disease Not Treated According to Current Recommendations". Di Gioia G, **Pellicano M**, Toth GG, Casselman F, Adjedj J, Van Praet F, Stockman B, Degrieck I, Trimarco B, Wijns W, De Bruyne B, Barbato E. J Cardiovasc Transl Res. 2016 Apr;9(2):145-52.

- *"Significance of Intermediate Values of Fractional Flow Reserve in Patients With Coronary Artery Disease"*. Adjedj J., De Bruyne B., Floré V., Di Gioia G., Ferrara A., **Pellicano M.**, Toth G.G., Bartunek J., Vanderheyden M., Heyndrickx G.R., Wijns W., Barbato E. Circulation 2016 Feb 2;133(5):502-8.

- *"Intracoronary adenosine: dose-response relationship with hyperemia"*. Adjedj J., Toth G.G., Johnson N.P., **Pellicano M.**, Ferrara A., Floré V., Di Gioia G., Barbato E., Muller O., De Bruyne B. JACC Cardiovasc Interv. 2015 Sep;8(11):1422-30.

- *"Validation of a novel catheter for thermodilution-derived measurement of absolute coronary blood flow and microvascular resistances"*. Adjedj J., Toth G.G. , Ferrara A., **Pellicano M.**, Floré V., Barbato E., De Bruyne B. Transcatheter Cardiovascular Therapeutics (TCT) Congress, San Francisco, 11-15 October 2015.

- *"Continuous intracoronary infusion of saline at room temperature induces steady state maximal hyperemia".* Adjedj J., Floré V., Toth G.G., Ferrara A., **Pellicano M.**, Barbato E., De Bruyne B. Transcatheter Cardiovascular Therapeutics (TCT) Congress, San Francisco, 11-15 October 2015.

- *"FFR Gray zone and clinical outcome".* Adjedj J., De Bruyne B., Floré V., Di Gioia G., Ferrara A., **Pellicano M.**, Toth G.G., Bartunek J., Vanderheyden M., Wijns W. , Barbato E. Cardiovascular Therapeutics (TCT) Congress, San Francisco, 11-15 October 2015.

- *"Contrast-induced microvascular dilatation: implications for*

fractional flow reserve measurements". Adjedj J., Toth G.G., Johnson N.P., **Pellicano M.**, Ferrara A., Di Gioia G., Floré V., Barbato E., Muller O., De Bruyne B. Transcatheter Cardiovascular Therapeutics (TCT) Congress, San Francisco, 11-15 October 2015.

- *"Effects of prasugrel versus clopidogrel on coronary microvascular function in patients undergoing elective percutaneous coronary intervention: a randomized double-blind study"*. Mangiacapra F., **Pellicano M.**, Di Serafino L., Bressi E., Peace A., Di Gioia G., Bartunek J., Wijns W., De Bruyne B., Barbato E. ESC congress, London 29 August – 2 September 2015.

- *"Intracoronary adenosine: dose-response relationship with hyperemia"*. Adjedj J., Toth G., Johnson N.P., **Pellicano M.**, Ferrara A., Floré V., Di Gioia G., Barbato E., Muller O., De Bruyne B. ESC congress, London 29 August – 2 September 2015.

- *"Procedure related platelet activation in long lesions treated with bioresorbable vascular scaffold versus xience xpedition implantation (PROACTIVE trial)".* **Pellicano M.**, Di Gioia G., Toth G., Ferrara A., Adjedj J., Delrue L., Bartunek J., Wijns W., De Bruyne B., Barbato E. ESC congress, London 29 August – 2 September 2015.

- *"Single string technique for complex coronary bifurcation stenting".* Toth G.G., Pyxaras S., Mortier P., Di Gioia G., Adjedj J., **Pellicano M.**, Barbato E., De Bruyne B., De Beule M., Wijns W. ESC congress, London 29 August – 2 September 2015.

- *"Image-based FFR during coronary catheterization".* Kornowski R., Lavi I., **Pellicano M.**, De Bruyne B. ESC congress, London 29 August – 2 September 2015.

- *"FFR gray zone and clinical outcome".* Adjedj J., De Bruyne, V., Flore V., Di Gioia G., Ferrara A., **Pellicano M.**, Bartunek J., Vanderheyden M., Wijns W., Barbato E. ESC congress, London 29 August – 2

September 2015.

- *"Fractional flow reserve-guided revascularization in patients with aortic stenosis: a propensity matched analysis".* Di Gioia G., **Pellicano M.**, Toth G., Casselman F., Van Praet F., Stockman B., Degrieck I., Trimarco B., De Bruyne B., Barbato E. ESC congress, London 29 August – 2 September 2015.

- *"High platelet reactivity and periprocedural myocardial infarction in patients undergoing percutaneous coronary intervention: A significant association beyond definitions".* Mangiacapra F., Cavallari I., Ricottini E., **Pellicano M.**, Barbato E., Di Sciascio G. Int J Cardiol. 2015 Jul 1;190:124-5.

- *"Single String Technique for Coronary Bifurcation Stenting: Detailed Technical Evaluation and Feasibility Analysis".* G Toth G., Pyxaras S., Mortier P., De Vroey F., Di Gioia G., Adjedj J., **Pellicano M.**, Ferrara A., De Schryver T., Van Hoorebeke L., Verhegghe B., Barbato E., De Bruyne B., De Beule M., Wijns W. JACC Cardiovasc Interv. 2015 Jun;8(7):949-59.

- *"FFR gray zone and clinical outcome".* Adjedj J., De Bruyne B, Floré V., Di Gioia G., Ferrara A., **Pellicano M.**, Toth G., Bartunek J., Vanderheyden M., Heyndrickx G., Wijns W.,Barbato E. EuroIntervention Supplement May 2015, Abstracts of EuroPCR Congress, Paris, 19-22 May 2015.

- *"The single string technique for complex coronary bifurcation stenting".* Toth G.G., Pyxaras S., Mortier P., De Vroey F., Di Gioia G., Adjedj J., **Pellicano M.**, Verhegghe B., Barbato E., De Bruyne B., De Beule M., Wijns W. EuroIntervention Supplement May 2015, Abstracts of EuroPCR Congress, Paris, 19-22 May 2015.

- *"Validation of a novel monorail coronary thermodilution catheter for measuring coronary microvascular resistances".* Adjedj J., Floré

V., Ferrara A., **Pellicano M.**, Toth G., Barbato E., De Bruyne B. EuroIntervention Supplement May 2015, Abstracts of EuroPCR Congress, Paris, 19-22 May 2015.

- *"Angiogram-based FFR during coronary catheterization".* Kornowski R., Lavi I., Assali A., Vaknin-Assa H., Valtzer O., **Pellicano M.**, Floré V., De Bruyne B. EuroIntervention Supplement May 2015, Abstracts of EuroPCR Congress, Paris, 19-22 May 2015.

- *"Unrecognized anomalous left circumflex coronary artery arising from right sinus of Valsalva: a source of perioperative complication",* **Pellicano M.**, Toth G., Di Gioia G., Rusinaru D., Wijns W., Barbato E., De Bruyne B., Degrieck I., Van Mieghem C.; J Cardiovasc Med (Hagerstown), 2015 Feb 11.

- Response to letter regarding article, *"revascularization decisions in patients with stable angina and intermediate lesions: results of the international survey on interventional strategy".* Toth G.G., Toth B., De Vroey F., Di Serafino L., Pyxaras S., Rusinaru D., Di Gioia G., **Pellicano M.**, Barbato E., Van Mieghem C., Heyndrickx G.R., De Bruyne B., Wijns W., Johnson N.P. Circ Cardiovasc Interv. 2015 Feb;8(2): e002296.

- *"Reversed Single String Technique for Coronary Bifurcation Stenting – first report in vitro case demonstrations".* Adjedj J., Toth G., **Pellicano M.**, Ferrara A., Floré V., Di Gioia G., Barbato E., De Bruyne B., Wijns W. 26es Journées Européennes de la Société Française de Cardiologie, 13-16 Janvier 2015.

- *"Accuracy of visual estimation compared to objective anatomical and functional measurement, QCA and FFR, in coronary lesions".* Adjedj J., Toth G., Di Gioia G., Ferrara A., Floré V., **Pellicano M.**, Barbato E., Wijns W., De Bruyne B. 26es Journées Européennes de la Société Française de Cardiologie, 13-16 Janvier 2015.

- *"Pump flushing versus manual flushing for optimal optical coherence tomography imaging".* Ferrara A., Toth G., Di Gioia G., **Pellicano M.**, Lenaerts B., De Vroey F., Wijns W., De Bruyne B., Barbato E. Giornale Italiano di Cardiologia vol 15, suppl 2 al n 12, dicembre 2014.

- *"Impact of patients' hemodynamic status on the accuracy of Fractional Flow Reserve measurement".* **Pellicano M.**, Toth G.G., Di Gioia G., Ferrara A., Rusinaru D., Adjedj J., Wijns W., De Bruyne B., Barbato E. Giornale Italiano di Cardiologia vol 15, suppl 2 al n 12, dicembre 2014.

- *"Revascularization decisions in patients with stable angina and intermediate lesions: results of the International Survey on Interventional Strategy (ISIS)"* Toth G.G., Toth B., Johnson N., De Vroey F., Di Serafino L., Pyxaras S., Rusinaru D., Di Gioia G., **Pellicano M.**, Barbato E., Van Mieghem C., Heyndrickx G., Wijns W., De Bruyne B.; Circ Cardiovasc Interv. 2014 Dec;7(6):751-9.

- *"Clinical outcome of patients with aortic stenosis and coronary artery disease undergoing incomplete treatment strategies",* Di Gioia G., **Pellicano M.**, Ferrara A., Toth G., Adjedj J., Wijns W., Degrieck I., Casselman F., De Bruyne B., Barbato E.; Abstracts of ESC Congress, Barcelona 30 August-03 September 2014.

- *"Acute coronary syndromes in patients with multivessel disease: the key role of optical coherence tomography",* Di Gioia G., Toth G., Rusinaru D., **Pellicano M.**, Wijns W., De Bruyne B., Barbato E.; J Cardiovasc Med (Hagerstown). 2014 Jun 28.

- *"Clinical outcome of patients with multivessel disease and moderate to severe aortic stenosis undergoing PCI",* Di Gioia G., **Pellicano M.**, Toth G., Adjedj J., Casselman F., Van Praet F., Stockman B., Degrieck I., Wijns W., De Bruyne B., Barbato E.; Abstracts of EuroPCR Congress, Paris, 20-23 May 2014.

- *"Impact of patient's haemodynamic status on the accuracy of FFR measurement",* Toth G.G., Rusinaru D., Di Gioia G., **Pellicano M.**, Adjedj J., Nelis O., Wijns W., De Bruyne B., Barbato E.; Abstracts of EuroPCR Congress, Paris, 20-23 May 2014.

- *"Treatment of no-reflow during primary angioplasty: head to head dipyridamole versus verapamil",* Scappaticci M., Mukred K., **Pellicano M.**, Cocco N., Tanzilli A., Tafani F., Al Kindy S., Tanzilli G, Gaudio C.; Giornale Italiano di Cardiologia vol 14, suppl 1 al n 5, Dicembre 2013.

- *"Histopathological characteristics of coronary thrombus in patients with acute myocardial infarction and large thrombus burden"* Tanzilli A., Cerbelli B., Scappaticci M., Mukred K., **Pellicano M.**, Cocco N., Tanzilli G., Gaudio C., Gallo P.; Giornale Italiano di Cardiologia vol 14, suppl 1 al n 5, Dicembre 2013.

- *"Clinical and electrocardiographic findings in a rare case of midventricular Tako-Tsubo cardiomyopathy"* Gentile P., Petriello G., Creo F., **Pellicano M.**, Paravati V., Barillà F., Gaudio C; Atti del 44° Congresso Nazionale ANMCO di Cardiologia, 30 maggio-01 giugno 2013.

- *"Hypertensive crisis as initial presentation of midventricular Tako-Tsubo cardiomyopathy: a clinical case report"* Gentile P., Petriello G., **Pellicano M.**, Creo F., Rauseo E., Pannarale G., Paravati V., Barillà F., Mangieri E., Gaudio C.; 23rd European Meeting of Hypertension & Cardiovascular Protection (ESH) June 14-17 2013

- *"Is there still a role for Glycoprotein IIb/IIIa antagonists in acute coronary syndromes?"* Iannetta L., Puddu P.M., Cuturello D., Saladini A., **Pellicano M.**, Schiariti M.; Cardiology Research Vol. 4, No.1, Feb 2013.

- *"Long-term efficacy of dual antiplatelet treatment with indobufen and clopidogrel in a subset of patients with hypersensitivity to aspirin undergoing percutaneous coronary intervention",* Barillà F., Mangieri E., Tanzilli G., Acconcia C., Dominici T., **Pellicano M.**, Paravati V., Pulcinelli F.M., Gaudio C. Platelets 2013;24(3):183-8.

- *"Clopidogrel plus indobufen in patients with hypersensitivity to aspirin undergoing percutaneous coronary intervention"* Barillà F., Dominici T., Pannarale G., Giordano F., Jacomelli J., **Pellicano M.**, Sergi S.C., Gaudio C.; ESC congress, Munich 25-29 August 2012.

- *"ST-segment elevation during levosimendan infusion"* Barillà F., Giordano F., Jacomelli I., **Pellicano M.**, Dominici T.; J Cardiovasc Med (Hagerstown). 2012 Jul;13(7):454-6.

- *"Effetti clinici ed emodinamici dell'Ivabradina in pazienti con scompenso cardiaco acuto post-infartuale",* Petriello G., Basile C., **Pellicano M.**, Jacomelli I., Giordano F., Sergi S.C., Donatiello M.G., Dominici T., Barillà F.; Atti del 43° Congresso Nazionale ANMCO di Cardiologia, 30 maggio-02 giugno 2012.

- *"Monitoraggio dell'aggregazione piastrinica come guida per l'ottimizzazione della terapia antiaggregante in pazienti con SCA trattati con PTCA ed impianto di stent",* Basile C., Petriello G., Dominici T., Giordano F., Jacomelli I., Sergi S.C., Donatiello M.G., **Pellicano M.**, Barillà F.; Atti del 43° Congresso Nazionale ANMCO di Cardiologia, 30 maggio-02 giugno 2012.

- *"Clinical and haemodynamic effects of ivabradine in patients with acute ischemic heart failure",* Jacomelli I., **Pellicano M.**, Dominici T., Giordano F., Basile C., Petriello G., Nusca B., Torromeo C., Gaudio C., Barillà F.; Giornale Italiano di Cardiologia vol 12, suppl 3 al n 12, dicembre 2011.

- *"Monitoraggio dell'aggregazione piastrinica e sviluppo di eventi in pazienti con SCA trattati con PTCA ed impianto di stent*", Giordano F., Dominici T., **Pellicano M.**, Jacomelli I., Basile C., Petriello G., Nusca B., Paravati V., Gaudio C., Barillà F.; Giornale Italiano di Cardiologia vol 12, suppl 3 al n 12, dicembre 2011.

- *"Clinical and haemodynamic effects of ivabradine in patients with acute ischemic heart failure",* Barillà F., Jacomelli I., Giordano F., **Pellicano M.**, Dominici T., Torromeo C., Paravati V., Petrini N., Gaudio C.; Policlinico Umberto I, "Sapienza" University of Rome – Italy, poster session of Heart Failure ESC congress, May 2011, Gothenburg, Sweden.

- *"Ivabradina: efficacia e tollerabilità nei pazienti con scompenso cardiaco acuto post-infartuale",* Jacomelli I., Giordano F., **Pellicano M.**, Dominici T., Torromeo C., Moschella Orsini F., Petriello G., Barillà F.; Atti del 42° Congresso Nazionale ANMCO di Cardiologia, maggio 2011.

- *"Monitoraggio dell'aggregazione piastrinica e sviluppo di eventi in pazienti con SCA rivascolarizzati mediante PTCA ed impianto di stent",* Giordano F., Jacomelli I., **Pellicano M.**, Dominici T., Carbotta S., Basile C., Pulcinelli F.M., Barillà F.; Atti del 42° Congresso Nazionale ANMCO di Cardiologia, maggio 2011.

- *"Efficacia e tollerabilità della doppia terapia antiaggregante con Clopidogrel ed Indobufene nei pazienti con cardiopatia ischemica sottoposti ad angioplastica coronarica transluminale percutanea ed impianto di stent",* Barillà F., Dominici T., Pulcinelli F.M., **Pellicano M.**, Petrini N., Roselli L., Jacomelli I., Giordano F., Paravati V., Gaudio C.; Giornale Italiano di Cardiologia vol 11, suppl 1 al n 12, dicembre 2010.

- *"Efficacia e tollerabilità dell'Ivabradina sul controllo della frequenza*

cardiaca in pazienti con scompenso cardiaco acuto post-infartuale"; **Pellicano M.**, Jacomelli I., Giordano F., Dominici T., Roselli L., Petrini N., D'Alessandro G., Acconcia C., Paravati V., Barillà F., Giornale Italiano di Cardiologia vol 11, suppl 1 al n 12, dicembre 2010.

- *"Valore predittivo del monitoraggio dell'aggregazione piastrinica sullo sviluppo di eventi nel follow-up in pazienti con sindrome coronarica acuta rivascolarizzati con angioplastica coronarica transluminale percutanea ed impianto di stent",* Jacomelli I., Giordano F., **Pellicano M.**, Dominici T., Torromeo C., Madeo A., Carbotta S., Gaudio C., Pulcinelli F.M., Barillà F.; Giornale Italiano di Cardiologia vol 11, suppl 1 al n 12, dicembre 2010.

- *"Prevenzione dell'IRA post imaging coronarografia: la nostra esperienza",* Lanzi L., Petrassi M., Tersigni F., Sergiacomi R., Garante C.M., **Pellicano M.**, D'Ambrosi A., Alessandri N.; Atti del XVII Congresso Nazionale della Società Italiana di Ricerche Cardiovascolari, ottobre 2010.

- *"Elasticità/distensibilità dell'aorta ascendente in condizioni di base e di microgravità simulata",* Di Matteo A., Tufano F., Sergiacomi R., Garante C. M., Tersigni F., **Pellicano M.**, Perna R., Alessandri N.; Atti del XVII Congresso Nazionale della Società Italiana di Ricerche Cardiovascolari, ottobre 2010.

- *"Cardiovascular functional adjustments in young healthy subjects in normobaric conditions and in microgravity",* Petrassi M., Alessandri N., Tufano F., Di Matteo A., Lanzi L., Coluzzi G., Fusco L., **Pellicano M.**, De Angelis C., Tomao E.; Acts of 31st Annual ISGP Meeting, 11th ESA Life Sciences Symposium, ELGRA Symposium, Trieste, giugno 2010.

- *"Inibitori di pompa protonica e resistenza al Clopidogrel in pazienti con Sindrome Coronarica Acuta trattati con PTCA ed impianto di stent",* Barillà F., Pulcinelli F.M., Petrini N., Dominici T., **Pellicano M.**, Paravati V., Torromeo C., Jacomelli I., Di Biagio D., Gaudio C.;

Giornale Italiano di Cardiologia vol 10, suppl 1 al n 11-12, dicembre 2009.

- *"Efficacia e tollerabilità della doppia terapia antiaggregante piastrinica con Indobufene e Clopidogrel in pazienti con SCA ed allergia documentata all'Aspirina, sottoposti a PTCA ed impianto di stent",* Barillà F., Pulcinelli F.M., Dominici T., Petrini N., **Pellicano M.**, Paravati V., Jacomelli I., Di Biagio D., Gaudio C.; Giornale Italiano di Cardiologia vol 10, suppl 1 al n 11-12, dicembre 2009.

- *"Aumento dei livelli sierici di Anticorpi anti-transglutaminasi tissutale e sviluppo di rimodellamento ventricolare sinistro nel post-infarto"*, **Pellicano M.**, Picarelli A., Petrini N., Dominici T., Paravati V., Barillà F., Giordano F., Gaudio C.; Giornale Italiano di Cardiologia vol 10, suppl 1 al n 11-12, dicembre 2009.

- *"Correlazione tra livelli sierici di pro-BNP ed Anticorpi anti-tTG in pazienti con Sindrome Coronarica Acuta: possibile nuovo marker di rimodellamento ventricolare?",* Barillà F., Petrini N., Di Tola M., **Pellicano M.**, Moschella Orsini F., Paravati V., Gaudio C., Picarelli A.; Giornale Italiano di Cardiologia vol 9, suppl 1 al n 12, dicembre 2008.

- *"Correlazione tra livelli sierici di Anticorpi anti-tTG e sviluppo di eventi cardiovascolari nel post-infarto",* Barillà F., Petrini N., Di Tola M., **Pellicano M.**, Faiella A., Chialastri C., Gaudio C., Picarelli A.; Giornale Italiano di Cardiologia vol 9, suppl 1 al n 12, dicembre 2008.

- *"Tollerabilità ed efficacia della terapia combinata Indobufene-Clopidogrel in pazienti con allergia all'Aspirina trattati con PTCA ed impianto di stent medicato",* Barillà F., Petrini N., **Pellicano M.**, Donato L.M., Torromeo C., Paravati V., Faiella A., Moschella Orsini F., Gaudio C.; Giornale Italiano di Cardiologia vol 9, suppl 1 al n 12, dicembre 2008.

- *"Influenza della Rosuvastatina sull'attività antiaggregante del Clopidogrel nei pazienti con Sindrome Coronarica Acuta",* Barillà F., Donato L.M., Petrini N., Riondino S., **Pellicano M.**, Paravati V., Torromeo C., Gaudio C., Pulcinelli F.M.; Giornale Italiano di Cardiologia vol 9, suppl 1 al n 12, dicembre 2008.

- *"Influenza della Terapia di Resincronizzazione Cardiaca sulla Heart Rate Varibility",* Magrì D., Chialastri C., Faiella A., Panetta G., **Pellicano M.**, Carucci A., Arrivi A., Magnanti M., Matera S., Pasquazzi E., Schifano E., Vellitti S., Mitra M., Cipriani E., Marigliano V., Piccirillo G.; Geriatric Medicine Journal, suppl. al vol.1, n. 1 , gennaio/aprile 2007.

- *"Effetto del Metoprololo e del Carvedilolo sulla variabilità del QT in soggetti con scompenso cardiaco sistolico",* Magrì D., Chialastri C., Faiella A., Moschella F., Petrini N., **Pellicano M.**, Magnanti M., Matera S., Pasquazzi E., Schifano E., Vellitti S., Mitra M., Cipriani E., Marigliano V., Piccirillo G.; Geriatric Medicine Journal, suppl. al vol.1, n. 1 , gennaio/aprile 2007.

- *"QT Variability e Rischio Cardiovascolare Globale nello scompenso cardiaco di grado moderato",* Magrì D., Chialastri C., Panetta G., **Pellicano M.**, Faiella A., Leonetti S., Magnanti M., Matera S., Pasquazzi E., Schifano E., Vellitti S., Mitra M., Cipriani E., Marigliano V., Piccirillo G.; Geriatric Medicine Journal, suppl. al vol.1, n. 1 , gennaio/aprile 2007.

- *"Rosuvastatin effects on platelet inhibition by Clopidogrel in cardiovascular patients"* Petrini N., Donato L., Riondino S., Pulcinelli F, **Pellicano M.**, Torromeo C., Paravati V., Barillà F.; Giornale Italiano di Cardiologia vol 9, suppl 2 al n 5, maggio 2008.

Acknowledgments

I wish to sincerely thank Bernard De Bruyne for his crucial role as scientific guide in the intense journey that allowed me to complete this thesis, as well as for having been my coronary physiology teacher during the outstanding years spent at the Cardiovascular Center of Aalst. An heartfelt thanksgiving to Emanuele Barbato, my mentor of interventional cardiology, science and professional life, a person who has always believed in me and who has taught me to see the "half-full glass" in life and work. A sincere thanks to William Wijns for showing me a transversal perspective in cardiology and for being a constant source of ideas and inspiration. Thanks a lot to Jozef Bartunek and Marc Vanderheyden for turning on, since the beginning, the “clinical light” in my world of interventional cardiologist. Thanks to all the Fellows of the Cardiovascular Center of Aalst with whom I have spent these years among challenging procedures, many coffees and healthy laughter. A greatful thanks to Tullio Tesorio and all the Staff of the Montevergine Clinic for having routed me to other branches of percutaneous interventions (peripheral and structural). The last but certainly not the least are my wife Alessia, who I thank for being always by my side, and my family for being my background in the life.

Thanks to Cathworks Ltd (Raanana, Israel) for giving me the copyright of two images used for the main figure of the cover page.